Volume 9, No. 1

July, 1961

THE SOVIET JOURNAL OF

ATOMIC ENERGY

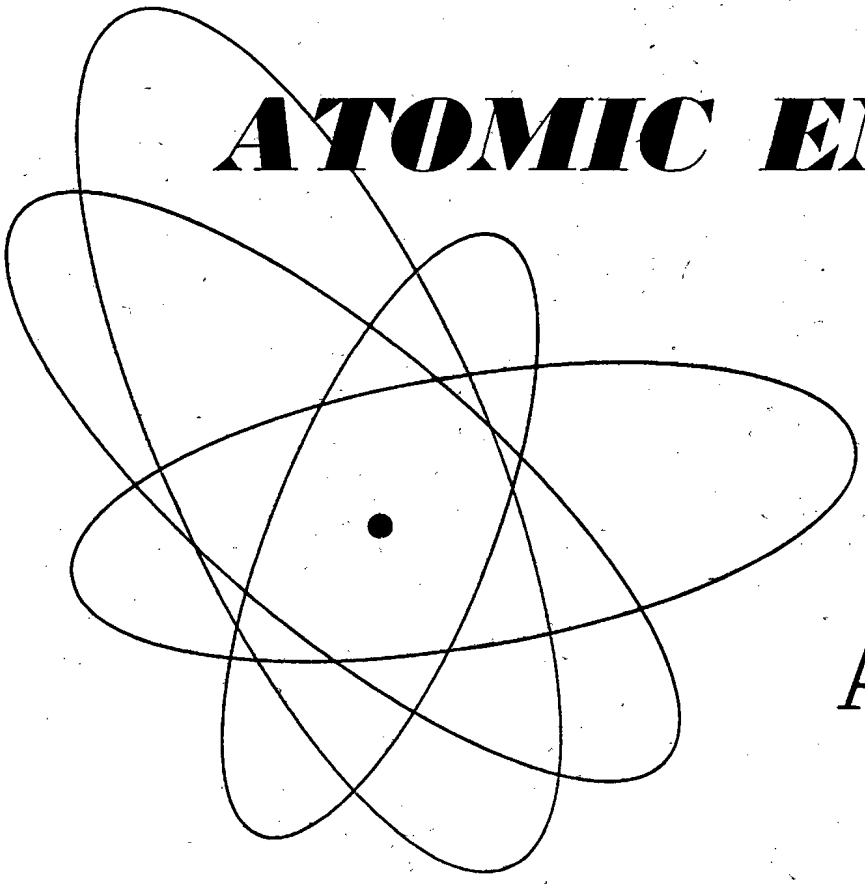

Атомная энергия

TRANSLATED FROM RUSSIAN

CONSULTANTS BUREAU

the latest Soviet techniques!

CONTEMPORARY EQUIPMENT for WORK with RADIOACTIVE ISOTOPES

A comprehensive review of the Soviet methods and technological procedures used in the production of isotopes and the preparation of labelled compounds from them. The shielding and manipulative devices are described as well as illustrated in detail. It is an excellent guide for all scientists and technologists concerned with radioactive isotopes.

CONTENTS

durable paper covers *67 pages* *illus.* *$15.00*

(c/b) CONSULTANTS BUREAU
227 W. 17th ST., NEW YORK 11, N. Y.

THE SOVIET JOURNAL OF

ATOMIC ENERGY

A translation of ATOMNAYA ÉNERGIYA, a publication of the Academy of Sciences of the USSR

(Russian original dated July, 1960)

Vol. 9, No. 7 July, 1961

CONTENTS

Annual subscription $75.00
Single issue 20.00
Single article 12.50

CONTENTS (continued)

NOTE

The Table of Contents lists all material that appears in Atomnaya Énergiya. Those items that originated in the English language are not included in the translation and are shown enclosed in brackets. Whenever possible, the English-language source containing the omitted reports will be given.

Consultants Bureau Enterprises, Inc.

ON THE STABILITY THEORY OF HOMOGENEOUS BOILING NUCLEAR REACTORS

B. V. Ershler, B. Z. Torlin, and L. Ya. Suvorov

Translated from Atomnaya Énergiya, Vol. 9, No. 7, pp. 5-9, July, 1960
Original article submitted July 24, 1959

This article presents the derivation of the kinetic equations for homogeneous boiling reactors where the characteristics of the water moderator volume boiling are taken into account. The parameters characterizing the reactor operating conditions are indicated, the pulse regimes arising in the case of stability disturbance are described, and the effect of some factors on stability are considered.

* * *

Fluctuations in the volume of the vapor contained in the water moderator of a homogeneous boiling reactor affect its reactivity to a great extent, which can lead to unstable conditions. Therefore, it would be of interest to obtain a semiquantitative or at least qualitative determination of the influence of different factors on the reactor operating stability. For this purpose, we shall consider the simplified stability theory for such reactors.

Under the conditions in question, the basic vapor mass is generated inside the liquid volume and not near the walls. The lack of a complete theory of volume boiling makes it difficult to find the reactor kinetics equations. The following factors can be used for the first approximation.

A characteristic of volume boiling is the difficult formation of vapor embryos. For instance, in our experiments, not less than several hours are required for the formation of a vapor bubble in 10 ml of water or solution in overheating by 10-20°C, and even the fission of uranium nuclei in the liquid volume does not appreciably accelerate this process. Neither is it influenced by the presence of uranium oxide powder in the water. Similar observations were made in [1]. On the other hand, by supplying heat with sufficient intensity to the volume, a relatively stable volume boiling can be secured even for an excess temperature of only several degrees. It follows from these two facts that stable volume boiling is not necessarily connected with the often-described [2 and 3] fluctuation mechanism of vapor embryo generation, for which large overheating values are required. In the absence of a fluctuation mechanism, the generation of new bubbles can occur due to the breaking-up of large bubbles by the liquid vortex flow. In contrast to the fluctuation mechanism, the hydrodynamic boiling mechanism does not presume large overheating values. We shall adduce certain data illustrating these assumptions.

Water or a salt solution which are free from vapor bubbles and centers necessary for their formation may sometimes not boil even in heating to 200°C under atmospheric pressure. These observations, described by many authors [4] as early as the past century, were considerably expanded in connection with work in designing homogeneous boiling reactors [1 and 5]. They indicate that a stable "embryonic" volume boiling mechanism, i.e., the generation of bubbles in the water volume, is not possible. However, if heat is continuously and intensively introduced into the water volume by electrolysis while taking great care to prevent electrolytical gas bubbles from passing into the water, the liquid cannot be overheated by 10 to 15°C without visible boiling. These experiments will be described in more detail below. They indicate that the hydrodynamic boiling mechanism is applicable in this case.

For deriving the reactor kinetics equations for such a boiling mechanism, we shall denote the vapor volume, weight, and density in the moderator by V_v, M_v, and γ_v; by V_l, M_l, and γ_l, we shall denote the same quantities for the liquid; we shall also denote the liquid height in the reactor in the absence of boiling by H_l, and S will denote the cross section of the reactor, which consists of a vertical cylinder. Moreover, we shall introduce the

notation $\varphi = \frac{V_V}{V_V + V}$ and $\upsilon = \frac{V_V - (V_V)_0}{(V_V)_0}$. The index 0 in all cases indicates that the values of the corresponding quantities pertain to the reactor steady-state conditions. It is considered that the value of $M_l + M_V$ is constant* or, in other words, that, M_l is constant, since $M_l \gg M_V$.

The temperature, the neutron flux, and the distribution of vapor bubbles in the reactor are assumed to be sufficiently uniform; they are replaced by certain average values which are considered as constant throughout the entire volume. Some calculations pertaining to the statics of boiling homogeneous reactors, which were performed by taking into account the nonuniform bubble distribution throughout the core volume, indicate that such approximations are permissible.

We shall represent the water overheating temperature Δt as the sum of two components:

$$\Delta t = \Delta t_1 + \Delta t_2.$$

Here, Δt, represents the water overheating with respect to the vapor in the bubbles, and Δt_2 is the overheating of the vapor in bubbles with respect to the vapor which is above the liquid mirror in the reactor. The water temperature is $t = t_0 + \Delta t$, where t_0 is the steady-state temperature of saturated vapor above the liquid mirror in the reactor.

Under the assumption of a hydrodynamic boiling mechanism, the following inequality holds for the radii of all bubbles:

$$r \gg \frac{2\sigma}{P},$$

where P is the saturated vapor pressure, and σ is the surface tension.

The rate of heat supply to the evaporating water bubble is

$$w = k4\pi r^2 \Delta t_1, \tag{1}$$

where k is a function of r and of the hydrodynamic conditions for boiling water.** Since, under the assumption of a hydrodynamic boiling mechanism, there should be no large bubbles because of their fragmentation nor very small bubbles because of the absence of embryos, we can assume that r is almost constant. Then, the heat used up per second for vapor generation will be

$$W_1 = \frac{V_V}{4/_3 \pi r^3} w,$$

or

$$W_1 = \frac{k}{r/3} V_V \Delta t_1 = f_1 V_V \Delta t_1 ***, \tag{2}$$

Hence, noting that the reactor heat output Q is expended only on two processes, the increase in the overheating temperature Δt and the generation of vapor W_1, we obtain an equation which provides the relationship between the thermal neutron flux N, the overheating, and V_V:

$$Q = f_2 N = C\Delta t + f_1 V_V \Delta t_1. \tag{3}$$

Here f_2 is the proportionality factor, and C is the total heat capacity of the vapor and water in the core. It is obvious that $f_2 = \epsilon \sigma_5 N_5$, where ϵ is the energy released during one U^{235} fission event, σ_5 is the U^{235} thermal neutron fission cross section, and N_5 is the number of U^{235} nuclei in the core.

*It is assumed that after the vapor leaves the liquid, its condensation and return to the core occur instantly.

**k is the thermal conductivity coefficient of the thin cooled water layer around the bubble per 1 cm^2 of the bubble surface. In stationary water, k depends only on r [5 and 6]. With an increase in the vortex motion intensity, the layer thickness decreases and k increases.

***It is obvious from the above-mentioned that the value of the f_1 constant depends on water flow conditions; this will be considered in more detail below.

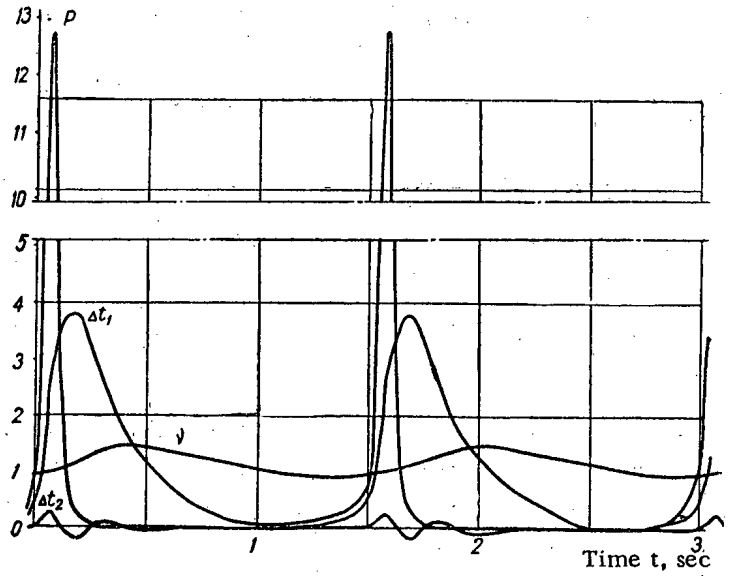

Fluctuations of relative power level values p, overheating values Δt_1 and Δt_2, and the relative vapor volume ν in the water under typical pulse conditions in a boiling homogeneous reactor.

The vapor volume W_2, generated per 1 m^2 of the water mirror, i.e., the vapor volume per second passing through 1 m^2 of the surface of the liquid saturated with bubbles, is equal to $a[\varphi/(1-\varphi)]$, where a is a constant. Since $\varphi/(1-\varphi) = V_v/V_l$ the discharge of vapor from the entire moderator surface is

$$W_3 = \gamma_v W_2 S = \gamma_v \frac{aS}{V_l} V_v = f_3 V_v. \tag{3a}$$

It is obvious that $f_3 = \dfrac{(\gamma_v)_0 aS}{M_l/(\gamma_l)_0}$.* Hence, we obtain the equation taking into account the vapor weight variation in the vapor-water mixture:

$$\dot{M}_v = \frac{1}{l} f_1 V_v \Delta t_1 - f_3 V_v, \tag{4}$$

where $M = V_v \gamma_v$, and l is the evaporation heat. If we do not neglect the changes in γ_v caused by small temperature fluctuations, the following can be substituted in Eq. (4):

$$\dot{M}_v = \dot{V}_v \gamma_v + V_v \frac{\partial \gamma_v}{\partial t} \Delta t_2.$$

In order to take into account the inertia of the moderator mass, we shall note that, if the mirror of the water-vapor mixture that boils according to the hydrodynamic mechanism is at rest, the vapor pressure P_v inside the bubbles is practically equal to the pressure P above the liquid,** and, consequently,

$$\Delta P = P_v - P = 0.$$

For the vertical motion of the mirror with acceleration $\ddot{x}$, which takes place due to the increase in V_v, the pressure head ΔP required for this motion is given by

*The a constant entering the expression for f_3 depends on temperature; it is given in [7]. The small fluctuations of γ_v and γ_l in reactor operation can be neglected, and f_3 can be considered as a constant.

**In considering the growth of an individual immobile bubble, the radius of which became much larger than the critical radius value, i.e., $r \gg 2\sigma/P$, we can neglect the inertia forces [5 and 6] as well as surface tension.

$$\Delta P = \frac{M'}{S}\ddot{x} = \frac{{}^1/_2\frac{Ml}{g}}{S}\ddot{x}, \tag{5}$$

where M' is the effective moving mass.*

Since $\ddot{x} = \frac{(V_V)_0}{S}\ddot{V}_V$ and, besides, for small Δt_2 values, we have $\Delta P = \frac{\partial P}{\partial t}\Delta t_2$, we obtain the following from Eq. (5):

$$\left(\frac{{}^1/_2 Ml}{\frac{g}{S^2\partial P/\partial t}}\right)\ddot{V}_V = f_4\ddot{V}_V = \Delta t_2, \tag{6}$$

where f_4 is a constant, and the value of $\partial P/\partial t$ is found from tables. Equation (6) takes into account the overheating Δt_2, which is necessary for overcoming the inertia of the moderator mass.

The equations for the time dependences of the neutron flux and the concentration of delayed neutron sources for small reactivities Δk are of the following form

$$\dot{N} = \frac{\Delta k - \sum_i \beta_i}{T}N + \sum \lambda_i C_i, \tag{7}$$

where C_i, λ_i, and β_i are the density of sources in the i-th group of delayed neutrons in the reactor, their decay constant, and the yield per single U^{235} fission event, respectively; T is the effective lifetime of a thermal neutron. In boiling homogeneous reactors, $T = T_{\varphi=0}(1-\varphi)^{-1}(1-\varphi\nu)$. If, for a constant fuel mass, the density of the medium in the reactor does not vary within a very wide range, it can be shown that, in the age approximation, the reactor reactivity is

$$\Delta k = -K\varphi_0\nu(1 + {}^1/_2\,\varphi_0\nu),$$

while

$$K = 2\left(\frac{2.4}{K_{\text{eff}}}\right)^2\left(\tau + \frac{L^2}{1+\alpha^2L^2}\right),$$

where K_{eff} is the reactor effective radius, τ is the age of thermal neutrons, L is their diffusion length, and α^2 is the geometric parameter of the cylindrical reactor [8].

Equations (3), (4), (6), and (7) describe the reactor behavior in time. For an analysis of these equations, it is convenient to substitute the dimensionless variables ν, $p = N/N_0$, and $t = \Delta t/\Delta t_0$ (where Δt_0 is the steady-state value of the water overheating) for V_V, N, and Δt. In calculating the constants f_1, f_2, f_3, and f_4, it was assumed that S = 2 m^2 and M_l = 2000 kg. The method for calculating these constants is clear from the corresponding equations.

A consideration of these constants indicates the following.

The f_2, f_3, and f_4 constants are well defined by the water moderator temperature and the reactor dimensions. Actually, the values of σ_5, a, γ_l, γ_V, and $\partial P/\partial t$, with respect to which the constants are calculated by means of the corresponding equations, are functions of temperature only and they are found from the well-known tables and paper [7]. The other quantities necessary for calculating these constants, namely, S, M_l and N_5 are determined by the reactor dimensions and charge.

*The value of M' is of the order of the water mass in the reactor, while it is obvious that $M' \leq 1/2(Ml/g)$. In choosing for the purposes of analysis the conditions which are most unfavorable to the preservation of stability, we used the maximum value of M', since stability decreases with an increase in M'. It should be noted that, in our approximation, where φ is considered as constant for any point in the liquid volume, the equality $M' = 1/2\,(M_l/g)$ must hold.

The f_1 constant cannot be obtained from any table data and must be considered separately. In connection with this, we shall first note that, for constant temperature, $f_1 = W_1/(V_V)_0\Delta t_0$ or $f_1 \simeq 1/\Delta t_0$. These relations are obtained as a result of combining Eqs. (2) and (3a) and the $\Delta t_1 = \Delta t_0$ identity, which is obvious for the steady-state boiling regime. Thus, as was mentioned before, the values of Δt_0 and f_1 are well defined by Eqs. (1) and (2), i.e., by water flow conditions in the core. In this, it is qualitatively obvious that, in the case where the vortex flow of the boiling moderator is intensified, the value of f_1 increases and that of Δt_0 decreases. The numerical values of Δt_0 (or f_1) for different water flow conditions are not yet known. However, by using the calculated constants f_2, f_3, and f_4, we can determined some of the essential characteristics of boiling reactors in spite of this indeterminancy by analyzing the reactor kinetics equations given earlier. In such analysis, Δt_0 should be given as an arbitrary variable parameter of the reactor operating conditions.

The other parameters are the power level, characterized by $(V_V)_0$ or φ_0, and the temperature.

For certain given values of Δt_0 and $(V_V)_0$ and calculated f_2, f_3, and f_4 values, an analysis of Eqs. (3), (4), (6), and (7) indicates that there is an interval of Δt_0 values where the system is stable in a considerable power level interval ($0 < \varphi_0 \leq 0.25$). For our reactor dimensions, the Δt_0 interval corresponding to stable operation varies from a few tenths of a degree to several degrees. Its upper limit decreases with an increase in pressure. In the case where the value of Δt_0 exceeds the upper or lower limits of this interval, the first-approximation analysis indicates that stability vanishes even for low power level values. If the power level value exceeds a certain limit, stability vanishes even for overheating Δt_0 values lying within the interval corresponding to stable conditions. This maximum power level value decreases with an increase in Δt_0.

In the case of stability loss, the system operates under pulse conditions, for which typical variations of p, ν, Δt_1 and Δt_2 in time are shown in the figure. The amplitude of all parameters under pulse conditions increases with an increase in Δt_0.

In the case of sufficiently large Δt_0 values ($\sim 10°C$), the region where the system is stable in the case of small disturbances can simultaneously represent the region of steady-state pulse regimes, which are attained after rather large disturbances are introudced. Thus, for large Δt_0 values, there is a region of two regimes. It should be noted that, in the case of large overheating values, such pulse regimes may not vanish if the power is reduced. The magnitude of disturbances which transfer the system from a stable regime to a pulse regime increases with a decrease in the power level.

As was indicated before, the maximum overheat value for which the system is still stable throughout the entire investigated power level interval considerably increases with an increase in pressure. Moreover, in the case of equal overheats, the amplitudes in pulse regimes are smaller for higher pressures and larger for low pressures (approximately 5 atm abs).

The physical meaning of these results is the following. The reactor kinetics is determined by the value of Δt_0, which depends on the boiling water flow conditions; Δt_0 decreases with an intensification of vortex flow. For very intensive flow, the value of Δt_0 can become too small, and, for an insufficiently intensive motion, this value can become too large. In both cases, Δt_0 can assume values lying outside the limits of the stable operation interval.

Thus, dynamic stability can be improved by reducing or intensifying the liquid turbulent motion. This can be achieved by changing the core geometry, introducing baffles, etc.

It should be noted that, in deriving the kinetic equations, many simplifications were made, which, as a rule, negatively affect the stability. Thus, the dissipation of the water flow mechanical energy and the decrease in Δt_0 with an increase in the water turbulent motion when power is stepped up (which can widen the operating power level interval) have not been taken into account, other boiling mechanisms beside the hydrodynamic mechanism have been neglected, etc. Thus, in the present analysis, we strived as much as possible to consider conditions which are more unfavorable to the preservation of reactor stability.

SUMMARY

1. For small overheating values (of a few degrees), the hydrodynamic boiling mechanism can take place in boiling homogeneous reactors.

2. For a hydrodynamic boiling mechanism, the steady-state overheating values Δt_0 are determined by the boiling water flow conditions in the reactor. The value of Δt_0 can serve as the characteristic of these conditions.

3. An analysis of the kinetic equations for a reactor where the hydrodynamic boiling mechanism prevails showed that there is a certain given interval of Δt_0 values corresponding to stable operating conditions within a considerable interval of power level values. If the Δt_0 value lies outside the limits of this interval, the stability is lost and pulse regimes occur even for low power level values. The upper limit of the Δt_0 interval rises with an increase in pressure.

4. Stability improves with a decrease in the moderator vapor content, a decrease in Δt_0, and an increase in pressure.

5. The amplitudes of all parameters under pulse conditions decrease with an increase in pressure for constant water flow conditions.

6. The measurement of overheating can serve as a method for investigating volume boiling.

I. L. Il'ina, A. S. Kronrod, and Z. S. Ryabovaya kindly analyzed the equations, and the authors are very thankful to them for the large amount of work they did in performing the calculations and in analyzing the results. The greatest part of the calculations was performed by means of the N. I. Bessonov RVM machine.

The authors extend their thanks to A. I. Alikhanov and A. D. Galanin for their continued interest in the work and the valuable discussion.

LITERATURE CITED

1. J. Ghormley, Nuclear Energy 6, 300 (1958).
2. Ya. I. Frenkel', Kinetic Theory of Liquids [in Russian] (Izd. AN SSSR, Moscow-Leningrad, 1945).
3. L. D. Landau and E. M. Lifshits, Theoretical Physics. Statistical Physics [in Russian] (Fizmatgiz, Moscow, 1958) Vol. 4.
4. O. D. Khvol'son, Physics Course [in Russian] (Gosizdat, 1925) Vol. 3, pp. 510-511.
5. M. Plesset and S. Zwick, J. Appl. Phys. 25, 493 (1954).
6. M. Forster and N. Zuber, J. Appl. Phys. 25, 479 (1954).
7. A. I. Filimonov, et al., Teploénergetika, 10, 22 (1957).
8. A. D. Galanin, Theory of Thermal Neutron Nuclear Reactors [in Russian] (Atomizdat, Moscow, 1959).

INVESTIGATION OF START-UP CONDITIONS IN ATOMIC POWER STATIONS WITH A GRAPHITE-URANIUM REACTOR WITH SUPERHEATED STEAM

V. V. Dolgov, V. Ya. Kozlov, L. A. Kochetkov, O. A. Sudnitsyn, and G. N. Ushakov

Translated from Atomnaya Énergiya, Vol. 9, No. 7, pp. 10-15, July, 1960
Original article submitted August 17, 1959

This article presents the results obtained in investigating start-up conditions in an atomic power station with a graphite-uranium reactor where the steam is superheated directly in the reactor. The experiments were performed in the vapor-water loop of the First Atomic Power Station. The loop and various start-up methods are described. The results of experimental work are given and the deficiences and advantages of different start-up methods are noted; on the basis of a comparative analysis of these methods, conclusions are drawn regarding the possibility of starting up an atomic power station of this type without the use of an extraneous steam generator.

* * *

For one of the atomic power stations with graphite-uranium reactors which are under construction, a two-loop layout with steam superheating directly in the reactor was adopted [1]. The first loop of the technological layout includes a group of the reactor evaporating channels from which the heat is removed by boiling water (with a vapor content of ~ 33% by weight at the outlet) under a pressure of 140-150 atm abs, and the second loop includes a group of channels for superheating the steam generated in the steam generators under a pressure of 100 atm abs, for which the heat from the first loop is used.

Such a layout has not been used before in thermal engineering practice; this was because, for designing such a layout, it was necessary to study its operating characteristics as well as a number of problems connected with the physical processes occurring in the loops.

From among the physical problems that had to be studied were the problems of the effect of the reactor coolant boiling on the reactivity and the coolant flow hydrodynamic conditions, where the specific conditions for a given reactor were taken into account. The investigation results are partially presented in [2 and 3].

Technological problems (problems connected with steam superheating conditions in the reactor channels and various power station start-up methods) also had to be studied.

The possibility of steam superheating directly in the reactor depends on securing a reliable cooling of the steam superheating channels (SSC) under transient conditions, especially in raising the power from the zero level. Since the reactor is "cold" at the moment when the power level has to be raised, and steam necessary for cooling SSC is not available, one can visualize two basically different conditions for securing nominal parameter values in the second loop. In the first case, we have start-up conditions where an extraneous steam generator is used, when SSC are cooled by steam from this generator during the initial period of raising the reactor power level; in the second case, we have start-up without an extraneous steam generator, when the SSC cooling is secured by the second loop coolant (with a gradual replacement of water by steam).

This article is concerned with the investigation of various start-up methods where no extraneous steam generators are used.

The investigations were performed in a special vapor-water loop,* which was mounted on the base of the First Atomic Power Station reactor.

Figure 1 shows the schematic diagram of a two-circuit loop, which is basically similar to the layout of the future atomic power station [1].

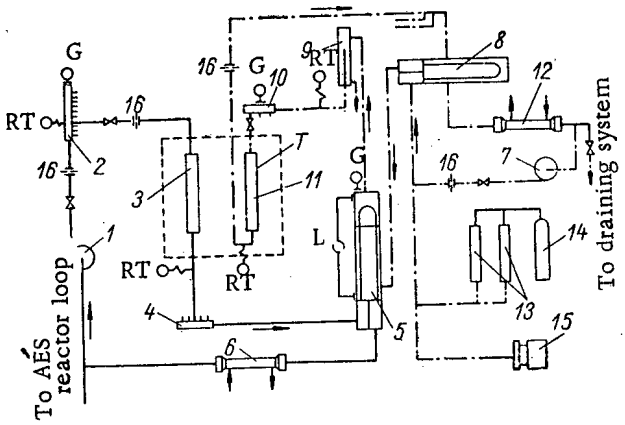

Fig. 1. Schematic diagram of the two-circuit loop. 1) First circuit pump; 2) distributive collector of the first circuit; 3) evaporation channels; 4) first circuit collecting collector; 5) evaporator; 6) cooler; 7) second circuit pump; 8) regenerative heat exchanger; 9) film separator; 10) distributive collector of the second circuit; 11) steam superheating channels; 12) cooler; 13) volume compensator; 14) compressed-air tank; 15) boosting pump; 16) flow measurement throttle; ——) first circuit; — · —) second circuit; RT) resistance thermometer; T) thermocouple; G) pressure gauge; L) level meter.

Ten process channels of the atomic power station reactor were used as evaporating channels in the first circuit of the loop. In order to eliminate the pulsation and spread of the water flow in these channels, a throttling baffle with a diameter of 2.4 mm was mounted at the inlet into the tube of each fuel element. The baffle diameter was determined as a result of investigations performed in individual channels as well as in a large number (51) of the reactor channels operating under boiling conditions [2 and 3].

Three (in certain experiments, two) process channels of the atomic power station reactor, where, however, a smaller degree of enrichment with U^{235} than that in the evaporating channels was used, served as steam-superheating channels in the second loop. Disk baffles with a diameter of 2.8 mm were provided at the fuel element tube inlets in SSC in order to secure hydrodynamic stability in operation under transient conditions. The baffle diameter was determined by preliminary experiments.

The thermodynamic parameters were measured with respect to the layout shown in Fig. 1. The basic parameter determining the safety of a certain start-up method is the temperature of the outside walls of SSC fuel elements, which is measured by means of special thermocouples.

Three methods for effecting the transition from the "cold" state to steam superheating conditions were tested in the vapor-water loop.

The First Method. Before raising the power level, the water was made to circulate through SSC at a flow rate by weight which was three to five times as large as the nominal steam flow. The water pressure in the first and the second circuits as well as the water flow in the first circuit were set at their nominal values. The heating of the circuits until the saturation temperature was attained at the SSC outlet was secured only by raising the reactor power level without manipulating any of the heat exchange equipment. It should be noted that this stage in raising the reactor power level can be extended in time, which does not lead to any basic changes in water flow and pressure in the second circuit; therefore, this stage does not differ in any way from the heating conditions in the first circuit.

From the moment when the temperature at the SSC outlet attained the saturation temperature, an accelerated process of the second circuit heating began; this process is connected with the operating characteristics of a regenerative heat exchanger under conditions applicable to the loop layout under consideration. In this, a very small decrease in the reactor power level resulted in the fact that the water in SSC was first replaced by a vapor-water emulsion and then by steam. The transient process took place in the following manner: the water temperature rise at the SSC inlet caused an increase in the vapor content at the SSC outlet, which, due to an increase in hydraulic resistance and, consequently, a reduction in coolant flow, led to a further increase in vapor content

*By the term "loop", we understand an experimental arrangement consisting of one or several fuel elements and a circulation circuit with a pump and a cooler, where the heat generated in the element is dissipated.

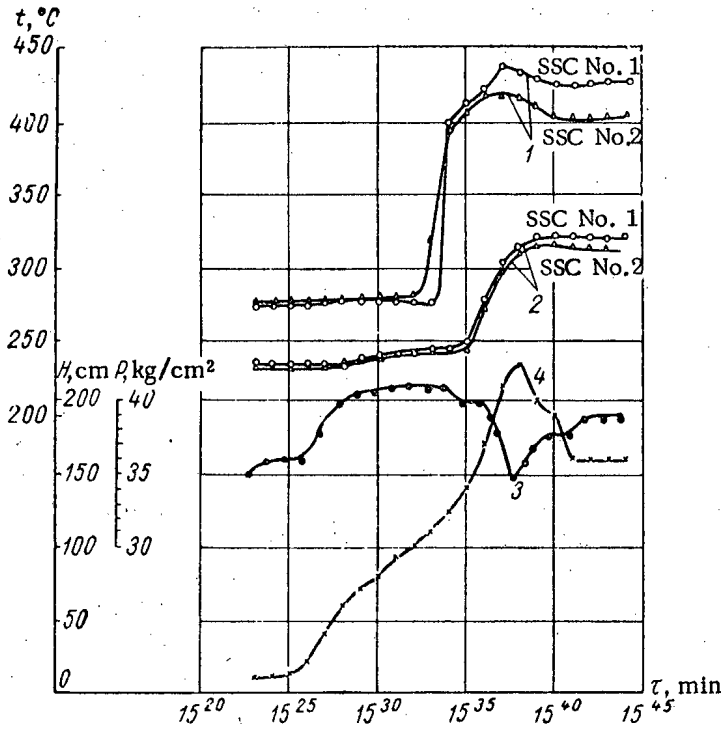

Fig. 2. Variation in time of the second-circuit parameters in the loop under start-up conditions specified by the first method with fast power level rising. 1) Fuel element temperature; 2) steam temperature at the steam-superheating channel outlets; 3) pressure of the second-circuit coolant in the evaporator; 4) water level in the evaporator measured from the top point.

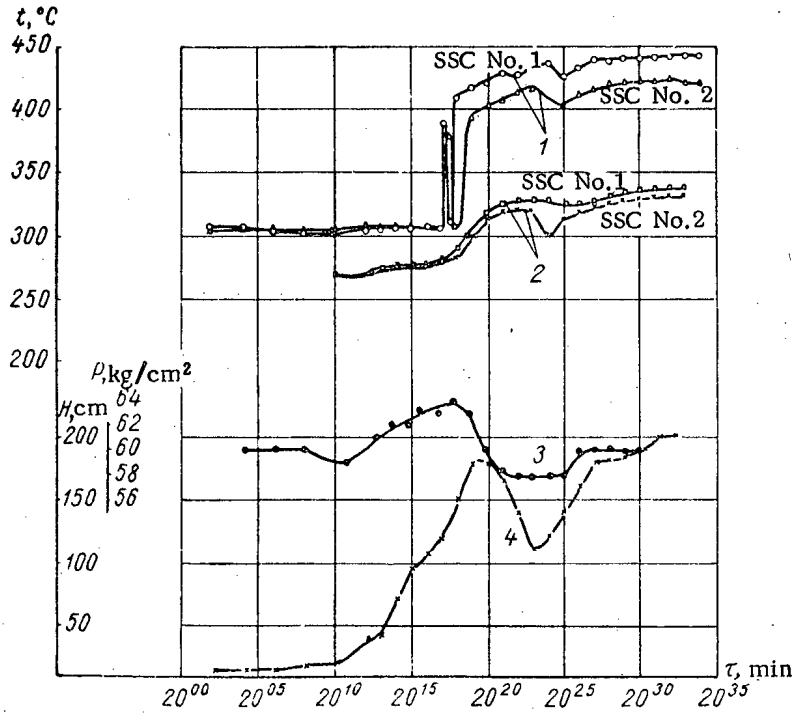

Fig. 3. Variation in time of the second-circuit parameters in the loop under start-up conditions specified by the first method with slower power level build-up (the notation is the same as in Fig. 2).

in the channels. In this, a portion of the water was removed from the second circuit due to the blow-through. The final stage of the transient process consisted in the appearance of water and a reduction in its level in the evaporator, when almost dry saturated vapor appeared at the SSC inlet. The appearance of a water layer in the evaporator was always accompanied by an increase in pressure and a stabilization of the coolant flow in individual channels. Only after this did we observe a sharp increase in the temperature of the fuel elements, which had a critical character, as well as a sharp increase in the steam temperature at the SSC outlet. With this, the basic transient process was completed, and stable rated parameters were established: the steam pressure in the evaporator was 60 atm, the steam flow through one SSC was 500 kg/hr, the superheated steam temperature was 370°C, and the fuel element maximum temperature was 470°C.

A typical diagram representing changes in the characteristic parameters under transient conditions is shown in Figs. 2 and 3.

The Second Method. The system was heated in the same way as when the first method was used. After the water at the SSC outlets was heated to the boiling temperature, the reactor power was reduced to the minimum controllable level. Immediately, after this, an intensive blowing-through of the second circuit in the loop was initiated. As a result of the blow-through, the pressure in the circuit was reduced, and water began to boil in the hottest sections (in the first place, in SSC and the channel beyond). As the water was removed from the circuit, the vapor content in the coolant flow at the SSC inlet increased and attained 100% at a given pressure. After this, SSC were cooled almost entirely by steam. Thus, the transient process (replacement of water by steam in SSC) in using the second method was secured for the minimum controllable reactor power level. After this, the reactor power level was raised in order to stabilize the steam superheating conditions and to raise the pressure to the rated value.

During the replacement of water by steam, only the SSC fuel element temperature and the coolant temperature at the channel outlets dropped; these temperatures did not fluctuate. Fig. 4 shows the diagrams representing the variation of the characteristic parameters during the transient process resulting from the use of the second method.

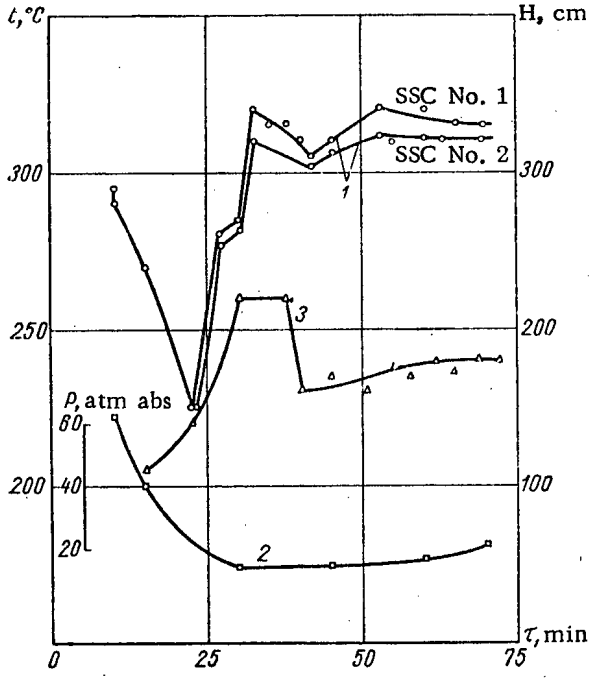

Fig. 4. Variation in time of the second-circuit parameters in the loop under start-up conditions specified by the second method. 1) Fuel element temperature; 2) pressure in the evaporator; 3) water level in the evaporator measured from the top point.

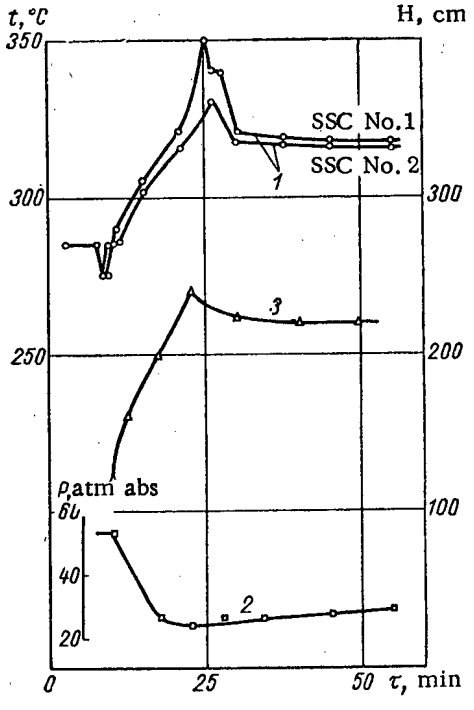

Fig. 5. Variation in time of the second-circuit parameters in the loop under start-up conditions specified by the third method (the notation is the same as in Fig. 4).

The Third Method. The system was heated according to a method similar to the method described above. The transient process consisted of two stages. The basic portion of the process, from the moment when the water started to boil and the beginning of the blow-through until the coolant flow stabilization in SSC, occurred practically for the same power level for which the water began to boil in the second circuit. The termination of the transient process and the generation of superheated steam occurred for a lower reactor power level. In these experiments, this level amounted to ~ 30% of the rated loop power. After superheated steam was produced with a lower power level, the latter was raised to its rated value. The power build-up rate was determined only by the maximum allowable rate of increase in the fuel element temperature and by the steam superheating rate. A typical variation of parameters during the transient process is shown in Fig. 5.

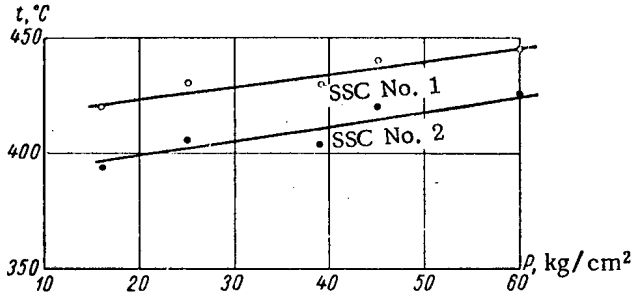

Fig. 6. Dependence of the fuel element temperature on the pressure of steam cooling the fuel elements.

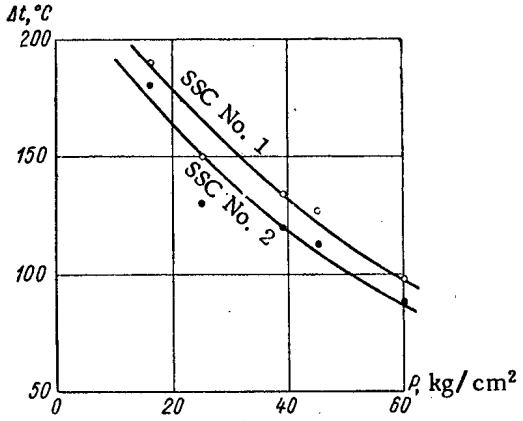

Fig. 7. Dependence of the temperature jump in the fuel elements in the steam superheating channels on pressure under start-up conditions (first method).

RESULTS

The analysis of various methods for establishing the rated operating conditions where superheated steam is used should be performed on the basis of the following evident requirements.

1. The start-up method must provide for a quick raising of power from the zero to the rated level;

2. The maximum fuel element temperatures under transient conditions must not exceed the maximum fuel element temperature specified for the rated operating conditions;

3. During the transient regime, it is necessary to secure a smooth rise of the fuel element temperature in time;

4. The start-up method must provide for a minimum number of operations with the processing equipment.

The first method for initiating the transient process (see Figs. 2 and 3) has the following characteristics:

1) a sharp increase in the fuel element temperature (by 100-150°C over a period of 1 min) which has the character of the crisis;

2) the superheating regimes in individual SSC in the loop are not initiated simultaneously, which is connected with the separating action of the input collector;

3) a considerable change in pressure in the second circuit, which necessitates an intensive blow-through of this circuit.

For the purpose of determining the effect of pressure in the evaporator on changes in the fuel element temperature under transient conditions, we performed a series of experiments for different pressures in the second circuit. As a result, it was established that, with an increase in pressure in the evaporator, the maximum level of the fuel element temperature increases (Fig. 6) and the fuel element temperature jump decreases after the superheating regime has been attained (Fig. 7).

It should be noted that the rate of the power level rise hardly affects the time during which the sharp temperature rise occurs, i.e., the time of a single jump; however, it affects the number of these jumps: for power rise rates lower than a certain given rate, the fuel element temperature repeatedly increased and dropped, while, for high rates, only a single temperature change was observed (see Fig. 2).

The second method secures reliable SSC cooling during the transient process, since the entire transition takes place for the minimum reactor power level. However, as can be seen from Fig. 4. a sharp decrease in temperatures (due to a reduction in the reactor power level and pressure) and a subsequent increase in temperatures (due to an increase in the reactor power level) take place in this case.

The rate at which the reactor power level decreased and the subsequent pressure drop in the second circuit of the loop were determined with respect to the system heat capacity and the magnitude of thermal losses. It is obvious that systems with larger heat capacities make it possible to lower the pressure in the circuit and to reduce or raise the reactor power level at a lower rate, whereby the deficiency of this method – fast changes in the coolant and the metal structure temperature – is minimized.

The third method makes it possible to minimize the temperature jump. This was achieved by combining the first and the second method. The upward temperature jump was prevented by reducing the power level before the superheating regime was initiated; the downward temperature jump was reduced by lowering the power level to a lesser extent and by reducing the SSC blow-through time. As can be seen from Fig. 5, the transient process is more smooth if the third method is used.

In performing the above experiments, the feasibility of realizing a thermal layout with superheating the system directly in the reactor was verified for the first time. The absence of sharp changes in the SSC fuel element temperature under transient conditions when using the third method indicates that this method is technologically the most advanced and that it is acceptable for atomic power stations with medium and high steam parameter values. The relative simplicity of the first methodsuggests that it can be used for power stations with high steam pressure in the second circuit, since the jump in the SSC fuel element temperature will decrease with an increase in pressure.

However, it should be noted that an actual power station layout with an open second circuit will require certain modifications of the start-up methods developed for this loop.

The team of engineers headed by P. I. Aleshchenkov collaborated in solving the technical problems.

The entire atomic power station team contributed much to the experimental work.

The authors hereby express their gratitude to A. K. Krasin and A. N. Grigor'yants for their helpfulness and continued interest in the work.

LITERATURE CITED

1. N. A. Dollezhal', Atomnaya Énerg. 3, 11, 391 (1957).*
2. N. A. Dollezhal', et al., Atomnaya Énerg. 5, 3, 223 (1958).*
3. N. A. Dollezhal', et al., Transactions of the Second International Conference on the Peaceful Uses of Atomic Energy (Geneva, 1958) Reports by Soviet Scientists: Nuclear Reactors and Nuclear Power Engineering [in Russian] (Atomizdat, Moscow, 1959) Vol. 2, p. 15.

*Original Russian pagination. See C. B. translation.

0.04-4.0 Mev NEUTRON FISSION CROSS SECTION OF Pu^{240}

V. G. Nesterov and G. N. Smirenkin

Translated from Atomnaya Énergiya, Vol. 9, No. 7, pp. 16-20,
July, 1960
Original article submitted January 3, 1960

A detailed investigation of the Pu^{240} nucleus cross section is of interest with regard to an experimental verification of theoretical concepts of the energy dependence of fission probability as well as regarding possible uses of Pu^{240} as a nuclear fuel in fast neutron reactors.

We measured the energy dependence of the fast neutron fission cross section of Pu^{240} for neutrons with the energy E_n = 0.04-4.0 Mev. The $T(p, n)He^3$ reaction served as the neutron source. The Pu^{240} fission cross section in the plateau region (1-4 Mev) amounts to ~ 1.6 barn and is equal to only one-half of this value for the neutron energy $E_n \simeq 0.7$ Mev. A sharp decrease in the fission cross section value occurs as E_n decreases to 0.3 Mev; for a further decrease in E_n, the cross section value drops less sharply, and it remains practically constant (~ 0.065 barn) for $0.04 < E_n < 0.15$ Mev. The correlation between the irregularities in fission cross section values and the levels of Pu^{240} nuclei which correspond to inelastic scattering channels is discussed.

* * *

The energy dependence of the Pu^{240} fast neutron fission cross section is given in [1 and 2]. A number of Pu^{240} fission cross section values were also measured for Ra-Be sources and some photoneutron sources [3]. The data obtained in these papers on the fission cross section in the neutron energy region $E_n > 0.3$ Mev are in good agreement with each other, and they lie close to the same curve within limits of measurement error. However, for $E_n < 0.3$ Mev, the cross section values given in [1 and 2] do not agree. We have established earlier [1] that the steep drop in cross section values which is observed in the 1-0.3 Mev energy region changes into a flatter curve for smaller energy values. Data from [2] indicate that the sharp decrease in the Pu^{240} fission cross section values continues in the $E_n < 0.3$ Mev region.

The present paper is concerned with a more detailed study of the energy dependence of the Pu^{240} fission cross section and with obtaining more accurate data on this dependence for energies $E_n < 0.3$ Mev. A detailed investigation of the Pu^{240} nucleus fission cross section is of interest with regard to an experimental clarification of theoretical concepts of the energy dependence of fission probability as well as regarding the possibility of using Pu^{240} as a nuclear fuel in fast neutron reactors [4].

Experimental method. The ratio of the Pu^{240} fission cross section to the Pu^{239} fission cross section was measured experimentally. The measurements were performed by means of a double fission chamber where Pu^{240} and Pu^{239} layers ~ 0.2 mg/cm^2 thick were deposited on a common high-voltage electrode and therefore were exposed to equal neutron fluxes. By using a suitable electrode geometry, by filling the chamber with a mixture of argon (93%) and carbon dioxide (7%) under reduced pressure (~ 120 mm Hg) and by using broadhand amplifiers with a transmission band upper limit of 10 Mc, we succeeded in obtaining satisfactory counting responses for the chambers and in securing a reliable separation of fission fragments and multiple superpositions of α-particles. This made it possible to perform an almost 100%-recording of fission events and to eliminate the effect of the angular anisotropy of fragments.

A Pu^{239} layer weighing 4 mg had an admixture of Pu^{240} nuclei equal to $\alpha_0 = 1.80 \pm 0.05\%$, and the concentration of Pu^{239} nuclei in a Pu^{240} layer weighing 2.5 mg was 7.35 ± 0.15%. The content of Pu^{241} nuclei in the first layer was negligibly small, and it was less than 0.2% in the second layer.

The $T(p, n)He^3$ reaction, which was produced in a Van de Graff generator with the maximum energy of accelerated protons equal to 5 Mev, served as the source of monochromatic fast neutrons. The range of the neutron energies under investigation was covered by changing the proton energies and the angle between the proton beam direction and the chamber axis. For measurements in the $0.3 < E_n < 4$ Mev region, the plutonium layer was perpendicular to the proton beam (the maximum angle between the chamber axis and the neutron direction of incidence to the layer was 20°).

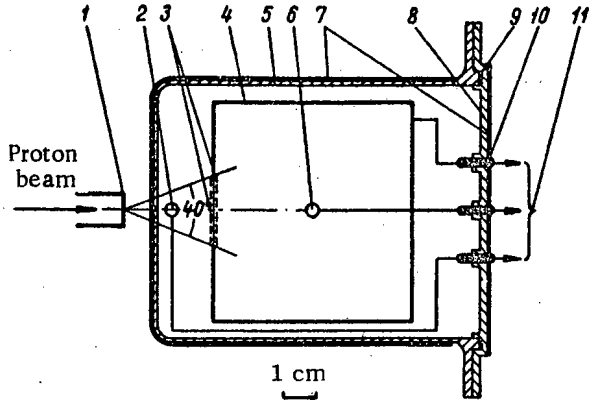

Fig. 1. Experimental arrangement and the double fission chamber for 0° angle measurements. 1) Target; 2) chamber collecting electrode with Pu^{239}; 3) Pu^{239} and Pu^{240} layers; 4) common high-voltage electrode; 5) chamber lid; 6) chamber collecting electrode with Pu^{240}; 7) cadmium casing; 8) chamber bottom; 9) rubber gasket; 10) teflon insulator; 11) electric lead-outs.

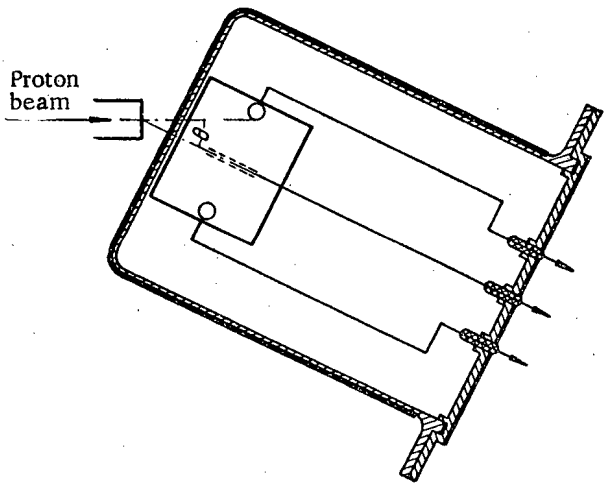

Fig. 2. Experimental arrangement for measurements at angles from 30 to 75°.

The design of the double fission chamber which we used and the experimental arrangement are shown in Fig. 1. A hard tritium target on a molybdenum base layer 0.2 mm thick was used in these experiments (the proton energy loss was 25 kev). In measurements in the $E_n < 0.3$ Mev region, in order to improve the angular and the energy resolution, the layers of fissionable substances were placed in a plane which coincided with the direction of neutrons outgoing to the proton beam under the angle θ (from 30 to 75°), as is shown in Fig. 2. A target with an energy loss of 45 kev was used in these experiments. The angular scattering of neutrons causing fission in the layers did not exceed 5°. During the measurements, the fission chamber was enclosed on all sides by means of a cadmium casing, which had a thickness of 0.5 mm.

The value of N_{40}/N_{39} – the ratio of fission events in the Pu^{240} and Pu^{239} layers – was measured for the given energy region. In order to determine the ratio of the effective quantities of fissionable substances in both chamber halves, we measured the ratio of fission intensities N_{40}^T/N_{39}^T in a flux of thermal neutrons, which were obtained by moderating fast neutrons in a paraffin block. The respective contributions of resonance neutrons and fast neutrons which passed through the paraffin were eliminated by the method of the cadmium difference. The mass-spectrometry analysis results available to us made it possible to determine α – the ratio of the number of Pu^{240} nuclei to the number of Pu^{239} nuclei in the Pu^{240} specimen, which enters directly the equation for calculating the fission cross section – only with an accuracy of ~ 10%. The value of α and the above value of the concentration of Pu^{239} nuclei in the Pu^{240} layer were determined by comparing the intensities of spontaneous fission and fission due to thermal neutrons in both chamber halves. As a result of numerous measurements, the value $C = \alpha/\alpha_0 = 675 \pm 15$ was found. The ratio of the number of Pu^{240} nuclei to the number of Pu^{239} nuclei in the Pu^{239} specimen was measured earlier by using several independent methods. The Pu^{240} fission cross section can be expressed in terms of the experimentally determined quantities by the following equation:

$$\sigma_{40} = \sigma_{39} \frac{A-1}{\alpha_0 (C-A)}, \text{ where } A = \frac{N_{40}}{N_{39}} \frac{N_{39}^T}{N_{40}^T}.$$

In this equation, the Pu^{240} thermal neutron fission cross section was assumed to be equal to zero (as in [5]). If we take into account the presence of Pu^{241} nuclei in the specimens used, a small correction, which is reduced from 3 to 0.2% as E_n increases from 0.1 to 1 Mev, can be introduced into the Pu^{240} fission cross section. The energy dependence of the Pu^{239} fission cross section which was used for calculating the absolute value of the energy dependence of the Pu^{240} fission cross section, was obtained by averaging the data from [2 and 6].

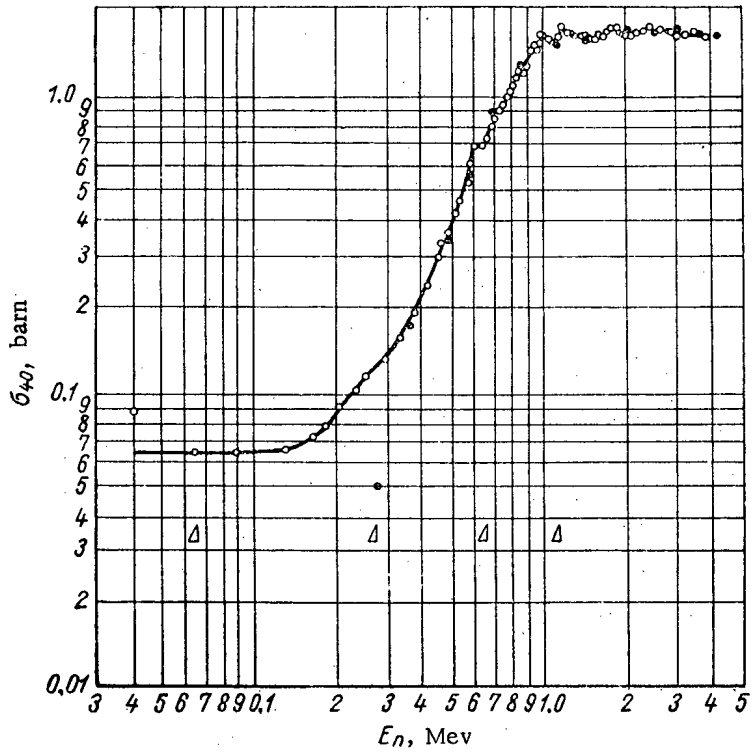

Fig. 3. Energy dependence of the Pu^{240} fission cross section in the E_n = 0.04-4 Mev region. O) Data given in the present paper; ●) data from [2].

Measurement Results and Their Discussion. The energy dependence of the Pu^{240} fission cross section, obtained by averaging the results of several measurement series, is shown in Figs. 3 and 4. The errors in determining the σ_{40}/σ_{39} ratio, which are shown in Fig. 4, are mainly determined by the statistical accuracy of the A, α_0, and C values and are equal to ~4% in the plateau region (1-4 Mev); in the region of the sharp drop in the Pu^{240} fission cross section values (0.3-1 Mev), the error amounts to ~5-10%, and, for E_n < 0.3 Mev, the error is equal to 10-20%. In the E_n < 0.3 Mev region, the main contribution to the final error in measuring σ_{40}/σ_{39} is due to the error connected with the subtraction of a large number of spontaneous Pu^{240} fission events (~0.5 fission/sec), which amounts to 50-80% of the total number of recorded fissions. The root-mean-square error in counting the number of spontaneous fission events in the Pu^{240} layer in the course of prolonged measurements did not exceed 2%. The energy resolution Δ (i.e., the width of the energy distribution of fission-producing neutrons, at the distribution half-height) was determined by the target thickness and the magnitude of the solid angle used in irradiation. The value of Δ indicated in Fig. 3 increases from 15 to 35 kev as the neutron energy increases. The background due to neutrons scattered in the target and the chamber did not exceed 1.5% in the 0° angle experiments and 5% in measurements performed for different angles. Considering the inaccuracy (5%) of the Pu^{239} fission cross section, the Pu^{240} fission cross section in the plateau region is equal to 1.65 ± 0.1 barn; it drops sharply for E_n < 1 Mev, and is reduced to one-half of this value for $E_n \simeq 0.7$ Mev. The sharp drop in the Pu^{240} fission cross section value continues down to $E_n \simeq 0.3$ Mev, after which the cross section value decreases less sharply until $E_n \simeq 0.15$ Mev is reached, where it is equal to 0.065 ± 0.02 barn; thereafter it remains practically constant for energy values as low as E_n = 0.04 Mev. The relatively small variation of the Pu^{240} fission cross section for E_n < 0.3 Mev does not agree with data from [2] and the prevalent concepts of the exponential variation of fission

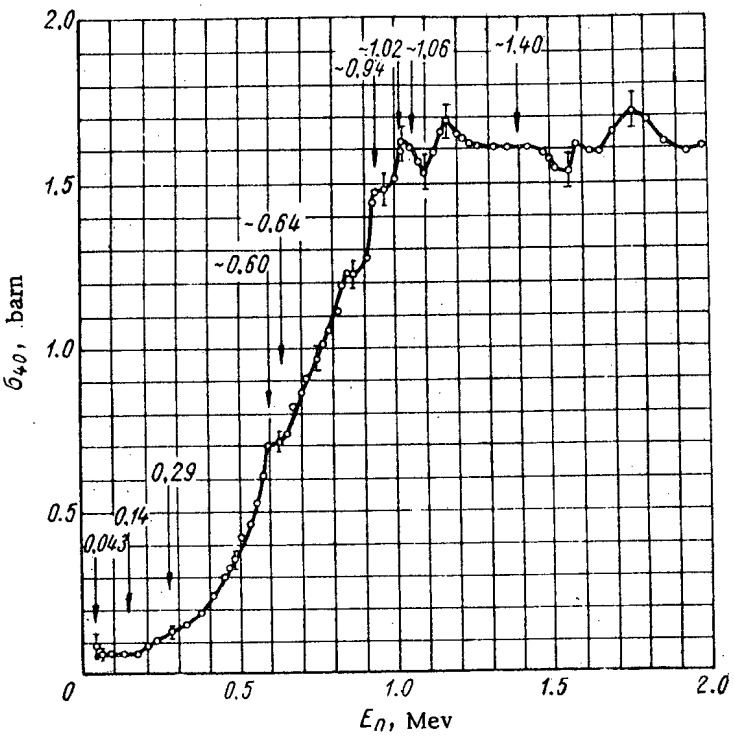

Fig. 4. Energy dependence of the Pu^{240} fission cross section in the E_n = 0.04-2 Mev region. The arrows indicate the position of known levels of Pu^{240} nuclei [9].

probability near the threshold. From among the factors which could cause this effect, we considered Pu^{240} fission by epicadmium neutrons and photofission by γ-rays with an energy of ~20 Mev, which are emitted in the $T(p, \gamma)He^4$ reaction (it was shown that the contribution of both these processes to the measured Pu^{240} fission cross section value is negligibly small). Differences between the distribution of Pu^{240} fission and Np^{237} fission along the radius of the BR-1 reactor with a uranium reflector [4] (Fig. 5) also indicate the correctness of the results obtained in the present paper. Pu^{240} and Np^{237} cross sections [2 and 7] almost coincide in the $E_n > 0.3$ Mev region. The increasing divergence between the curves in Fig. 5 as the distance from the reactor center increases and the softening of the neutron spectrum are apparently due to the difference between the Pu^{240} and Np^{237} fission cross section values for small E_n.

A number of irregularities characteristic of the fission cross section values of all even-even isotopes having the threshold in the region of positive E_n values is observed in the energy dependence of the Pu^{240} fission cross section. As was shown in [8], the effects consisting of a slowdown in the rise of fission cross section values in the threshold region and of dips at the initial plateau portion are explained by the opening of inelastic scattering channels, or, in other words, by the concurrence of fission and neutron widths. According to this view, the positions of the peculiarities on the Pu^{240} fission cross section curve under discussion must correspond to the levels of the target-nuclei with small spin values. It is obvious from Fig. 4 that the irregularities in the measured energy dependence of the Pu^{240} fission cross section are correlated with the position of the known levels of Pu^{240} nuclei (data from [9]): ~0.6 Mev (1^-), ~0.64 Mev (3^-), ~0.940 Mev (0^+), ~1.02 Mev (2^+), ~1.06 Mev (3^+), and ~1.4 Mev (1^-). Apart from these E_n values, there is a step in the Pu^{240} fission cross section curve in the $E_n \simeq$ $\simeq$ 0.8-0.9 Mev region. As follows from Fig. 4, the relative measurement accuracy secured in these experiments allows us positively to affirm the presence of the above particularities on the Pu^{240} fission cross section curve. Measurements of the relative Pu^{239} fission cross section values, performed by means of an all-wave fast neutron monitor, indicate that the irregularities observed in the Pu^{240} fission cross section values cannot be caused by similar effects in the energy dependence of the Pu^{239} fission cross section values.

One of the possible explanations of the behavior of the Pu^{240} fission cross section values for $E_n < 0.3$ Mev is the assumption that the Pu^{240} fission threshold lies below 40 kev, and that the constancy of the Pu^{240} fission cross section values in the $0.04 < E_n < 0.3$ Mev region and the relatively slow rise of these values in the $0.15 <$ $< E_n < 0.3$ Mev interval are caused by the concurrence of inelastic scattering of the 43 kev (2^+) and 142 kev (4^+)

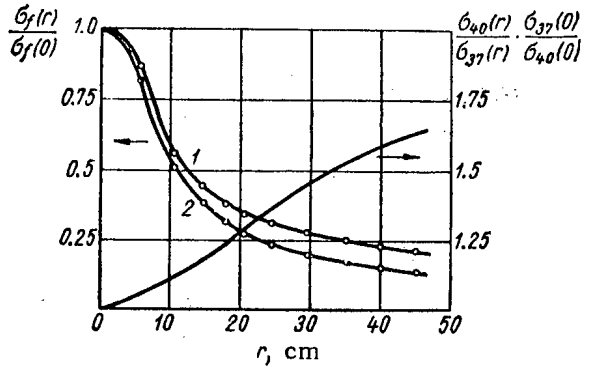

Fig. 5. Ratio of the Pu^{240} (curve 1) and the Np^{237} (curve 2) fission cross section values to the Pu^{239} fission cross section in dependence on the distance from the reactor BR-1 center. The values of the ratios at the core center are assumed to be equal to unity. $\frac{\sigma_{40}(r)}{\sigma_{37}(r)} \cdot \frac{\sigma_{37}(0)}{\sigma_{40}(0)}$ is the ratio of the Pu^{240} fission cross section to the Np^{237} fission cross section reduced to the fission cross section at the reactor center.

energy levels [9]. On the basis of the example of U^{238} nuclei [10], where, for small E_n, inelastic scattering mainly occurs at these levels, it could be naturally assumed that, also in the case of Pu^{240} nucleus scattering, these levels can considerably affect the Pu^{240} fission cross section values in this E_n region. Neither does the observed effect contradict the possibility of fission through two channels, one of which has a threshold of $E_n \simeq 0.6$-0.7 Mev, and the other apparently opening at considerably lower E_n values or, generally, in the $E_n < 0$ region. It should also be noted that the sharp drop in the fission cross section values for lower E_n values is not only peculiar to Pu^{240} nuclei. A similar tendency is observed in the case of U^{234} nuclei and, to a lesser extent, U^{236} nuclei [2]. The constancy of Np^{237} fission cross section values ($\sim$ 20 mbarn) for $E_n < 0.2$ Mev was also observed in [7].

The authors extend their heartfelt thanks to A. I. Leipunskii and I. I. Bondarenko for their helpfulness and interest in the work, to L. N. Usachev for the discussion of the results, to Yu. I. Baranov and N. E. Tokmantseva for their help in measurements, and to V. A. Romanov, G. A. Strigin, and Yu. I. Parfenov, who kept the accelerator in good running order.

LITERATURE CITED

1. V. G. Nesterov and G. N. Smirenkin, Zhur. Éksp. i Teoret. Fiz. 35, 533 (1958).
2. D. Hughes, and R. Schwartz, Neutron Cross Sections, BNL-4 (1958).
3. G. A. Dorofeev and Yu. P. Dobrynin, Atomnaya Énerg. 2, 1, 10 (1957).*
4. A. I. Leipunskii, et al., Transactions of the Second International Conference on the Peaceful Uses of Atomic Energy (Geneva, 1958) Reports by Soviet Scientists: Nuclear Reactors and Nuclear Power Engineering [in Russian] (Atomizdat, Moscow, 1959) Vol. 2, p. 377.
5. C. Bigham, Canad. J. Phys. 36, 503 (1958).
6. A. Hemmendinger, Transactions of the Second International Conference on the Peaceful Uses of Atomic Energy (Geneva, 1958) Selected reports by scientists from abroad: Neutron Physics [Russian translation] (Atomizdat, Moscow, 1959) Vol. 2, p. 89.
7. B. M. Gokhberg, G. A. Otroshchenko, and V. A. Shigin, Doklady Akad. Nauk SSSR 128, 1157 (1959).
8. J. Wiler, Atomnaya Énerg. 5, 71 (1956).*
9. B. S. Dzhelepov and L. K. Peker, Modes of Decay of Radioactive Nuclei [in Russian] (Izd. AN SSSR, Moscow, 1958) p. 739.
10. L. Cranberg and J. Levin, Phys. Rev. 109, 2063 (1958).

*Original Russian pagination. See C. B. translation.

THE USE OF THE ISOTOPIC COMPOSITION OF LEAD FOR PROSPECTING URANIUM ORES

D. Ya. Surazhskii and A. I. Tugarinov

Translated from Atomnaya Énergiya, Vol. 9, No. 7, pp. 21-26, July, 1960
Original article submitted December 17, 1959

The article examines the probable causes of the appearance of anomalous leads and the possibility of the use of isotopic anomalies in leads for prospecting uranium deposits. It is assumed that the apperance of leads with an unusually high content of radiogenic isotopes (Pb^{207}, Pb^{206}) is due to the following geological processes: 1) the rapid accumulation of young sediments as a result of the intense erosion of ancient uranium deposits; 2) the assimilation by magma and deep-seated granitization of uranium-bearing rocks which appeared long before magmatism; 3) hydrothermal metamorphism of uranium ore bodies; 4) supergenesis in the oxidation zone of uranium deposits.

* * *

The lead of the earth's crust consists of four isotopes: Pb^{204}, Pb^{206}, Pb^{207}, Pb^{208}. The isotopes Pb^{206}, Pb^{207}, and Pb^{208} are the end products of nuclear reactions in the series U^{238}, U^{235}, and Th^{232}, respectively; Pb^{204} does not have radioactive precursors.

The radioactive decay of uranium and thorium contained in rocks leads to a continuous increase in the content of radiogenic lead in the earth's crust, whereas, the Pb^{204} content probably remains the same as at the moment of formation of the earth.* For this reason, the evolution of the isotopic composition of natural lead is usually expressed by the continually increasing ratios Pb^{206}/Pb^{204}, Pb^{207}/Pb^{204}, and Pb^{208}/Pb^{204} [1].

The enrichment of primary lead with radiogenic isotopes takes place until all the lead, both primary and secondary, has separated from the enriched magmas or parent rocks, forming lead ore deposits practically free from radioative elements. In such cases the isotopic composition of lead remains the same as it was during the period of ore formation.

The relative abundance of various lead isotopes in the earth's crust is mainly a function of time and the associated relationships usually employed for determining the absolute age by the lead-lead method:

$$\frac{Pb^{206}}{Pb^{204}} = 19.04 - 12.15\,(e^{0,154t-1}); \quad (1)$$

$$\frac{Pb^{207}}{Pb^{204}} = 15.69 - 0.089\,(e^{0,972t-1}); \quad (2)$$

$$\frac{Pb^{208}}{Pb^{204}} = 39.00 - 46.48\,(e^{0,0499t-1}), \quad (3)$$

where t is the age of the mineral in 10^9 years; 19.04, 15.69, and 39.00 are the Pb^{206}/Pb^{204}, Pb^{207}/Pb^{204} Pb^{208}/Pb^{204} ratios in the lead of recent muds of the Pacific Ocean; 12.15, 0.089, and 46.48 are coefficients calculated on the basis of the clarkes accepted at present: $U^{238} - 3 \cdot 10^{-4}\%$, $U^{235}/U^{238} = 1/138$, Th/U = 3.7, Pb – $1.6 \cdot 10^{-3}\%$; $0.154 \cdot 10^{-9}$ years – 1; $0.972 \cdot 10^{-9}$ years – 1; $0.0499 \cdot 10^{-9} - 1$ are the decay constants of U^{238}, U^{235}, and Th^{232}, respectively.

*If it is assumed that there is not a substantial introduction of nonradiogenic lead from extraterrestrial sources or the depths of the Earth.

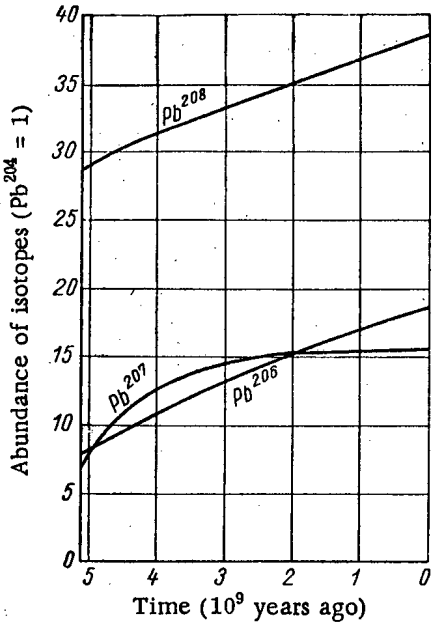

Fig. 1. Abundance of lead isotopes (Pb^{204} = 1), represented as a function of time [9].

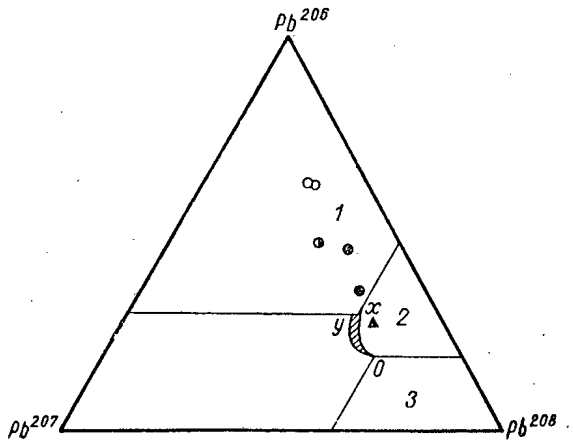

Fig. 2. Diagram of the isotopic ratios of lead: Oxy) field, characterizing ordinary lead; 1) field, characterizing anomalous leads from a region of uranium deposits; 2) field, characterizing anomalous leads from a region of thorium deposits; 3) field, characterizing anomalous leads from a region of uranium-thorium deposits. ○) Colorado; ◑) Witwatersrand; ●) Blind River; ▲) Sudbury [14].

The changes in the Pb^{206}/Pb^{204}, Pb^{207}/Pb^{204}, and Pb^{208}/Pb^{204} ratios during the course of geological time are shown in Fig. 1.

Naturally, in the case of serious deviations of the uranium, thorium, and lead contents in the parent rocks or magmas, with which the lead ores are associated, from the mean contents of these elements in the earth's crust, lead with an isotopic composition different from the mean lead content characteristic of the given epoch may appear [2]. This is clearly evident, for example, from a comparison of the isotopic ratios in the lead of ore occurrences associated with the trappean formation of the Siberian Platform [3,4] and formed at the end of the Paleozoic – beginning of the Mesozoic (Table 1), with isotopic ratios in the lead of ore occurrence genetically associated with Upper Variscian granitoids of Saxony, the North Caucasus, the Ukraine, and Central Asia [5-8] (Table 2).

Lead, the isotopic composition of which corresponds roughly to the age of the ores, is called normal or ordinary lead. Lead which contains a considerable excess of radiogenic isotopes compared with the normal proportion is called anomalous lead. It is found primarily in regions of uranium deposits [9] (Table 3). Its occurrence is generally associated with an abnormally high uranium content in the enriched magma or parent rock. The causes of such anomalies are not always clear. Analysis of data on this problem shows that the following geological processes may assist the appearance of anomalous leads:

1. The formation of deposits in a lead mineralization of sedimentary origin in regions of intense denudation of previously formed uranium deposits. Anomalies of the isotopic composition of lead will be more marked the more intense is the process of denudation, the greater is the difference in age between erosion and redeposition and the more limited is the region of accumulation (coastal zone, intermontane depression, etc.).

Excellent examples of distinct anomalies of this type are found in regions of Central Asia [8] where the Pre-Jurassic deposits are characterized by lead of normal isotopic composition, and the Post-Jurassic deposits, i.e., formed in the period of intense erosion of Variscian uranium and thorium deposits, by lead of anomalous composition with a marked increase in the content of Pb^{206} and Pb^{208} (Table 4).

Rejuvenation of such an anomalous lead, accumulated during sedimentation, may lead to the formation of vein and metasomatic deposits of the Missouri type with anomalous lead.

TABLE 1

Isotopic Composition of Lead of Ore Occurrences Associated with the Trappean Formation of the Siberian Platform (from data of A. P. Vinogradov, G. G. Moor, S. I. Zykov, and L. S. Tarasov [3, 4])

Sampling site	Sample	Isotopic composition of lead		
		$\frac{Pb^{206}}{Pb^{204}}$	$\frac{Pb^{207}}{Pb^{204}}$	$\frac{Pb^{208}}{Pb^{204}}$
Norilsk deposit	Lead from chalcopyrite	17.81	15.24	37.54
The same	Lead from platinum	17.90	15.29	37.53
The same	Lead from galena	17.88	15.27	37.50
Lake Taimyr	Galena	17.84	15.03	37.07
Region of Taimyr	The same	17.96	15.38	37.87
Stony Tunguska River	Galena veins in Silurian limestones	17.97	15.35	37.72
Kotui River	Galena in minor intrusions of syenites	17.98	15.36	37.65
Mean of seven determinations		17.90	15.27	37.55
Isotopic composition of the lead of the earth's crust 200 million years ago		18.66	15.67	38.54

2. Assimilation by magma and deep-seated granitization of deposits with an increased uranium content. In cases where the magma assimilates uranium-bearing deposits which have appeared shortly before the commencement of magmatic activity, for example, during rapid and fairly deep submersion of the deposits in a geosynclinal zone, the appearance of anomalous leads soon after this inversion is not very probable. This is natural, because during the brief interval between the formation of sedimentary rocks and the occurrence of intrusive activity appreciable amounts of uranium lead could not be accumulated in the sedimentary series. Examples of provinces in which magmatic assimilation of sediments of similar age occurred are, in particular, Saxony and the North Caucasus (see Table 2).

TABLE 2

Isotopic Composition of the Lead of Ore Occurrences of Upper Triassic Age, Associated with Granitoids of Saxony, the North Caucasus, the Ukraine and Central Asia (according to the data of A. P. Vinogradov, A. I. Tugarinov, S. I. Zykov and others [5-8])

Province	Isotopic composition of the lead		
	$\frac{Pb^{206}}{Pb^{204}}$	$\frac{Pb^{207}}{Pb^{204}}$	$\frac{Pb^{208}}{Pb^{204}}$
Saxony (mean of seven determinations)	18.24	15.26	37.12
North Caucasus (mean of five determinations)	18.01	15.22	37.25
Ukraine (mean of three determinations)	18.48	15.92	39.22
Central Asia (mean of nine determinations)	18.52	15.93	38.75
Isotopic composition of the lead of the earth's crust 250 million years ago	18.50	15.66	38.40

In the case of assimilation of magma or the granitization of an ancient sedimentary series with an unusually high content of radioactive elements, formed considerably earlier than the intrusive bodies, the appearance of anomalous leads in galenas accompanying the uranium ores must be considered highly probable. In this case,

TABLE 3

Isotopic Composition of the Lead of Galenas from Certain Uranium Deposits [9]

Deposit	Isotopic composition of the lead		
	$\frac{Pb^{206}}{Pb^{204}}$	$\frac{Pb^{207}}{Pb^{204}}$	$\frac{Pb^{208}}{Pb^{204}}$
Happy Jack Mine, Colorado	92.62	20.12	37.77
Monument No. 2, Colorado	88.81	18.75	36.36
Witwatersrand, Union of South Africa	58.94	24.10	40.19
Algom, Blind River, Canada	34.00	15.08	44.26
The same	59.48	18.61	52.49
Sudbury, Ontario, Canada	26.00	16.94	52.21

the Pb^{207} anomaly will be greater the older is the series of deposits subjected to assimilation by the magma and the higher is its uranium content. Anomalies of such type are noted, in particular, in Variscian lead deposits in the Ukraine and in Central Asia, characterized by a higher Pb^{207} and Pb^{208} content than in Saxony and the North Caucasus. It may be assumed that this phenomenon is linked with the substantial participation of the Precambrian foundation, composed of crystalline rocks with a higher content of radioactive elements in the formation of the lead ores. Certain American investigators [10] formed a similar conclusion with regard to the causes of the appearance of anomalous lead in nonradioactive minerals in the Colorado Plateau.

TABLE 4

Isotopic Composition of Lead of Central Asian Polymetallic Deposits [1, 8]

Type of deposits	Isotopic composition of the lead		
	Pb^{206}	Pb^{207}	Pb^{208}
Stratiform deposits in Devonian and carboniferrous limestones (mean of 11 determinations)	17.52	15.31	37.76
Hercynian skarn and vein deposits	18.52	15.93	38.75
Disseminated and stratiform deposits in Cretaceous limestones	19.55	16.17	39.79

3. Hydrothermal metamorphism of ancient uranium deposits with isolation of radiogenic lead and uranium and the deposition of these elements in situ in the form of regenerated pitchblende and secondary galena [11]. In some cases uranium and radiogenic lead are transferred beyond the limits of the primary deposit [12], with the formation of a characteristic zonality in the aureole around the ore. Galenas consisting only of radiogenic lead are found in the direct vicinity of ore bodies. At a distance of several meters the galenas already contain about 10% of ordinary lead. At distances of the order of hundreds of meters the galenas contain only ordinary lead (Table 5).

Anomalous lead of such origin may undoubtedly be considered as an indicator that uranium deposits are located at a comparatively short distance. It must be borne in mind, however, that such anomalies may also arise during the process of redeposition of lead ores in cases where this redeposition is caused by solutions which have appropriated radiogenic lead from uranium-bearing rocks. Such anomalies are characteristic for many ore regions. They occur most clearly in the Sander Bay deposits (Ontario, Canada). The results of investigations [13] make it possible to divide the lead of this region into two groups. One group includes lead from galenas in rocks of Keewatin age, with a more or less constant isotopic composition corresponding fairly accurately to the epoch of formation of the ores (of the order of $2 \cdot 10^{-9}$ years). The second group, associated with deposits of the Grenville formation, is characterized by extremely varied and markedly anomalous isotopic ratios. It may be

assumed that this lead is the result of the mixing of two different leads: ordinary (Keewatin) and radiogenic with a Pb^{208}/Pb^{206} ratio = 0.37 and a Pb^{207}/Pb^{206} ratio = 0.185.

Employing the value of the first ratio (Pb^{208}/Pb^{206}), it can be calculated that the ratio of thorium to uranium in rocks from which lead of such composition was extracted must be 1.4. The value of the second ratio (Pb^{207}/Pb^{206}) shows that the age of these rocks – assumed to be the source of the lead – may vary from 2740 ± 40 to 1700 ± 30 million years [13].

As may be seen from Table 6, lead of the Sander Bay deposit contains 14-36% radiogenic lead, which was probably formed in the surrounding rocks and transported from them by hydrothermal solutions which redeposited the lead ores.

TABLE 5

Isotopic Composition of Lead of Galenas of a Uranium Deposit [12]

Sampling site	Isotopic composition of lead			
	Pb^{204}	Pb^{206}	Pb^{207}	Pb^{208}
Directly from the ore deposit	0.02	100.00	13.04	0.58
10 m from the ore deposit from the tectonic zone cut by it	0.50	100.00	22.22	18.88
100 m from the ore deposit	1.00	16.86	15.86	37.00

Under such conditions, mobilization and concentration of the originally dispersed uranium may also take place, with the formation of true uranium ore deposits.

4. Processes of supergenesis in the oxidation zone of uranium deposits. In regions with a humid climate, the uranium in the oxidation zone is generally completely leached. In such cases, the prospects of uranium yield in a primary ore zone can be assessed from the results of an isotopic analysis of lead from relatively stable se-

TABLE 6

Isotopic Composition of Lead of Galenas of Ore Occurrences of the Sander Bay and Keewatin Regions in Canada

Sampling site	Isotopic composition of the lead		
	$\frac{Pb^{206}}{Pb^{204}}$	$\frac{Pb^{207}}{Pb^{204}}$	$\frac{Pb^{208}}{Pb^{204}}$
Galenas from ore occurrences present in rocks of Keewatin age	13.66	14.78	33.46
	13.74	14.61	33.20
	13.80	14.69	33.37
	13.37	14.59	33.38
	13.32	14.54	33.16
Galenas from ore occurrences of the Sander Bay type	18.19	15.81	37.78
	18.32	15.89	37.14
	18.55	15.95	37.82
	20.72	16.40	38.28
	30.05	18.26	41.17
	30.65	18.10	41.45
	30.71	18.21	41.23
	33.88	18.69	43.98

condary lead minerals of the wulfenite or cerussite type. Under these conditions an increased content of radiogenic isotopes can be considered as an indication of the probability of finding uranium minerals at depth. Anomalous lead of this type can be accumulated in soils above uranium deposits and particularly in argillaceous formations of the sedimentary mantle.

All the above leads to the conclusion that investigations of the variations of the isotopic composition of lead in specific geological conditions may be very useful during the prospecting of blind uranium deposits and when an assessment is made of the uranium reserves of particular geological regions. The results of such work are best interpreted with respect to the Pb^{206}: Pb^{207}: Pb^{208} ratios as a sum taken as 100%, i.e., deducting Pb^{204}, the accuracy of the determination of which is very low at present.

It was established that in a radiogenic component of ordinary lead from nonradioactive deposits these ratios vary within very narrow limits. The narrow sickle-shaped figure 0xy in the triangular diagram of Fig. 2, compiled from the results of a large number of analyses, gives an idea of them [14]. The position of this figure is corroborated by theoretical calculations of the isotopic evolution of a certain "primordial" lead* during geological time in regions of the earth's crust with a low clarke content of uranium and thorium.

Lead from nonradioactive minerals in uranium-bearing areas is characterized by completely different isotopic ratios. In such cases the results of analyses plotted on the three-component diagram of Fig. 2 transgress far beyond the limits of the sickle-shaped figure of ordinary lead. The Pb^{207}: Pb^{206} ratio remains almost constant for the same region, while for different regions it varies as a function of the age of the ores.

The progress of present-day analytical methods makes it possible to determine the isotopic ratios in leads from minerals other than lead, such as iron and copper sulfides, etc., in which, as was correctly noted in [14], the degree of dilution of radiogenic lead by ordinary lead is much less than in galenas.

Many important questions relating to the problem of the use of the isotopic ratios in lead for the practical aims of uranium ore prospecting are not yet clarified but the possibility of such utilization is, in general, quite clear.

LITERATURE CITED

1. A. P. Vinogradov, Izvest. Akad. Nauk SSSR, Ser. Geol., 3, 3 (1954).
2. A. I. Tugarinov, Izvest. Akad. Nauk SSSR, Ser. Geol., 4, 31 (1955).
3. G. G. Moor and S. I. Zykov, Doklady Akad. Nauk SSSR 24, 1, 168 (1959).
4. A. P. Vinogradov, S. I. Zykov, and L. S. Tarasov, Geokhimiya, 6, 515 (1958).
5. A. Winogradow, et al., Freiberger Forschungsh., 57, 73 (1959).
6. A. I. Tugarinov, S. I. Zykov, and A. V. Zmeenkova, Proceedings of Fifth Session of the Committee for the Determination of the Absolute Age of Geological Formations [in Russian] (Gosgeoltekhizdat, Moscow, 1958) p. 64.
7. A. I. Tugarinov and S. I. Zykov, Geokhimiya 3, 42 (1956).
8. A. I. Tugarinov, Report: Geochemical Prospecting of Ore Deposits in the USSR [in Russian](Gosgeoltekhizdat, Moscow, 1957) p. 79.
9. Nuclear Geology. Ed., T. Fowler [Russian translation] (Il, Moscow, 1958).
10. L. Stieff, T. Stern, and R. Milkey, U. S. Geol. Surv. Circ., 271, 19 (1953).
11. W. Eckelman and L. Kulp, Geol. Soc. Am. Bull. 68, 1117 (1957).
12. A. I. Tugarinov, Report: Problems of Geology and Mineralogy [in Russian] (Izd. AN SSSR, Moscow, 1956) p. 94.
13. R. Farquhar and R. Russel, Trans. Am. Geophys. Union 38, 4, 552 (1957).
14. R. Cannon, L. Stieff, and T. Stern, Proceedings of the Second International Conference on the Peaceful Uses of Atomic Energy (Geneva, 1958) Selected Reports of Foreign Scientists. The Geology of Atomic Raw Material [Russian translation] (Atomizdat, Moscow, 1959) Vol. 8, p. 31.

* With an isotopic composition similar to the composition of the lead of meteorites.

INTERNAL FRICTION IN URANIUM

A. I. Dashkovskii, A. I. Evstyukhin, E. M. Savitskii,

and D. M. Skorov

Translated from Atomnaya Énergiya, Vol. 9, No. 7, pp. 27-32,
July, 1960
Original article submitted October 3, 1959

Studies have been made of the temperature dependence of internal friction and the shear modulus in uranium. The internal friction in α uranium depends on the heat treatment and is reduced after annealing in the β and γ regions. During polymorphous transformations the internal friction changes its value isothermally. The transitions $\alpha \rightarrow \beta$ and $\gamma \rightarrow \beta$ are accompanied by a reduction in the internal friction and $\beta \rightarrow \gamma$ and $\beta \rightarrow \alpha$ by an increase in the internal friction. Each polymorphous modification of uranium in the temperature ranges for its existence has its own value of internal friction.

* * *

The measurements were made by recording the damping of free torsional vibrations of the specimen on a relaxation type apparatus. The specimens were uranium wires of 99.9% purity, diameter 0.98 mm, and length 320 mm. The measurements were made at frequencies of about 2 vibrations per second in a vacuum of about $5 \cdot 10^{-5}$ mm Hg. The rates of heating and cooling were varied from 5 to 0.5 deg/min. The accuracy in measuring the temperature was ± 1.5°C. The shear modulus was determined at the same time as the internal friction.

It is well known that there are three polymorphous modifications of uranium: α uranium (with a rhombic lattice), β uranium (with a tetragonal lattice) and γ uranium (with a volume-centered cubic lattice). The temperature of the $\alpha \rightarrow \beta$ transition is 662°C, and the $\beta \rightarrow \gamma$ transition 769°C [1].

Figure 1 shows the change in the internal friction of α uranium from room temperature to 630°C. Cold drawn specimens having sharply defined texture of deformation were annealed at various temperatures. Curve 1 shows the behavior of specimens annealed for 30 min at 630°C. These specimens have a readily reproducible picture for the relationship between internal friction and temperature, except for the section from room temperature to 200-250°C, where the internal friction depends to a large extent on the conditions under which the specimen is cooled after annealing. Thus, on some specimens peaks were observed at a temperature of 100°C, reaching a value of 0.1 (curve 5, Fig. 1); however, their height depended to a large extent on the conditions of cooling.

In some cases much lower peaks were formed in the temperature range 180-200°C. It was noted that these low temperature peaks of internal friction were detected in cases where very small stresses were induced during cooling after annealing. We did not make a detailed study of the factors affecting the appearance and size of the peaks; it is possible that they are the same as those which cause a considerable increase in the tensile strength with simultaneous drop in the yield point in this temperature range [2].

The change in internal friction in uranium from room temperature to 350°C occurs almost linearly, and the same is observed for the shear modulus. Above 350°C the internal friction rapidly increases and the shear modulus falls rapidly; in both cases, the change is no longer linear. For most pure metals [3] at the recrystallization temperatures there is a inflection on the internal friction curve, in the case of uranium at 450-500°C.

There was no noticeable change in the value of internal friction and the shear modulus during repeated heating to 630°C and cooling to room temperature (5 cycles). The effect mentioned in [4-6] of the cyclic heat treatment of uranium in the α region was not observed under these conditions. The reason for this was the low

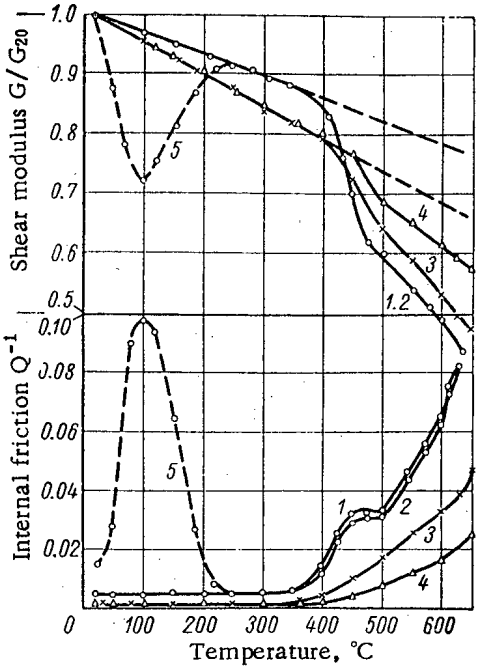

Fig. 1. The temperature dependence of internal friction (bottom) and shear modulus (top) of α uranium (the shear modulus is given in the form of the ratio to its value at a temperature of 20°C): 1) after annealing at 630°C for 30 min; 2) the same, during cooling; 3) after annealing in the β region at 720°C for 30 min; 4) after annealing in the γ region at 960°C for 30 min; 5) after annealing in the γ region and cooling in the stressed state.

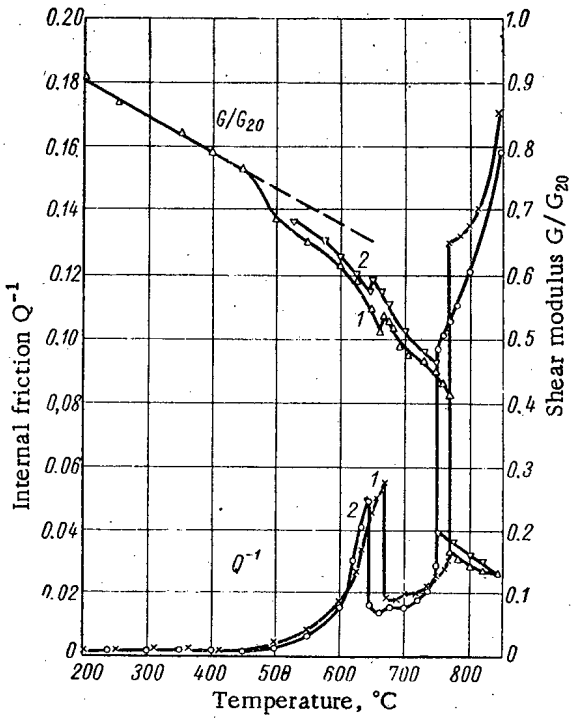

Fig. 2. Temperature dependence of internal friction (bottom) and shear modulus (top) of uranium (up to 850°C): 1) heating curve; 2) cooling curve.

rate of heating and especially cooling obtaining in these experiments since the effect of cyclic heat treatment increases considerably with increase in the rate of cooling [4, 5]. It is also possible that the number of cycles was insufficient. In all cases, the cooling curve passed somewhat below the heating curve in the region of high temperatures (curve 2, Fig. 1).

Annealing in the β region (at 720°C for 30 min) leads to a considerable reduction in the internal friction in α uranium (curve 3, Fig. 1) and to the disappearance of the inflection on the curve in the temperature range 450-500°C. The linearity of the change in internal friction and shear modulus is then maintained to 400°C. The modulus for the linear part passes lower, and after 450°C, higher, than for specimens annealed in the α region. Since the inflection on the curve of internal friction of pure metals in the region of recrystallization temperatures is usually connected with relaxation of stresses at the grain boundaries, it can be assumed that the disappearance of this inflection for uranium is due to reduction in the mobility of the grain boundaries due to annealing in the β region.

The viscous behavior of the grain boundaries in α uranium also explains the sharp change in the shear modulus in relation to the temperature. It has been found theoretically [7] that the maximum for shear relaxation is determined by the expression

$$1 - \frac{G_p}{G_H} = 1 - \frac{2\,(7+5\mu)}{5\,(6-4\mu)}, \qquad (1)$$

where G_p is the shear modulus of a polycrystalline specimen for the case where the relaxation of shear stress along the grain boundaries has taken place completely; G_H is the shear modulus in the absence of slip at the grain boundaries; μ is the Poisson ratio.

At low temperatures the shear modulus of uranium changes linearly (curve 1, Fig. 1); it can then be assumed that there is no relaxation at the boundaries. The curve 1 extended by a dotted line can therefore be considered as relating to the nonrelaxing modulus. Then, for any temperature the ratio of the relaxing modulus G_p to the nonrelaxing modulus G_H will be equal to the ratio of the squares of the corresponding frequencies of vibrations:

$$\frac{G_p}{G_H} = \left(\frac{f_p}{f_H}\right)^2. \quad (2)$$

From Fig. 1 (curve 1, shows G/G_{20} after annealing in the α region) it can be established that relaxation along the grain boundaries becomes equal to a certain constant value on approaching the temperature of 630°C. Assuming that relaxation takes place completely at the boundaries, on the basis of equality (2) we determine the value $G_p/G_H = 0.56$. This means that part of the complete shear stress which can relax along the grain boundaries is equal to 1-0.56 = 0.44.

Taking the Poisson ratio for uranium (according to [8]) equal to 0.23, from equation (1) we find the theoretical value $G_p/G_H = 0.535$. Therefore, the agreement of the experimental value $G_p/G_H = 0.56$ with the theoretical (0.535) derived from the concept of viscous behavior of the grain boundaries is perfectly satisfactory.

Annealing in the β region leads not only to an increase in viscosity of the boundaries but also to a change in the slope of the nonrelaxed section of the shear modulus curve (curve 3, Fig. 1). It is well known that annealing in the α region does not completely remove the grain texture which exists after plastic deformation [9], and the temperature dependence of the shear modulus is linked with the presence of a preferred orientation. Annealing in the β region, accompanied by phase recrystallization, destroys the deformation texture, and the temperature relationship of the shear modulus in this case corresponds to a polycrystal with disordered orientation of the grains.

The experimental value of relaxation at the grain boundaries after annealing in the β regions, determined for G/G_{20} from curve 3 of Fig. 1, is 0.29 instead of 0.44, i.e., is considerably reduced, which supports the hypothesis of change in mobility of the grain boundaries due to annealing in the β region.

Specimens annealed in the γ region at 960°C for 30 min had a much lower level of internal friction in the α region (curve 4, Fig. 1). The value of the internal friction and the shear modulus up to 450°C remains almost the same as after annealing in the β region, but above 450°C the internal friction has a much lower level than after β annealing, and the shear modulus also relaxes to a much smaller extent.

Change in the crystalline structure during polymorphous transformation is accompanied by a sharp change in the physical and mechanical properties of a material [10]. The internal friction, as a structural sensitive characteristic, should also undergo considerable changes.

Change in the internal friction during polymorphous transformations in pure metals has only been studied for cobalt [11, 12].

Figure 2 shows curves for internal friction and shear modulus of uranium in relation to the temperature (up to 850°C) for specimens annealed at 960°C. The internal friction increases, reaching a maximum value at a temperature of 670°C; during isothermal soaking at this temperature it is reduced to a certain stable value. With further heating to 768°C, the internal friction again gradually increases. At this temperature there is an isothermal increase in the internal friction to very large values (of the order of 0.13); with further increase in temperature it rapidly increases. The shear modulus at 670°C increases somewhat and at 768°C it drops sharply. The change in internal friction with time during isothermal soaking at 670 and 768°C occurs due to polymorphous transformations in uranium.

During cooling the transformations are accompanied by a reverse change in the internal friction and shear modulus, but occur at lower temperatures: 755 and 645°C. With change in the internal friction hysteresis is therefore observed which depends to a considerable extent on the rate of cooling (in the case of measurements without isothermal soaking).

Isothermal soaking at a temperature somewhat lower than the $\alpha \rightarrow \beta$ transformation temperature gives a certain reduction in the internal friction; however, with further heating to 670°C the internal friction again sharply increases. Only at this temperature, due to isothermal soaking does the internal friction reach a minimum value, corresponding to the level of the β region. Similar behavior is also observed with increase in internal friction during the $\beta \rightarrow \gamma$ transformation.

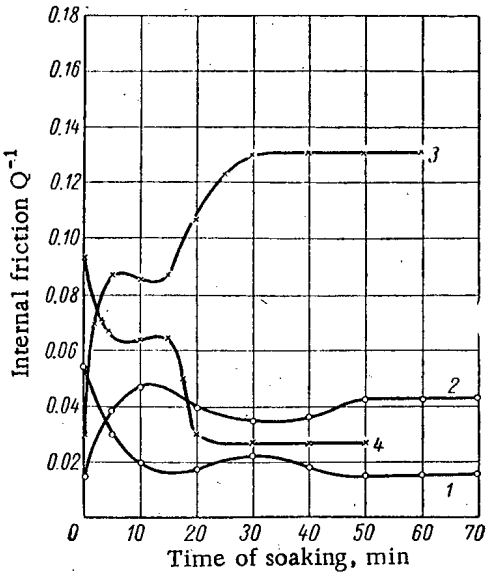

Fig. 3. Change in the internal friction in uranium in dependence on the time during isothermal soaking: 1) $\alpha \rightarrow \beta$ transition, 670°C; 2) $\beta \rightarrow \alpha$ transition, 645°C; 3) $\beta \rightarrow \gamma$ transition, 768°C, 4) $\gamma \rightarrow \beta$ transition, 755°C.

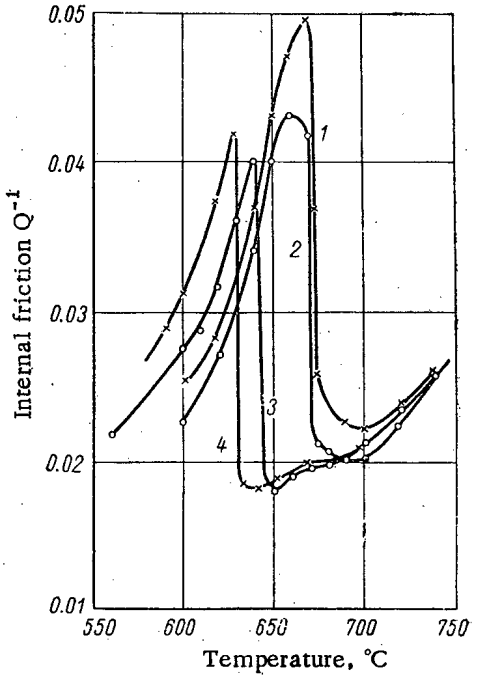

Fig. 4. The effect of rates of heating and cooling on the internal friction of uranium: 1) rate of heating 5 deg/min; 2) rate of heating 0.5 deg/min; 3) rate of cooling 0.5 deg/min; 4) rate of cooling 5 deg/min.

Figure 3 shows the change in internal friction in uranium during isothermal soaking at the temperatures of polymorphous transformations. In all cases after a certain time of soaking a certain stable value of internal friction is reached. Change in the internal friction in time during heating and cooling, respectively for each transformation, has a completely reversible character. The law for the change is such that after a rapid increase (or decrease) in the internal friction during the first minutes in soaking there is a certain reduction (or increase) and a further smooth attainment of the stable value.

The temperatures at which transformations take place during continuous heating or cooling depend on the rate of change in temperature. Figure 4 shows curves for the change in internal friction in the region of transformations for two rates of heating: 5 and 0.5 deg/min. Increasing the rate of heating does not lead to much increase in the transformation temperatures, since even on overheating by 5°C above the transformation temperature, the internal friction during this heating reaches the same value as after isothermal soaking at the transformation temperature. In other words, with increase in the degree of overheating the rate of transformation increases so strongly that it is impossible, by increasing the rate of heating (from 0.5 to 5 deg/min), to displace the transformation towards higher temperatures. However, increasing the rate of cooling considerably displaces the transformations to lower temperatures. Similar behavior is also observed when studying transformations of uranium by other methods [13].

Change in the internal friction in uranium during polymorphous transformations therefore differs considerably from such changes during relaxation processes. Change in the internal friction during polymorphous transformation occurs in time at a constant temperature, which is independent of the frequency of vibrations and is determined by the transformation itself. A definite level of internal friction is achieved by soaking, corresponding to the new phase state, i.e., to the new type of crystalline lattice.

Of special importance is the fact that internal friction decreases in the process of isothermal soaking during the $\alpha \rightarrow \beta$ transformation, and during the $\beta \rightarrow \gamma$ transformation it increases. This indicates that the value of the internal friction of various polymorphous modifications of uranium is different for the given temperature.

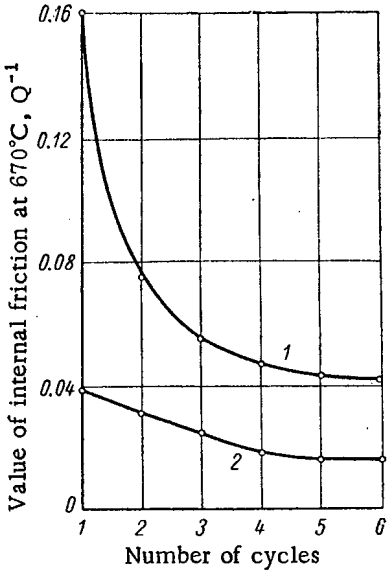

Fig. 5. Change in the internal friction during the $\alpha \rightarrow \beta$ transition in dependence on the number of subsequent transitions through the $\alpha \rightleftharpoons \beta$ transformation: 1) internal friction in α uranium; 2) internal friction in β uranium.

Depending on the type of crystalline lattice forming or disappearing during the polymorphous transition, there is a corresponding decrease or increase in the internal friction.

For repeated transitions through the $\alpha \rightleftharpoons \beta$ transformation the value of the internal friction in the α region decreases from cycle to cycle during the first few cycles; after about ten cycles the internal friction reaches a fixed and almost constant level both in the α and in the β region. Figure 5 shows the reduction in maximum value of internal friction near the transformation temperature in dependence of the number of $\alpha \rightleftharpoons \beta$ transitions.

The value of the observed effects does not depend to any great extent on the range of temperature change and remains approximately the same for the ranges 600-700 and 20-700°C. The minimum value reached by the internal friction in the β region after transformation is also somewhat reduced during the first cycles, but in a less abrupt form (curve 2, Fig. 5). These effects are presumably connected with the above phenomena: the removal of preferred orientation and reduction in the mobility of the grain boundaries due to the $\alpha \rightleftharpoons \beta$ transition.

The fact that after several cycles the value of the internal friction becomes constant and does not change during continuation of the cyclic heat treatment indicates that the known effect of cyclic heat treatment [4, 13] during the $\alpha \rightleftharpoons \beta$ transitions, accompanied by a change in the dimensions of the specimen, does not affect the value of internal friction under the given conditions (rate of change in temperature is $\sim$ 5 deg/min for about five to six cycles).

The curves shown in Figs. 2-4 were obtained for specimens which had first been subjected to five to six cycles of $\alpha \rightleftharpoons \beta$ transformations.

The following conclusions can be drawn:

1. The inflection on the curve of internal friction in the temperature range 450-500°C is due to the viscous behavior of the grain boundaries and disappears after annealing in the β and γ regions, which is due to reduction in the mobility of the boundaries due to phase recrystallization.

2. Polymorphous transformations in uranium are accompanied by isothermal change in the value of internal friction at a transformation temperature which has a reversible character during heating and cooling.

3. The plastic γ region of uranium, having a volume-centered cubic lattice is characterized by the maximum value of internal friction. The tetragonal β modification, which tends to be brittle, has a minimum value of internal friction (at the tmeperature of the $\alpha \rightarrow \beta$ transition the internal friction in β uranium is lower than in α uranium). The internal friction is therefore directly connected not only with the type of crystalline lattice but also with the capacity of a given modification for plastic deformation.

LITERATURE CITED

1. A. A. Bochvar, et al., Atomnaya Énerg. 5, 1, 5 (1958).*
2. G. Ya. Sergeev, et al., Atomnaya Énerg. 5, 6, 618 (1958).*
3. V. S. Postnikov, Uspekhi Fiz. Nauk 66, 1, 43 (1958).
4. A. A. Bochvar and G. P. Tomson, Atomnaya Énerg. 4, 6, 520 (1957).
5. Chiswich and Kellman, Material of the International Conference on the Peaceful Use of Atomic Energy (Geneva, 1955) [in Russian] (Leningrad, Goskhimizdat, 1958) Vol. 9, p. 184.
6. S. Pugh, J. Inst. Metals 86, 12, 497 (1958).
7. C. Zener, Phys. Rev. 61, 906 (1941).

*Original Russian pagination. See C. B. translation.

8. R. Seller, "Nuclear reactors," Materials for Nuclear Reactors [Russian translation] (IL, Moscow, 1956) Vol. 3, p. 285.
9. Fort, Materials of the International Conference on the Peaceful Uses of Atomic Energy (Geneva, 1955) [in Russian] (Goskhimizdat, Leningrad, 1958) Vol. 9, p. 51.
10. E. M. Savitskii, The Effect of Temperature on the Mechanical Properties of Metals and Alloys [in Russian] (Izd. AN SSSR, Moscow, 1957).
11. V. S. Postnikov, Tr. Kemerovskogo Pedinstituta 1, 191 (1956).
12. V. S. Postnikov, Fiz. Metalov. i Metalloved. 4, 344 (1957).
13. P. Lehr and J. Langeron, Rev. Metallurgie 55, 9, 829 (1958).

THE PHASE DIAGRAM FOR THE SYSTEM ZIRCONIUM – BERYLLIUM

V. S. Emel'yanov, Yu. G. Godin, A. I. Evstyukhin,

and A. A. Rusakov

Translated from Atomnaya Énergiya, Vol. 9, No. 7, pp. 33-38, July, 1960
Original article submitted February 3, 1960

Using the methods of metallographic, thermal, and x-ray qualitative phase analyses and by measuring the hardness, studies have been made of the system zirconium–beryllium, and its phase diagram has been plotted. The presence of four intermediate phases has been shown in the system: $ZrBe_2$, $ZrBe_6$, $ZrBe_9$, and $ZrBe_{13}$. The first three compounds formed by peritectic reactions at temperatures of 1235, 1475, and 1555°C, respectively; the last compound melts with an open maximum at 1645°C. At 965°C and 5 weight % beryllium a eutectoid forms between the $ZrBe_2$ and the zirconium. Additions of beryllium to the zirconium lead to a reduction in temperature of the $\alpha-\beta$ transformation and to the formation of a eutectoid at 800°C. The solubility of beryllium in α-zirconium is less than 0.1 weight % and in β-zirconium – less than 0.3 weight %. The solubility of zirconium in beryllium does not exceed 0.3 weight %.

* * *

The phase diagram of the system zirconium– beryllium has been insufficiently studied. According to a study carried out on specimens of alloys prepared by the powder metallurgy method [1], in the system zirconium–beryllium, it is possible to have a eutectoid in the region which is rich in zirconium and at least four intermediate phases. One has the composition $ZrBe_2$ and the other is close to 27 weight % beryllium; the remaining phases have an uncertain composition. The introduction of beryllium into the zirconium increases the temperature of the $\alpha-\beta$ transformation.

A later paper [2] confirmed the presence of the compound $ZrBe_2$ and a eutectoid at a temperature of 980°C and 5 weight % of beryllium. Apart from the compound $ZrBe_2$ the most probable is the existence of the intermetalloids $ZrBe_6$, $ZrBe_9$, and $ZrBe_{16}$. There is also the possible existence of a region of solid solutions of $ZrBe_2$ and $ZrBe_9$. Additions of beryllium to the zirconium lead to a reduction in the temperature of its $\alpha-\beta$ transformation and to the formation of a eutectoid. The existence in the zirconium-beryllium system of the compounds $ZrBe_2$ and $ZrBe_{13}$ is mentioned in [3]. The presence is also assumed of the intermediate phases $ZrBe_4$ and $ZrBe_7$, the latter possibly having a region of homogeneity.

A study of the structure of the compound $ZrBe_2$ [4] showed that it has a hexagonal lattice with parameters $a = 3.82$ Å, $c = 3.24$ Å, and $c/a = 0.848$. The compound $ZrBe_{13}$ has [5] a face-centered cubic lattice with parameter $a = 10.047$ Å.

Because of the contradictory data on the system zirconium–beryllium a systematic study was undertaken using the methods of microscopic investigation, thermal, and x-ray phase analyses and also by determining the hardness and microhardness.

The starting materials for the preparation of the alloys were bars of zirconium iodide of purity 99.7 weight % and distilled beryllium in the form of druses of purity 99.4 weight %.

The alloys were smelted in an arc furnace on a copper-floor cooled with water and in an atmosphere of purified argon. The alloyed specimens were subjected to repeated resmelting and were prepared in the form of bars weighing 20-40 g. The preparation of the alloys was complicated due to evaporation of the beryllium during

smelting, which changed the composition of the alloys and hindered observation of the melting and also cracking and splitting of the ingots during cooling or heating in the arc furnace as a result of high thermal stresses. This latter led to considerable losses in the weight of the ignots,reaching 10-20% of the weight of the charge in a number of cases.

Chemical analysis of the specimens showed a certain reduction in the content of beryllium in the alloys compared with the charge composition; in a number of cases this reduction was 1-2%.

A metallographic investigation was carried out on the cast alloys which had been quench-hardened after prolonged annealing. The heat treatment systems used on the alloys are given in the table.

Systems of Heat Treatment Used on Alloys

Annealing temp., °C	Duration of annealing, hr	Annealing temp., °C	Duration of annealing, hr
750	250	870	150
730	220	935	110
810	188	1000	70
830	170	1200	35

Note. At temperatures of 1000 and 1200°C annealing was carried out on alloys containing more than 17 weight % beryllium.

The alloys were annealed in quartz ampoules filled with argon in order to prevent evaporation of beryllium during the annealing. The alloys were quench-hardened by rapidly taking the ampoules from the furnace and plunging them into water.

The sections for the metallographic studies were prepared in the usual way. To prevent the brittle alloys from chipping during grinding the fine grain emery paper was rubbed with wax. The structure of the alloys was revealed by etching them in an aqueous solution of hydrofluoric and nitric acids.

The thermal analysis of the alloys was carried out in a vacuum with rates of cooling and heating of 5-7 deg/min. The critical points were determined for alloys containing 2.9, 5.04, and 8.9 weight % beryllium. The introduction of beryllium into the zirconium reduced the temperature of the $\alpha-\beta$ transformation. Eutectoid decomposition in the system zirconium–beryllium occurred at a temperature of about 800°C, and the melting point of the eutectic was 965°C.

The temperatures of the start of melting of the alloys were determined by the movement of a hollow in the center of the specimen (the method of Pirani and Altertum). The method used to heat the alloys in order to determine the temperatures of the start of fusion was to pass a current through the specimen compressed between electrodes in a vacuum. In extremely hard specimens which could not be machined in the usual way, the hollows were made by ultrasonic machining. The pyrometer was graduated from the melting points of pure metals: zirconium, iron, and nickel.

The x-ray investigation of the alloys was carried out by the photographic and ionization methods in K_α-radiation. In the first case, the x-ray photographs were taken with the RKU-86 camera with an asymmetric charge on the film, in the second case the URS-50I apparatus was used. The diffractograms of the investigated alloys obtained on the URS-50I apparatus were used to check the data of the photographic method. The powders of alloys rich in zirconium or beryllium were obtained by filing the alloys. The other alloys were crushed in a press and then the small pieces were ground in an agate mortar. To remove the internal stresses the powders were annealed for 2-3 hr in a high vacuum at a temperature of about 700°C.

The microhardness of the alloys was measured by a diamond cone on a Rockwell instrument with a 15 kg load. Attempts to measure the hardness with the usual load were unsuccessful due to the particles of the alloys shearing at the measurement points.

From the data of the investigation a phase diagram was plotted for the system zirconium–beryllium (Fig. 1).

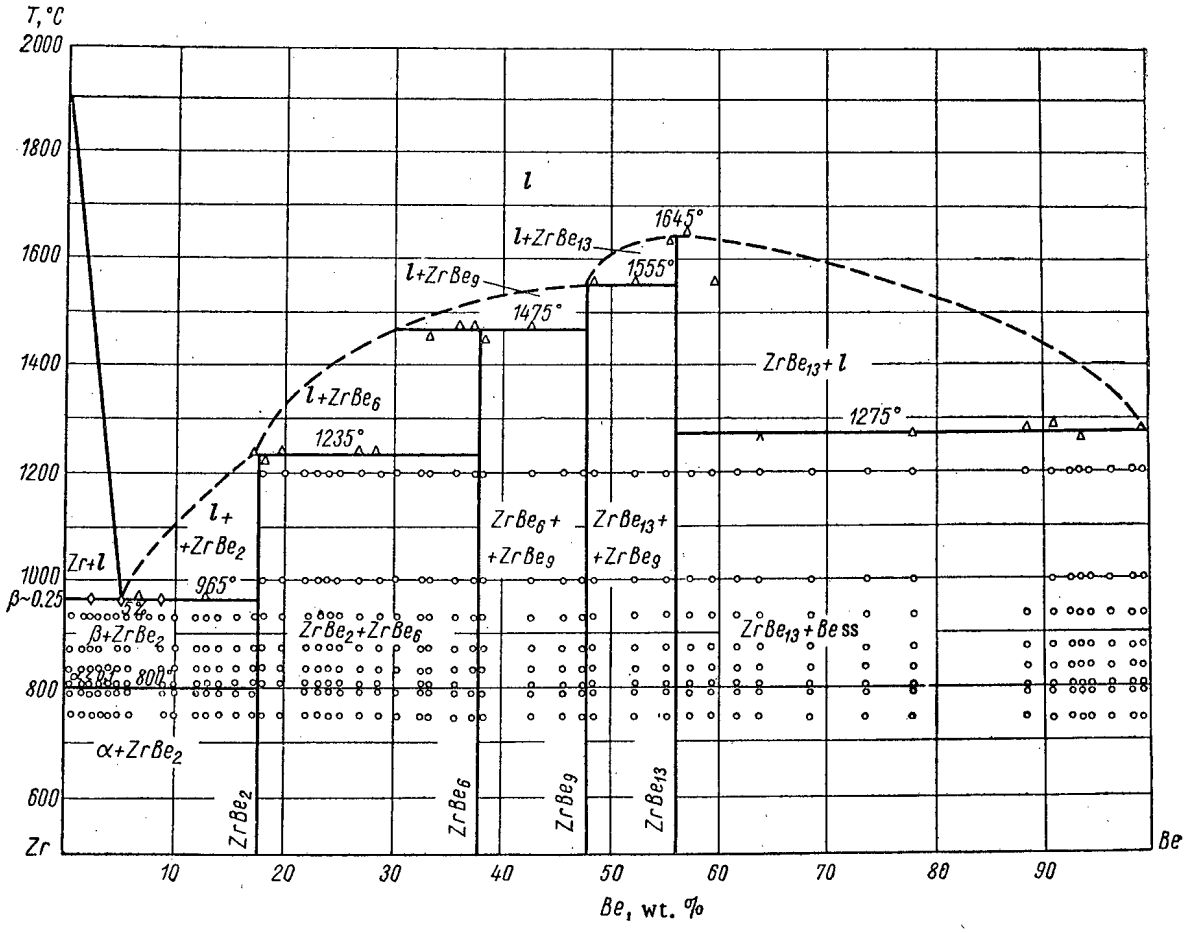

Fig. 1. Phase diagram for the system zirconium–beryllium: ○ – two phase alloys; Δ – temperature of the start of fusion of the alloys; ◇ – temperature of the start of fusion of alloys from the data of thermal analysis.

A microscopic investigation of cast specimens and also specimens used to determine the start of fusion and thermal analysis indicated that the eutectic point in the system zirconium– beryllium lies at a temperature of 965°C and corresponds to an alloy with ~ 5 weight % of beryllium.

A study of the structure of isothermally annealed alloys showed that the solubility of beryllium in β zirconium near the eutectic temperature is less than 0.3 weight%. Alloying zirconium with beryllium does not lead to stabilization of the β phase; due to quench-hardening the latter is transformed to the α' phase, which is a supersaturated solid solution of beryllium in α zirconium.

In the solid state the β phase decomposes at 800°C. The eutectic decomposition of $\beta \rightleftharpoons \alpha + ZrBe_2$ was determined from the data of thermal analysis and by studying the isothermally annealed alloys. The decomposition is characterized by structures shown in Fig. 2. The structure shown in Fig. 2a consists of a mixture of α and β phases obtained in the alloy with a 0.18 weight % of beryllium after annealing at 810°C; Fig. 2b shows the structure of the same alloy after annealing at 790°C. In this specimen, the β phase decomposed to the α phase and $ZrBe_2$, which coagulated during annealing. The eutectoid point of the system determined from the data of microscopic investigation corresponds to an alloy containing ~0.23 weight % of beryllium.

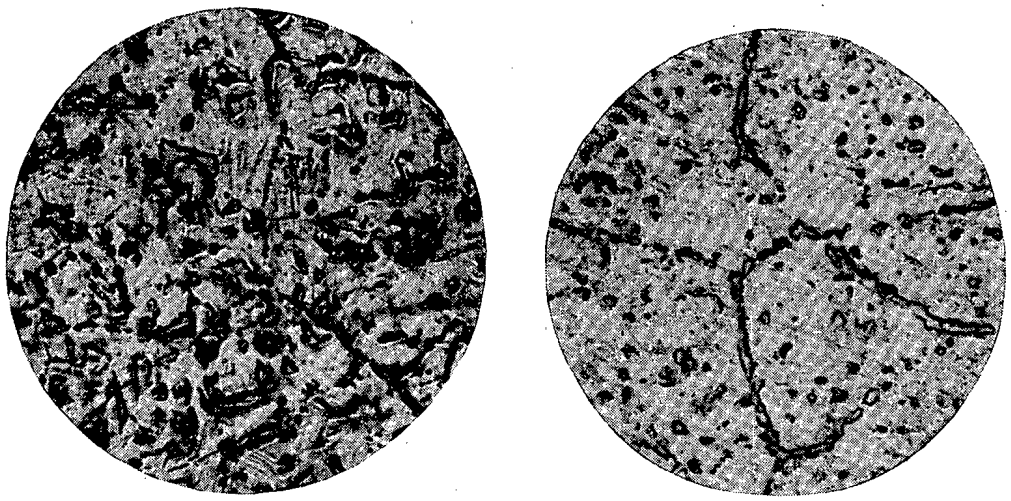

a b

Fig 2. Alloy with 0.18 weight % beryllium (× 340): a) quench-hardened from 810°C; b) quench-hardened from 790°C.

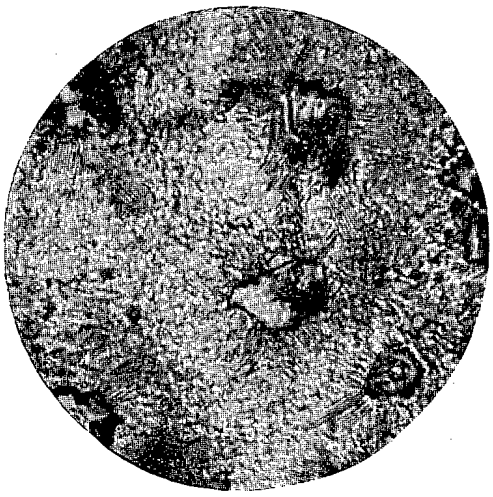

Fig. 3. Cast alloy with 5.87 weight % beryllium (× 500).

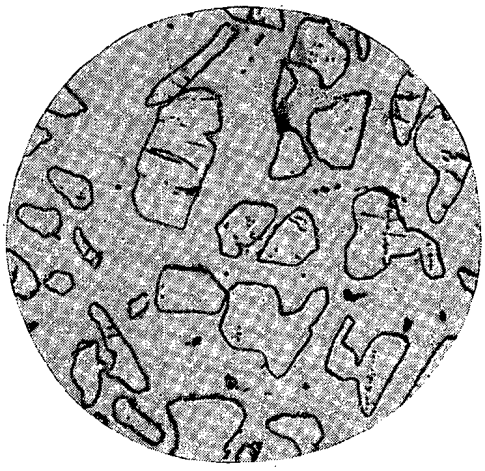

Fig. 4. Cast alloy with 17.65 weight % beryllium (× 340).

The value of the maximum solubility of beryllium in α zirconium can be judged from the structure of the alloy with 0.1 weight % beryllium. This alloy, cooled rapidly after annealing at 810°C, consisted of grains of the α phase at the base of which there was a small amount of isothermally formed grains of the β phase.

A study of the microstructure of successive series of cast and annealed alloys showed the presence of four intermediate phases in the system. The eutectic with 5 weight % beryllium consists of a mixture of the β phase and the intermediate phase $ZrBe_2$ (16.5 weight % beryllium). In the cast alloys with > 5 weight % beryllium the primary crystals of this phase are observed at the background of the eutectic mixture β + $ZrBe_2$, as can be seen from Fig. 3, which shows the microstructure of an alloy with 5.87 weight % beryllium. The alloy with 16.3 weight % beryllium consists almost completely of $ZrBe_2$ grains.

In Fig. 4, representing the microstructure of cast alloy with 17.65 weight % of beryllium, there can be seen primary crystals of the following intermediate phase at the base of the peritectically formed phase $ZrBe_2$. The structure of the alloy with 36.7 weight % beryllium consists of some grains of the second intermediate phase, due to which it was determined as $ZrBe_6$. Consequently, $ZrBe_2$ is formed at 1235°C due to the peritectic reaction $ZrBe_6 + l \rightleftharpoons ZrBe_2$. In the structure of the cast alloy with 30.4 weight % beryllium there are primary crystals of

the third intermediate phase, surrounded by the peritectic $ZrBe_6$ and lying in the mother liquor of $ZrBe_2$. The amount of beryllium in the latter phase is 47.1 weight %, due to which it was ascribed the formula $ZrBe_9$. The phase $ZrBe_6$ is formed due to the peritectic transformation $ZrBe_9 + l \rightleftharpoons ZrBe_6$, occurring at a temperature of 1475°C.

Figure 5 shows the microstructure of a cast alloy with 42.7 weight % beryllium, consisting of the primary grains of the intermediate phase $ZrBe_{13}$ (56.3 weight % beryllium) and peritectic formations of $ZrBe_9$, forming at 1555°C according to the reaction $ZrBe_{13} + l \rightleftharpoons ZrBe_9$.

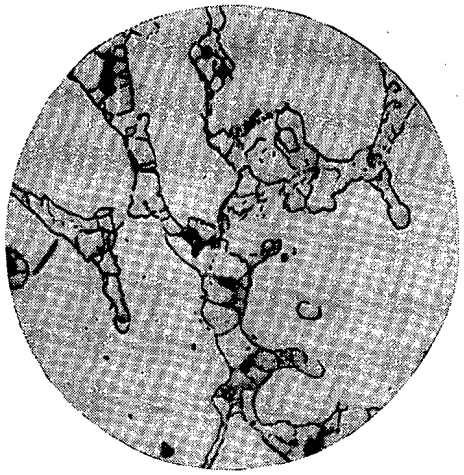

Fig. 5. Cast alloy with 42.7 weight % beryllium (× 340).

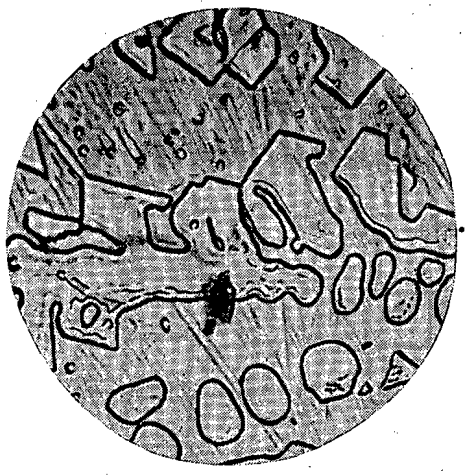

Fig. 6. Cast alloy with 77.9 weight % beryllium (× 200).

The compound $ZrBe_{13}$ melts with an open maximum at 1645°C. Alloys containing more than 56.3 weight % beryllium consist of a mixture of the phase $ZrBe_{13}$ and a solid solution rich in beryllium. This very wide two-phase region on Fig. 6 indicates the structure of an alloy with 77.9 weight % beryllium, consisting of primary crystals of $ZrBe_{13}$ in the matrix of a solid solution of zirconium in beryllium.

The character of the reaction between $ZrBe_{13}$ and beryllium (eutectic or peritectic) could not be established. The eutectic or peritectic points should lie in the concentration range 99.5-100 weight % of beryllium at 1275°C. We did not determine the solubility of zirconium in beryllium; however, it did not exceed 0.3 weight %.

To confirm the data of the metallographic investigation, x-ray photographs and diffraction diagrams were obtained for a number of alloys lying in various phase regions, and phase analysis was carried out on them. Figure 7 shows the x-ray photographs. The diffraction diagrams made it possible also to plot the extrapolation graphs to determine the concentrations corresponding to single-phase alloys. To plot them, measurements were made of the relative intensities of several pairs of diffraction maximums for alloys of varying compositions, in each pair strong maximums being taken, relating to various alloys.

In accordance with the results of the microscopic investigation, the obtained data showed the presence of four intermediate compounds in the system, corresponding to the compositions 16.5, 37, 47.1, and 56.3 weight % of beryllium. The lattice parameters of the intermetallides $ZrBe_2$, $ZrBe_6$, $ZrBe_9$, and $ZrBe_{13}$, as shown by precision measurements, did not change noticeably on departure from the stoichiometric compositions (the accuracy in determining the interplane distances at $\theta \simeq 85°$ was equal to ± 0.00004 Å). The interplane distances, calculated from the strong lines for $ZrBe_6$ and $ZrBe_9$ had the same values; however, the intensities of the diffraction lines differed noticeably. This fact indicates the similarity of the structures of both intermetallides.

The indication of the $ZrBe_{13}$ x-ray photograph confirmed the data on the presence of a face-centered cubic lattice in this compound. Its parameter is a = 10.009 Å.

The curve for the dependence of the hardness of cast alloys on their composition, shown in Fig. 8, has three maximums at compositions of 16.5, 37, and 47 weight % beryllium, which correspond to the positions of

the compounds $ZrBe_2$, $ZrBe_6$, and $ZrBe_9$. In an alloy containing 56.3 weight % beryllium and corresponding to the intermetallide $ZrBe_{13}$, there is no maximum on the hardness curve. This is apparently due to the presence of a large number of pores and microcracks in alloys containing about 56.3 weight % beryllium. The introduction of beryllium into zirconium considerably increases its hardness; a similar action, although to a lesser degree, is shown by the addition of zirconium to beryllium.

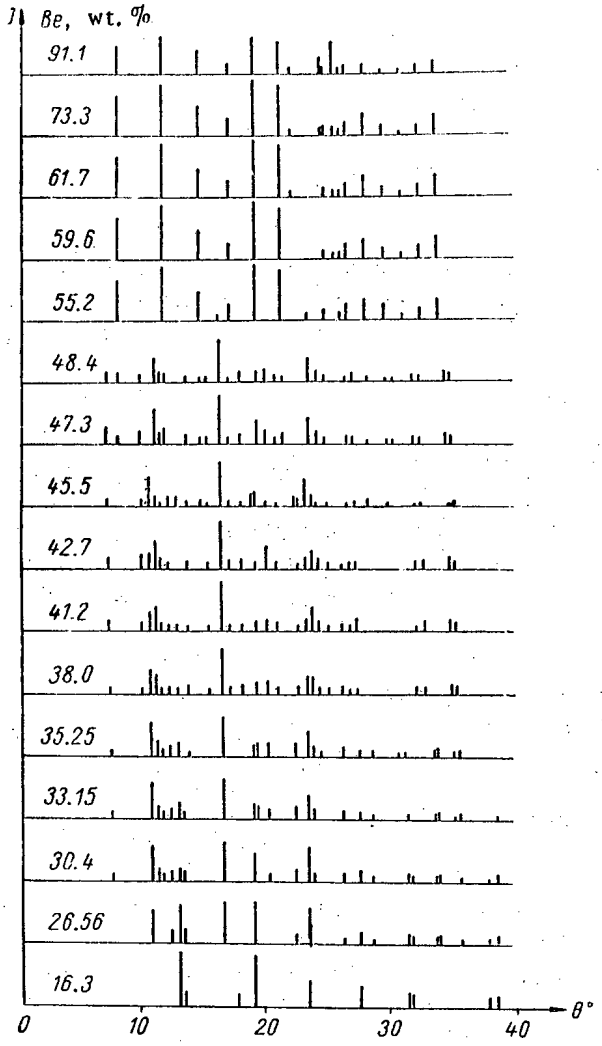

Fig. 7. X-ray photographs of zirconium–beryllium alloy powders.

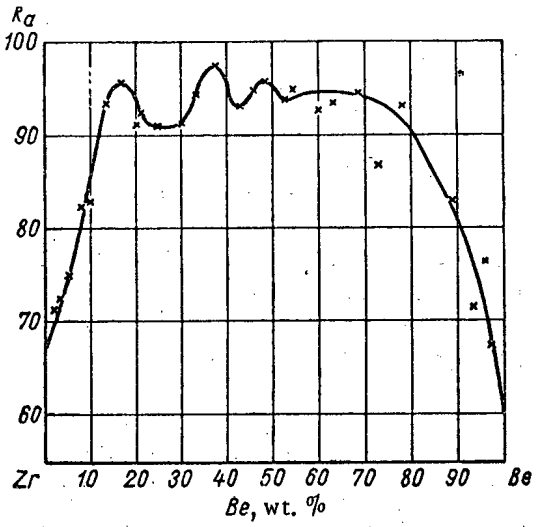

Fig. 8. Relationship between the hardness of cast zirconium–beryllium alloys and their composition.

The data for the measurement of microhardness confirmed the presence of four intermediate phases in the system. A very high microhardness (1580 kg/mm^2) is shown by the compound $ZrBe_{13}$ and the lowest microhardness (840 kg/mm^2) by the compound $ZrBe_2$. The microhardness of the phases $ZrBe_6$ and $ZrBe_9$ is equal to ~ 1145 and 1230 kg/mm^2, respectively. The microhardness of the eutectic is 244 kg/mm^2.

The phase diagram (see Fig. 1) is similar in general features to the approximate diagram given in [3]. In contrast to the previously published data, it was found that in the zirconium–beryllium system there are four intermediate phases of the daltonide type. In the region rich in beryllium there is an intermetallide $ZrBe_{13}$, melting with an open maximum and very difficult to fuse; the remaining compounds melt with a closed maximum. There are no solid solutions based on intermetallides in the system. It was also shown unambiguously that the introduction of beryllium to zirconium reduces the temperature of the $\alpha-\beta$ transformation of the latter.

LITERATURE CITED

1. H. Hausner and H. Kalish, J. Metals 188, 1, 59 (1950).
2. J. McGurty, et al., Report TID-5061 (April, 1951).
3. M. Hansen and K. Anderko, Constitution of Binary Alloys (New York, McGraw-Hill Book Co., 1958).
4. Acta Cryst. 7, 132 (1954).
5. Acta Cryst. 2, 258 (1949).

RATIO BETWEEN THE RADIATION DOSE AND THE ABSORBED DOSE

Yu. V. Sivintsev

Translated from Atomnaya Énergiya, Vol. 9, No. 7, pp. 39-47, July, 1960
Original article submitted February 8, 1960

The article indicates the difference between the concepts "radiation dose" and "absorbed dose"; specific formulas are given for calculating an absorbed dose from the results of absolute measurements of a radiation dose, and the conditions of electron equilibrium during dosimetric measurements of x-rays and γ-radiations of various energies within the 200 kev – 32 Mev range are stated.

* * *

Until recently, the opinion was predominant in radiobiology that the biologically significant part of the energy transmitted to living matter is only that part of the energy expended by the penetrating radiations on the ionization of the cell molecules. Consequently, the main emphasis in dosimetry was placed on measurement of the absolute value of the ionization of the medium irradiated, and the assessment of the energy transmitted to the matter was only an outcome of this. However, many radiobiological hypotheses which have been considered almost axiomatic have recently been modified. These changes were advanced, in particular, by one of the most important discoveries in this field, namely that of the process of migration of the excitation energy within the cell, leading to a considerable disintegrating effect on the protein molecules, which intensifies the ionization effect of the cells [1]. As a result, a reassessment was made of certain hypotheses of contemporary dosimetry, the principal problem of which was finally recognized, after years of dispute, to be the measurement of the energy transmitted to a gram of matter exposed to ionizing radiations. This solution found its repercussion in the recommendations of the International Commission on Radiological Units and Measurements (ICRU), published in 1957 [2].

We will first deal with the necessity for a clear-cut distinction between the concepts "absorbed dose" and "radiation dose". As already mentioned, the main problem of dosimetry is the determination of the absorbed dose D, i.e., the energy ΔE transmitted to a unit mass of matter Δm exposed to ionizing radiation. The value of the absorbed dose is the only strictly physical value determined in dosimetry proper. By definition

$$D = \frac{dE}{dm} = \frac{1}{\rho}\frac{dE}{dv}, \tag{1}$$

where $\Delta m = \rho \Delta u$. The dimension of the absorbed dose is

$$[D] = \frac{\partial_j}{kg} = \frac{w \cdot sec}{kg}. \tag{2}$$

The rad, numerically equal to

$$10^{-2}\ w.\ sec/kg = 10^2\ erg/g \tag{3}$$

is a special unit of the absorbed dose.

The term "absorbed dose" cannot be considered a fortunate choice, because any dose is the result of absorption of irradiation (no dose can be transmitted to a vacuum). Taking account of this, the Radiation Protection Commission of the Federal German Republic proposed the term "energy dose" for the absorbed dose, and "ionic dose" for the radiation dose [3]. But in the interest of preserving the unity of scientific terminology, in this communication we will adhere to the recent recommendations of ICRU.

In spite of the fact that the absorbed dose is physically strictly specific for any form of ionizing radiation and any medium, its measurement is extremely difficult and is only possible on the basis of the calorimetric method, which is only employed in certain cases of exceptionally high values of the effect measured and is, in principle, inapplicable to biological objects. However, this problem can often be solved by measuring the radiation dose, expressed in roentgens. This value, which characterizes only the radiation field and is independent of the composition of the object irradiated, can be found on the basis of the widely employed ionization measurement methods. For x-rays and γ-radiations the measurements are carried out in a standard medium, air, the basic advantage of which is that the relation between the linear absorption coefficient of the radiation and its energy is practically identical with the tissues of the living organisms. It is known that as a result of this fact, ionization chambers can be constructed, free from so-called hardness behavior in a wide energy range. The true sum of the measurement of a radiation dose by the ionometric method can be represented by the very simple relationship

$$I = \frac{dQ}{dm} = \frac{1}{\varrho_a}\frac{dQ}{dv}, \tag{4}$$

where Q is the amount of electricity, and ρ_a is the density of air.

The dimension of the radiation dose is

$$[I] = \frac{\text{k}}{\text{kg}} = \frac{\text{amp} \cdot \text{sec}}{\text{kg}} \tag{5}$$

The special unit of measurement of a radiation dose is the roentgen, numerically equal to

$$2.58 \cdot 10^{-4} \text{ amp} \cdot \text{sec/kg} = \frac{1 \text{ electrostatic unit of electricity}}{0.001293 \text{ g}} \tag{6}$$

The absorbed dose, the value of which is determined both by the irradiation field and the composition of the object irradiated, can be found (in addition to the above-mentioned calorimetric method) on the basis of the determination of the radiation dose, other ionization measurements, luminescence or chemical effects of radiation. Since the biological action of ionizing radiations is due primarily to the energy transmitted to the substance, the biological effect must obviously be more closely correlated with the absorbed dose than with the radiation dose. The necessity for a clear distinction between the radiation dose and the absorbed dose is indicated, for example, by the fact that for the same radiation dose (expressed in roentgens) the absorbed dose (expressed in rads) in bone tissue may be more than three times greater than the absorbed dose in the adjacent soft tissue [4].

In many cases, the absorbed dose can be easily calculated on the basis of measurements of the radiation dose, as a result of which the roentgen as a practical unit of the radiation dose by x-rays or γ-rays remains the principal value of present-day practical dosimetry.

According to definition, the ionization of air, caused by high-energy electrons formed by a beam of photons in 1 cm^3 of dry air under normal conditions and expressed in electrostatic units of electricity, is equal to the number of roentgens. In actual fact, the electrons formed in a given volume of air lose part of their energy outside the limits of the given volume. On the other hand, certain electrons which penetrate outside the volume in question cause additional ionization in the given volume, as a result of which the ionization loss may be partially or completely compensated. It is known that measurement in roentgens requires complete compensation, which may be achieved in practice, provided that the electron equilibrium present at any point of medium irradiated is maintained, if: 1) the intensity and the energy spectrum of the x-rays or γ-rays are unchanged in all directions of the region from the point in question, at least up to the maximum path of the electrons formed by the radiation measured, and 2) the mass absorption coefficient of the energy and the stopping power of the medium are constant throughout the whole extent of this region.

If these conditions are satisfied, for each electron leaving an infinitely small volume around the point in question there is another electron of almost the same energy, which enters this volume from outside sources. Thus, in this case, the energy transferred within the limits of the medium to an element of volume Δv by all the secondary electrons intersecting the volume is equal to the energy which the secondary electrons formed by the radiation within the limits of Δv transfer to the medium along the whole of its path. From this it follows that

electron equilibrium occurs both in a normal ionization chamber, the measuring volume of which is surrounded by a fairly large amount of air, and in an air-equivalent ionization chamber, if the thickness of its walls is not less than the maximum path of the secondary electron in the material of which the wall is made and is sufficiently small for the absorption of primary radiation within it to be neglected.

The following are typical examples of the absence of electron equilibrium:

1) a radiation field in the immediate vicinity of its source where the intensity changes rapidly;

2) boundary regions between materials with different atomic compositions of the medium (but not of the density [5]), such as soft tissues and bone tissue;

3) high-energy (in practice more than 3 Mev) x-rays or γ-rays, which undergo a considerable attenuation in the medium at a distance equal to the mean path length of the secondary electrons.

As far back as 1936, Gray [6] established that the absorbed dose can be assessed by means of the ratio between the ionization formed in the cavity filled with gas and located at the point in question of the material irradiated, and the energy transferred to a unit mass of the substance irradiated. At fairly small dimensions of the cavity the gas A which fills it, is subjected to the same current of ionizing particles as the substance B in question, exposed to radiation. Hence

$$D_B = S_{BA} D_A \tag{7}$$

where S_{BA} is the ratio of the mass stopping powers of the medium irradiated and the gas filling the cavity, for secondary electrons.

When a standard medium – air – is used, for a fairly small volume of the medium the relationship

$$D_a = U_i I, \tag{8}$$

applies, where U_i is a coefficient associated with the mean amount of energy W_i, expended on the formation of one pair of ions in air, by the relationship

$$U_i = \frac{W_i}{e}, \tag{9}$$

where e is the electronic charge.

According to recent investigations, the value of W_i for x-rays and γ-rays in air is in all probability between 33 and 35 ev. At present, for calculations (for x-rays and γ-rays with a photon energy of more than 20 kev) the use of the value $W_i = 34$ ev ($5.44 \cdot 10^{-11}$ erg) is recommended. Hence, with measurement of the value of the absorbed dose D_a in w·sec/kg, and the radiation dose I in amp·sec/kg, U_i is 34 v. With a radiation dose I of 1 r of x-radiation or γ-radiation the absorbed dose D_a at a specific point of the air (under normal conditions) or the air-equivalent substance (provided that electron equilibrium exists) is

$$\left(\frac{1 \text{ electrostatic unit of electricity}}{0.001293 \text{ g of air}}\right) \times \left(2.082 \cdot 10^9 \times \frac{\text{electrons}}{1 \text{ electrostatic unit of electricity}}\right) \times$$

$$\times \left(34 \frac{\text{ev}}{\text{electron}}\right)\left(1.602 \cdot 10^{12} \frac{\text{erg}}{\text{ev}}\right) \times \left(\frac{1 \text{ rad}}{100 \text{ erg/g}}\right) = 0.877 \text{ rad} \simeq 0.88 \text{ rad}.$$

Thus, with measurement of the radiation dose I in roentgens and the absorbed dose in air D_a in rads the coefficient

$$U_i \simeq 0.88 \text{ rad/r}. \tag{10}$$

From the above it follows than when an ionization chamber or some other measuring instrument, calibrated in roentgens by means of a standard chamber or another method records (under the conditions of electronic equilibrium within the walls of the chamber) a radiation dose I roentgens, then at the same measuring point in air, other conditions being equal, the absorbed dose is

$$D_a \simeq 0.88 \text{ I rad} \tag{11}$$

From this relationship it is evident that the roentgen, being the unit of the radiation dose, does not express the absorbed dose in air.

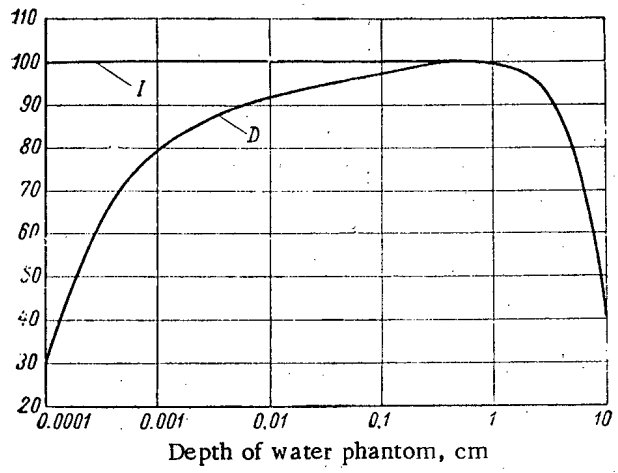

Fig. 1. Radiation dose I and absorbed dose D at different depths of a water phantom for 200 kev x-radiation (depth of establishment of equilibrium 0.3 mm).

To illustrate the hypothesis formulated, Figs. 1-3 give the values of the absorbed doses and radiation doses at different depths of a water phantom for x-radiation with an energy of 200 kev and bremsstrahlung with an energy of 2 and 31 Mev [7]. The radiation dose was calculated theoretically by means of the formulas given,* and the absorbed dose was measured by thimble chambers and in the frontal layers of the phantom by an extrapolation chamber in which the thickness of its upper electrode varied. The chambers were made of a mixture of bakelite and graphite; to improve the conductivity of the electrodes, their surface was coated with a fine layer of metal (vanadium or copper oxide) by spraying. From an examination of the diagrams, it is evident that for 200 kev x-radiation the absorbed dose can be found from the results of measurements of the radiation dose after the establishment of electron equilibrium, attained in the case of this radiation at a depth of 0.3 mm. For 2 Mev bremsstrahlung, electron equilibrium is attained at depth of 5-6 mm, but in this case only an approximate (within the limits of several percent) relation is retained between the radiation dose and the absorbed dose. For 31 Mev bremsstrahlung, the radiation dose expressed in energy units (the roentgen unit is inapplicable to these energies, equal to 93 erg/g) is plotted arbitrarily to illustrate the absence of its conformity to the absorbed dose. This is due to the fact that when electron equilibrium – established in the given case at depths of more than 60 mm – is reached the absorption of the primary radiation is already a substantial factor.

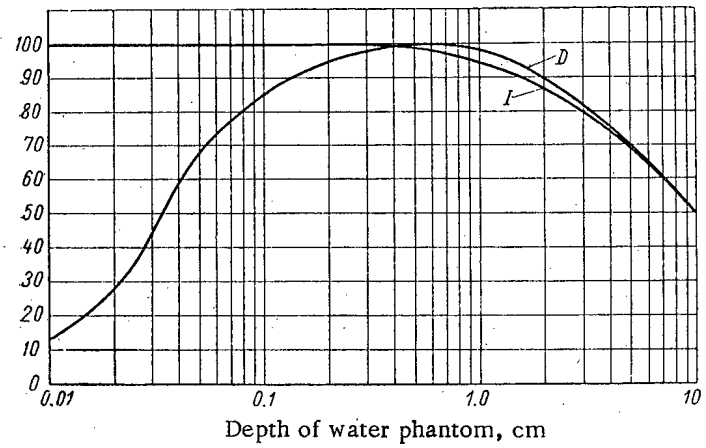

Fig. 2. Radiation dose I and absorbed dose D at different depths of a water phantom for 2 Mev bremsstrahlung (depth of establishment of equilibrium 5 mm).

Taking into account the above-given general equation (7), we may examine two practically important particular cases of electron equilibrium in air-equivalent walls of an ionization chamber. The first of these is associated with the use of an ionization chamber calibrated in roentgens by means of x-rays or γ-rays of the spectral composition which occurs at the point of interest to us of the medium irradiated. This case is most fre-

*The radiation dose curves indicate an attenuation of the primary radiation (in equivalent thicknesses of air, expressed in g/cm^2), on the assumption of absence of the phantom.

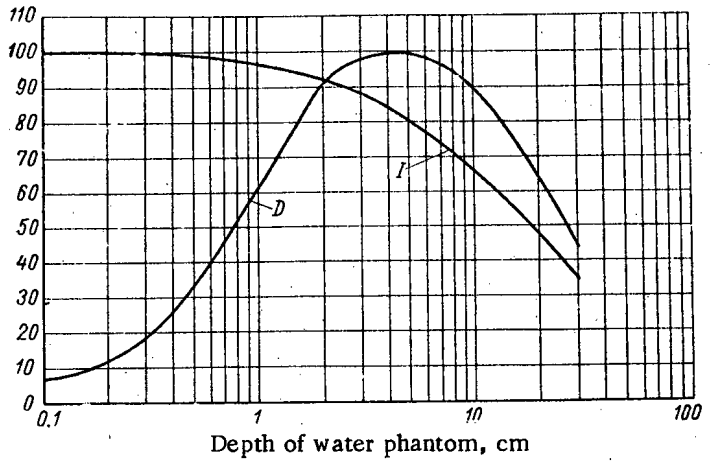

Fig. 3. Radiation dose I and absorbed dose D at different depths of a water phantom for 31 Mev bremsstrahlung (depth of establishment of equilibrium 60 mm).

quently found in radiobiological experiments where the radiation is still generally acute and is produced by means of special x-rays or γ-apparatuses, the radiation spectrum of which is well known and can be reproduced by calibration of the dosimeters. The only limitation (apart from the above mentioned electron equilibrium) imposed on the measuring apparatus is the necessity for fairly small dimensions of the ionization chamber in order that its introduction into the radiation field does not change the latter appreciably. Here the material of the wall may be selected arbitrarily because although it influences the ionization in the chamber, this effect is taken into account in practice when the dosimeter is calibrated by means of the standard chamber.

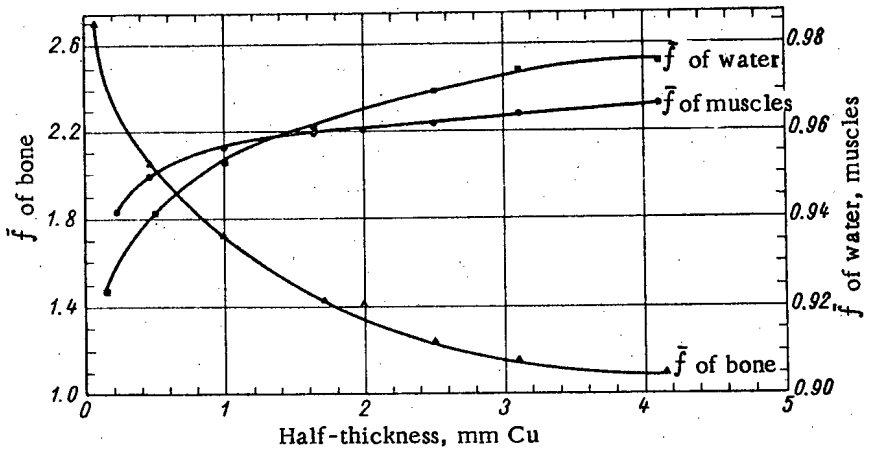

Fig. 4. Values of the coefficient $\bar{f}$ as a function of the half-thickness.

If these requirements are satisfied the absorption dose in medium B can be found from the results of measurement of the radiation dose in air by means of the following equations:

$$D_B = D_a \frac{(m\mu_{en})_B}{(m\mu_{en})_a}, \tag{12}$$

$$D_B = 0.88 I \frac{(m\mu_{en})_B}{(m\mu_{en})_a} = fI \text{ rad}, \tag{13}$$

where $m\mu_{en} = m^{\tau} + m^{\sigma}_{a} + m^{\kappa}$ is the mass absorption coefficient of energy by the medium (or by air), expressed in cm^2/g and calculated for the whole spectrum of the x-radiation or γ-radiation, penetrating the medium at the point in question; m^{τ}, m^{σ}_{a}, m^{κ} are the mass absorption coefficients for the photoeffect, the Compton effect and the process of vapor formation, respectively, and f is a coefficient numerically equal to the ratio of the value of the absorbed dose expressed in rads and the radiation dose expressed in roentgens.

Table 1 gives the values of the mass absorption coefficients of energy for water, soft tissue, and bone tissue in the case of monoenergetic photons, taken from the recent recommendations of the International Commission on Radiological Units and Measurements.

TABLE 1

Values of the Mass Absorption Coefficients of Energy and the Coefficient f

Energy of the photons, Mev	Mass absorption coefficient of energy $(m\mu_{en})$, cm^2/g,				$f\frac{0.88\,(m\mu_{en})\text{ medium B}}{(m\mu_{en})\text{ air}}$		
	Water	Air	Bone tissue	Soft tissue	$\frac{\text{water}}{\text{air}}$	$\frac{\text{bone tissue}}{\text{air}}$	$\frac{\text{soft tissue}}{\text{air}}$
0.010	4.80	4.66	19.0	4.96	0.92_0	3.58	0.93_3
0.015	1.32	1.29	5.80	1.36	0.89_7	4.00	0.92_5
0.020	0.523	0.516	2.51	0.544	0.88_7	4.27	0.92_5
0.030	0.147	0.147	0.743	0.154	0.87_7	4.43	0.91_9
0.040	0.0047	0.0640	0.305	0.0677	0.88_7	4.18	0.92_8
0.050	0.0394	0.0384	0.158	0.0409	0.90_0	3.61	0.93_4
0.060	0.0304	0.0292	0.0979	0.0312	0.91_3	2.94	0.93_7
0.080	0.0253	0.0236	0.0520	0.0255	0.94_0	1.93	0.94_8
0.10	0.0252	0.0231	0.0386	0.0252	0.95_7	1.47	0.95_7
0.15	0.0278	0.0251	0.0304	0.0276	0.97_1	1.06	0.96_4
0.20	0.0300	0.0268	0.0302	0.0297	0.98_2	0.98_8	0.97_2
0.30	0.0320	0.0288	0.0311	0.0317	0.97_7	0.94_7	0.96_5
0.40	0.0329	0.0296	0.0316	0.0325	0.97_5	0.93_6	0.96_3
0.50	0.0330	0.0297	0.0316	0.0327	0.97_4	0.93_3	0.96_6
0.60	0.0329	0.0296	0.0315	0.0326	0.97_5	0.93_3	0.96_6
0.80	0.0321	0.0289	0.0306	0.0318	0.97_4	0.92_9	0.96_5
1.0	0.0311	0.0280	0.0297	0.0308	0.97_4	0.92_7	0.96_5
1.5	0.0283	0.0255	0.0270	0.0281	0.97_3	0.92_9	0.96_6
2.0	0.0200	0.0234	0.0248	0.0257	0.97_4	0.92_0	0.96_3
3.0	0.0227	0.0205	0.0219	0.0225	0.97_1	0.93_7	0.96_3
4.0	0.0205	0.0186	0.0199	0.0203			
5.0	0.0190	0.0173	0.0186	0.0188			
6.0	0.0180	0.0163	0.0178	0.0178			
8.0	0.0165	0.0150	0.0165	0.0163			
10.0	0.0155	0.0144	0.0159	0.0154			

Here, the chemical composition of air, soft tissue and bone tissue was taken in accordance with international recommendations [2].

Table 2 and Fig. 4 give practically important values of the coefficient f, these being the average values of a number of x-ray spectra (both measured experimentally and calculated by means of Kramers' formula [8]).

The method of measuring the radiation dose can also be successfully employed for determining the activity of γ rays of known nature. Thus, for example, at the Second International Conference on the Peaceful Uses of Atomic Energy, a group of British scientists reported [9] that the activity of cobalt sources is easily determined with an accuracy of ± 5% by this method. This must be considered perfectly satisfactory for the majority of purposes.

The second practically important case of absolute measurements of the absorbed dose of x-rays or γ-rays under the conditions of electron equilibrium is associated with the use of a chamber, the walls of which are made of air-equivalent material. The requirements of the preservation of electron equilibrium lead to the imposition of two limitations on the design of the chamber: on the one hand, its walls must be sufficiently thick to exclude any secondary electrons from the external medium surrounding the ionization chamber, and on the other hand, the dimensions of the cavity must be small compared with the paths of the main mass of secondary electrons ionizing the gas of the cavity. The latter condition is difficult to satisfy during measurements of soft x-rays; in

TABLE 2

Mean Absorption Dose per 1 r of Radiation Dose in Water, Soft Tissue, and Bone Tissue with Various X-Ray Spectra

Voltage applied to the tube, kv	Filter thickness, mm	Half-thickness, mm	Spectrum	$\overline{f} = \overline{\frac{pag}{p}}$		
				Water	Soft tissue	Bone tissue
100	0.18 Cu	0,25 Cu or 5.5 Al	Measured	0.91	0.94	3.10
100	0.18 Cu	0.25 Cu or 5.5 Al	Calculated	0.91	0.94	3.13
150	0.075 Cu	0.2 Cu	»	0.92	0.94	2.69
200	0.20 Cu	0.5 Cu	»	0.94	0.95	2.05
250	0.17 Cu+3.0 Al	1.0 Cu	»	0.95	0.95	1.76
250	0.9 Cu+3.0 Al	2.0 Cu	»	0.96	0.96	1.42
280	—	1.7 Cu	Measured	0.96	0.96	1.44
280	—	2.5 Cu	»	0.97	0.96	1.22
280	—	3.1 Cu	»	0.97	0.965	1.13
400	—	4.16 Cu	»	0.97	9.7	1.11

this case, preference must, therefore, be given to the method employing chambers calibrated in roentgens by means of a standard chamber. When an air-equivalent chamber is used, the calculation of the absorbed dose is based on the use of the relation of the theory of the ionization of a cavity, taking into account the relative stopping power $S_{w,a}$ of the material of the wall and air

$$D_c = 0.88\, QS_{w,a}\,\text{rad}, \tag{14}$$

where Q is the charge (in electrostatic units of electricity) which is transferred by the ions of any sign, generated by the radiation investigated, in 1 cm^3 of air under normal conditions. It follows, therefore, that the absorbed dose in medium B can be found by means of the formula

$$D_B = 0.88 QS_{w,a}\frac{(m\mu_{en})_B}{(m\mu_{en})_a}\,\text{rad}. \tag{15}$$

Table 3 gives the values of the mean relative stopping power of carbon, water and muscle tissue in comparison with air, obtained by integration of the energy of the electrons between the limits of zero and the initial (monochromatic) energy of the electrons.

Table 4 gives the results of important practical calculations of the mean stopping power for carbon, water and tissue in comparison with air for the spectrum of Compton electrons formed by Co^{60} and Cs^{137} γ-radiation (including the correction for the density effect [10]).

The importance of using so-called air-equivalent materials as the material for the walls of ionization chambers is evident from the above. Until recently, graphite was considered to be a fairly satisfactory material in this respect; but the increasing accuracy required for radiobiological experiments has recently made it necessary to exclude even the small error associated with the use of graphite. This problem was solved in 1958 by a group of American dosimeter physicists under the leadership of Failla, who employed the method of selecting the composition of an "ideal" wall of conducting plastic, and obtained results, given in detail at the Second International Conference on the Peaceful Uses of Atomic Energy [11]. The composition of the materials, obtained by these investigators, was found analytically on the basis of the solution of a system of equations derived by comparing the ionization characteristics of these substances against air. Polyethylene (CH_2), nylon ($C_6H_{11}NO$), soot (C), silica (SiO_2), and calcium fluoride (CaF_2) were selected as the components of complex conducting plastics.

Data of the recommendations of the International Commission on Radiobiological Units and Measurements [2] were taken as the reference figures for the chemical composition of human muscle and bone tissue.

TABLE 3

Values of the Mean Mass Stopping Powers of Certain Substances in Comparison with Air $\bar{S}$ (Taking into Account the Density Effect)

Initial kinetic energy of electrons, Mev	Values of stopping powers		
	Carbon	Water	Tissue
0.01	1.050	1.202	1.182
0.02	1.044	1.191	1.172
0.03	1.041	1.185	1.166
0.04	1.039	1.181	1.163
0.05	1.038	1.179	1.160
0.06	1.037	1.177	1.159
0.07	1.036	1.175	1.157
0.08	1.035	1.174	1.156
0.09	1.034	1.173	1.155
0.1	1.034	1.172	1.154
0.2	1.030	1.166	1.148
0.3	1.027	1.163	1.145
0.4	1.024	1.161	1.143
0.5	1.022	1.159	1.141
0.6	1.020	1.158	1.140
0.7	1.017	1.156	1.138
0.8	1.016	1.154	1.136
0.9	1.014	1.152	1.134
1.0	1.012	1.150	1.132
2	1.001	1.139	1.121
3	0.985	1.121	1.103
4	0.976	1.110	1.093
5	0.968	1.108	1.084
6	0.961	1.093	1.076
8	0.950	1.080	1.063
10	0.940	1.069	1.052

To determine the numerical values of the percentage composition of the mixture of substances

$$(C)_a\,(CH_2)_b\,(C_6H_{11}NO)_d\,(SiO_2)_e\,(CaF_2)_g$$

the following principles were employed for deriving the equations: a) the values of the nitrogen, hydrogen, and carbon contents were suitably adjusted (in this connection, account was taken of the experimentally found fact that optimum conductivity occurs at a 13.5% free carbon content); b) the amounts of ionic vapor formed by Compton and photoeffects (the latter was standardized for 30 kev) were also suitably adjusted.

As a result of the calculations and a subsequent experimental check, conducting plastics (including tissue-equivalent plastics) were made by this method, making it possible to carry out direct measurements of the absorbed dose in rads, not only for photons in muscle and bone tissue but also for mixed currents of photons and neutrons; the latter is of particular importance in practical dosimetry in nuclear reactors and accelerators of elementary particles. The degree of discrepancy of measurement results obtained by means of these materials from the theoretical values for true tissues is very small, and even in the hitherto most complex region of low energies it is 3-5% (for example, a fiber-equivalent mixture of plastics – a muscle analog – irradiated with γ-rays or neutrons in the energy range of 20-50 kev gives a discrepancy of - 3.7 to + 6.0%, and a similar bone-tissue analog gives a discrepancy of - 1.1 to + 2.1%, etc.). Ionizing chambers with metal walls may, as formerly, be used for relative measurements by determining the correction factors by means of thimble chambers. The report presented to the Second International Conference on the Peaceful Uses of Atomic Energy by the Czech physicist Clumpar [12] may serve as an example of such work. But, the field of application of such transducers is severely limited by the possibility of using them only in radiation fields of known spectral composition.

TABLE 4

Values of the Mean Mass Stopping Powers of Certain Substances in Comparison with Air, Integrated Over the Initial Spectrum of Comptom Electrons Formed by Co^{60} or Cs^{137} γ-Radiation

γ-Ray source	Stopping powers of		
	graphite	water	tissue
Co^{60}	1.01_6	1.15_5	1.13_7
Cs^{137}	1.02_6	1.16_2	1.14_5

Together with the previously indicated advantages of absolute measurements, thimble chambers have certain essentially irremovable limitations which restrict the region of application and the universality of this method. For this reason, research is being conducted in a number of laboratories to find a method which can eliminate the basic limitations of the Bragg-Gray principle (small dimensions of the cavity, the negligibly small absorption of the radiation measured in the walls, the complete absorption of external secondary electrons in the walls), while retaining its advantages. A real success was obtained in this field by the Italian physicist Lonati [13], who developed a fluorescent plastic material

distributed in an irradiated phantom. The subsequent measurement of the total accumulated light, directly associated with the amount of energy absorbed by 1 g of substance, is carried out by means of a chamber to which the plastic detector is transferred. It is interesting to note that Lonati made effective use of two principles developed previously by I. B. Keirim-Markus and V. V. Antonov-Romanovskii and their co-workers in the Soviet Union. We are referring to the ILK method [14], in which the phenomenon of luminescence is employed for measuring the integral radiation dose and the original method, proposed in 1958, for measuring depth doses of thermal neutrons by the secondary γ- radiation of Na^{24} [15]. Lonati abandoned the use of a photoemulsion, which has a nonuniform sensitivity of β particles of different energies, and developed a new plastic material consisting of styrene (97.46 wt. %), terphenyl (2.5 wt. %) and terphenyl butadiene (0.03 wt. %).

Having a density of 1.1 g/cm^3 and a mean effective atomic number almost coinciding with the mean effective atomic number of human tissues, this material makes it possible to measure reliably depth doses of hard x-rays and γ-rays, because its sensitivity to β-particles is constant within a wide energy range.

In practice, it is very often necessary to carry out dosimetric measurements in the absence of electron equilibrium (for example, under conditions of transient effects at the boundaries of tissue-air or bone-tissue regions). In such cases, the present-day recommendation is to use an air ionization chamber with walls thick in comparison with the path of secondary electrons at the point in question of the medium irradiated. If the walls are so thin that they form a negligibly small part of the total ionization of the air cavity, the composition of the wall may be arbitrary. But, in practice, this requirement is difficult to satisfy and the walls of the chambers may therefore be made of a substance whose composition is closest to the composition of the medium directly surrounding the measuring apparatus. In such cases, the depth of the ionization chamber in the direction of the gradient of the absorbed dose must obviously be small. If, under these conditions, ions of any sign, formed by the radiation investigated in 1 cm^3 of air, transfer under normal conditions a charge of Q electrostatic units of electricity, the general relation of the theory of ionization of a cavity

$$D_B = 0.88 S_{Ba} Q \text{ rad}. \tag{16}$$

is applicable.

The above-mentioned materials indicate that in the majority of possible radiobiological and physical experiments for investigating the effect of nuclear radiations on a substance, the absorbed dose of x-rays and γ-rays can be found from the results of absolute measurements of the radiation dose. Since the concept of the roentgen is applicable to energies of radiations reaching 3 Mev, this method is employed in the most widely distributed energy range of x-rays and γ-rays.

LITERATURE CITED

1. A. M. Kuzin, Proceedings of the All-Union Conference on the Use of Isotopes and Nuclear Radiations. Radiobiology [in Russian] (Izd. AN SSSR, Moscow, 1958) pp. 3-13.
2. Report of the International Commission on Radiological Units and Measurements (ICRU). National Bureau of Standards Handbook 62 (1957).
3. H. Franz and W. Hubner, Report No. 971, presented by Federal German Republic Delegation to the Second International Conference on the Peaceful Uses of Atomic Energy (Geneva, 1958).
4. H. Woodard and F. Spiers, Brit. J. Radiol. 26, 301, 38 (1953).
5. U. Fano, Rad. Res. 1, 3, 237 (1954).
6. L. Gray, Proc. Roy. Soc. A156, 578 (1936).
7. W. Oosterkamp, Appl. Sci. Res. 3, 2, 100 (1953).
8. H. Kramers, Philos. Mag. 46, 836 (1923).
9. W. Eastwood, R. West, and E. Wiblin, Report No. 288, presented by the British Delegation to the Second International Conference on the Peaceful Uses of Atomic Energy (Geneva, 1958).
10. R. Sternheimer, Phys. Rev. 103, 3, 511 (1956).
11. F. Shonko, J. Rose, and G. Failla, Report No. 753, presented by the U.S. Delegation to the Second International Conference on the Peaceful Uses of Atomic Energy (Geneva, 1958).
12. I. Klumpar, Report No. 2108, presented by the Czechoslovak Delegation to the Second International Conference on the Peaceful Uses of Atomic Energy (Geneva, 1958).
13. R. Lonati, Report No. 1393, presented by the Italian Delegation to the Second International Conference on the Peaceful Uses of Atomic Energy (Geneva, 1958).

14. V. V. Antonov-Romanovskii, et al., Session of the Academy of Sciences, USSR, on the Peaceful Uses of Atomic Energy (Meeting of the Fiz-Math. Sci. Section) [in Russian] (Izd. AN SSSR, Moscow, 1955) p. 342.
15. A. G. Istomina and I. B. Keirim-Markus, Physics and Thermotechnics of Reactors. Supplement No. 1 to the Journal Atomnaya Energiya [in Russian] (Atomizdat, Moscow, 1958) p. 136.

ON THE He^7 ISOTOPE

V. V. Balashov

Translated from Atomnaya Énergiya, Vol. 9, No. 7,
pp. 48-49, July, 1960
Original article submitted May 9, 1959

In [1, 2] on the basis of a calculation of nuclear levels of Li^7, the author decided that a radiation stable nucleon of the He^7 isotope might exist. According to calculations, the first three states of the Li^7 nucleus with an isotopic spin T = 3/2 lie at energies of 10.1 Mev (J = 3/2), 12.4 Mev (J = 1/2), and 13.2 Mev (J = 5/2). In accordance with the rules of selection with regard to isotopic spin these states can appear in the reaction $Li^7(\gamma, n)Li^{6*}$ and are forbidden in the reaction $Li^7(\gamma, H^3)H^4$. In actual fact, experimental studies of the reaction (γ, n) indicate the existence in this region of energies of free levels at 10.8, 12.4, and 14.0 Mev, which are not observed in the reaction (γ, H^3), whereas the neighboring states at 9.3 and 17.5 Mev, having T = 1/2, are observed in both reactions [3].

A nucleus with T = 3/2 form an isotopic quartet; the basic state of the He^7 nucleus (and also B^7) corresponds to the lowest excited state of Li^7 with T = 3/2. It therefore follows that the energy of the He^7 bond with respect to decomposition to He^6 and a neutron is very small: it is several tens of kiloelectron volts (for the existence of the nucleus stable He^7 isotope, the first level of the Li^7 nucleus with T = 3/2 should lie not higher than 10.81 Mev). Since the accuracy of the experiments on which the identification of the Li^7 levels is based is low, the "safety factor" when determining the energy of the He^7 bond is very small. Strictly speaking, it should be assumed that the energy of the He^7 bond (within the limits of experimental errors) is equal to zero and therefore the problem of the existence of the He^7 isotope is open.

Some experiments are described below dealing with this problem.

Experiments on the preparation and direct detection of the He^7 isotope. The He^7 nucleus should be β active. During β decay there should be transitions to the basic and first excited (0.477 Mev) states of Li^7. The upper boundary of the β spectrum is equal to ~ 10 Mev. The value of $\log f\tau$, calculated from the model of shells in the approximation of the j–j bond, is equal to 3.26 and increases on deviation from the j–j bond arrangement. The life of the He^7 isotope should therefore be ~ 30-100 msec. Decay can be observed both directly and from the radiation transition between the first excited and basic states of Li^7.

The He^7 isotope can be obtained in the following reactions:

$Li^7(n, p)He^7$	$Li^7 + \pi^- \rightarrow He^7$
$Be^9(\gamma, 2p)He^7$	$Q \simeq -10$ Mev
$Be^9(n, He^3)He^7$	$Q \simeq -29$ Mev
$Li^7(d, 2p)He^7$	$Q \simeq -21$ Mev
$C^{12} + \pi^- \rightarrow He^7 + \alpha + p$	$Q \simeq -12$ Mev
$B^{11} + \pi^- \rightarrow He^7 + \alpha$	

In the case where the state corresponding to He^7 lies in the region of positive energy, it should appear in all the given reactions from the characteristic correlation of He^6 and a neutron.

It is stated in [4] that during the absorption of negative π-mesons in carbon, together with β activity caused by decay of B^{12} (τ = 20 msec), activity was detected with τ = 80 msec. Its nature is not clear to the authors. Although the life of the unknown nucleus agrees extremely well with the calculated life of the He^7 isotope, one experiment is not sufficient confirmation of the fact that the He^7 isotope exists.

Indirect experiments. Experiments in which levels of Li^7 with T = 3/2 are detected are very inaccurate: the energies of the levels are determined from the output curve. Experiments can be carried out which are immediately directed to the study of Li^7 and Be^7 levels with T = 3/2. As well as the mentioned reactions (γ, n) and (γ, H^3) which should have been studied more accurately, we observed the reactions $Li^6(p, p)Li^6$ and $He^4(He^3, He^3)He^4$.

Due to the disturbance in the purity of the states with regard to isotopic spin, connected with Coulomb reaction, the given width of the first level of Be^7 with T = 3/2 with respect to the canals $Li^6 + p$ and $He^4 + He^3$ is $\sim 1\%$ of the Wigner limit. The canal corresponding to the formation of Li^6 in the excited phase with T = 1 (J = 0; E = 3.57 Mev), is forbidden for s-protons, and for p-protons it is very weak, since the energy removed by the proton is equal to ~ 0.5 Mev. Therefore, the cross-sections of the indicated reactions should reveal sharp resonance peaks at energies corresponding to the first level of Be^7 with T = 3/2.

The author would like to thank Yu. M. Shirokov for his interest in the work.

LITERATURE CITED

1. V. V. Balashov, Report to the Ninth Annual Conference on Nuclear Spectroscopy [in Russian] (Kharkov, 1959).
2. V. V. Balashov, Dissertation [in Russian] (Izd. MGU, 1958).
3. F. Ajzenberg and T. Lauritzen, Rev. Mod. Phys. 27, 77 (1955).
4. J. Burgman, and I. Fiselur, Phys. Rev. Letter 1, 469 (1958).

THE THERMAL ELECTRON CONVERSION OF THERMAL ENERGY INTO ELECTRICAL ENERGY USING THORIUM CARBIDE

N. D. Morgulis and Yu. P. Korchevoi

Translated from Atomnaya Énergiya, Vol. 9, No. 7, pp. 49-51,
July, 1960
Original article submitted February 6, 1960

The problem of the direct conversion of nuclear (thermal) energy to electrical energy using thermal electron emission has recently attracted a considerable amount of interest. The first work in this field was presented in a review [1] where we considered the following cases:

1. The use of pure difficult-to-fuse metals as the cathode – tungsten in cesium vapors. With a cathode temperature T = 2500°K, in 1949, energy conversion efficiencies $\eta \simeq 1\%$ were obtained and useful power $\omega \simeq 1$ w/cm^2, specific with respect to the cathode. The principle of operation of similar converters with a cesium filler was given further development in other papers [1].

2. The use as a cathode of a two-component low temperature (Ba-W) metal film l -cathode in cesium vapors. In a similar way we obtained for T = 1300°C, $\eta \simeq 5\%$ and $\omega \simeq 0.6$ w/cm^2.

In the present work, we sought a cathode material of the single component type, which could give noticeable emission in the middle range of temperatures T ≃ 2000°K and which would not have a particularly small work of removal of the electron φ_c. The latter was necessary in order to provide: 1) a uniform and noticeable thermal ionization of cesium vapors over the whole surface of the cathode, neutralizing the electron space discharge, and 2) a high value of the emf $\delta \simeq (V_c + V_0) \approx V_c$, and values ω and η of a similar converter; here, $V_c = (\varphi_c - \varphi_a)$ is the contact difference in potentials between the cathode and the anode, which have a work of removal φ_c and φ_a, $V_0 = (2e/c)\, T_c - T_a$. From this point of view, from the existing very sparse data [2] thorium bicarbide (ThC_2) seemed to combine the above properties, for which reason it was chosen for the investigation. In [3] mention is also made of thorium carbide for the thermal electron conversion of energy, the values obtained being $\eta > 15\%$ and $\omega > 15$ w/cm^2.

In the first stage of the experiments, diodes in cesium vapors were used. The cathode was a narrow tungsten ribbon having a fine layer of ThC_2 on the middle section; the anode was made of tantalum and had protective rings on the ends; the distance between the electrodes was about 1.5 mm. The cathode temperature was determined by an optical micropyrometer on the assumption that ThC_2 radiates as a black body [2]. A drop of metallic cesium was introduced into the lamp; its vapor pressure p was determined by the temperature t of the lamp bulb, placed in a thermostat with controllable temperature. To prevent the distorting effect of the magnetic field of the filament current and the longitudinal drop in potential, the cathode was fed with alternating current with a rectifier in the filament circuit, using the known arrangement for determining the cathode parameter with an oscillograph in the half period blocking the filament current.

The electron parameters of ThC_2 were determined in parallel by the methods of electron and ionic emission. In the first case, the temperature dependence was determined for the electron emission I_e with a cold lamp bulb, i.e., with a very low vapor pressure p. A plot was made of the Richardson relationship $\lg(I_e/T^2) = f(1/T)$ (Fig. 1). From the angular factor of the obtained straight line it was found that $f_c = 3.2$ ev and the constant A = 200 amp/cm$^2 \cdot$ deg^2. In the second case, the temperature dependence was determined for the ionic emission I_p, i.e., the current of cesium ions obtained on the cathode by the thermal ionization of the atoms of its vapors; the lamp

bulb was heated to t ≃ 95°C where p ≃ $4 \cdot 10^{-4}$ mm Hg. A plot was made of the relationship lg $I_p = f(1/T)$, which, according to theory, was represented by the straight line 2 of Fig. 1. From its angular factor it was found that f_c = 3.4 ev. The value α, the probability of ionization of a cesium atom on the ThC_2 surface (for example, at 1900°K), was equal to ~ 7%, whereas theoretically (not distinguishing ThC_2 from the metal) $\alpha = 1/2 \exp [-e/kT \times (V_i - \varphi)] \simeq 2.4\%$. Both these methods therefore give a value of φ_c which is practically the same and close to that of [2], i.e., there is a noticeable and useful contact difference (as regards sign) in potentials $V_c \simeq$ ≃ 1.6 − 1.8 v relative to the anode covered with a film of cesium.

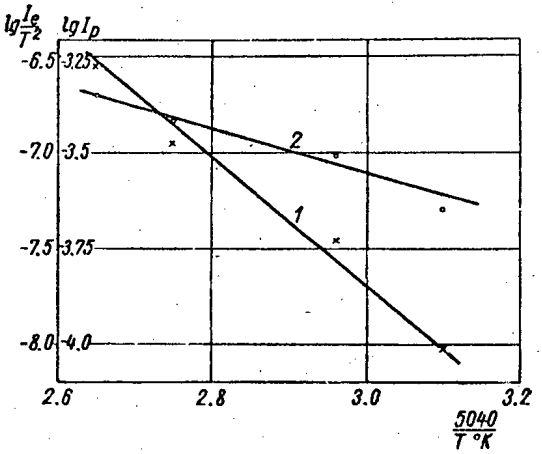

Fig. 1. The relationship between the electron (curve 1) and ionic (curve 2) emissions and the temperature.

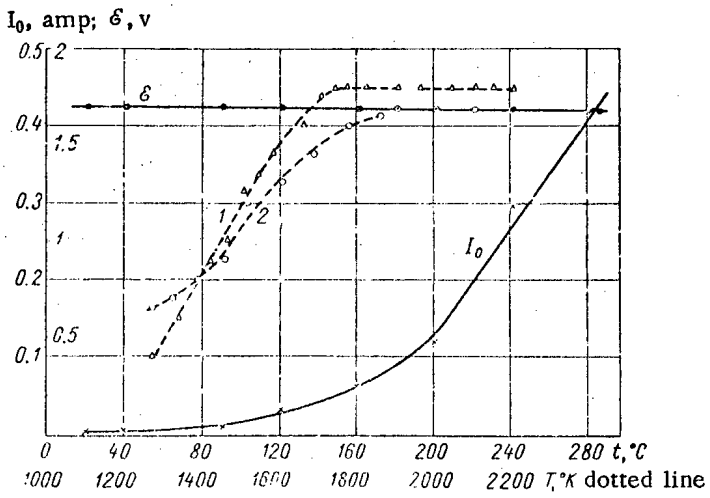

Fig. 2. The dependence of the short circuited current I_0 and the emf of conversion of $\mathcal{E}$ on the vapor pressure of cesium (expressed by t − the bulb temperature) at T = 2000°K (continuous curves) and the emf $\mathcal{E}$ on the cathode temperature T for t equal to 20 and 250°C (dotted curves 1 and 2, respectively).

We will consider the operation of lamps in a system of energy conversion. We will first determine the short circuited current I_0 and the emf of conversion $\mathcal{E}$ depending on the values of p or t for a fixed value of T. For T = 2000°K these relationships are given by the continuous curves of Fig. 2; we see here that the emf has an actually constant value $\mathcal{E}$ = 1.7 v which is close to V_c; the value of I_0 at t ≥ 100−120°C begins to increase rapidly, indicating the large store of emission at the cathode. The dotted curves of Fig. 2 show the relationship between the emf $\mathcal{E}$ and the temperature of the cathode T for the cases t = 20°C (curve 1) and t = 250°C (curve 2).

Now selecting t = 250°C (p ≃ 0.5 mm) and T = 2100°K, we plot the basic load characteristics of the conversion, i.e., the dependence of the current I_R, the drop in potential $V_R = I_R R$ and the useful power $W_R = I_R^2 R$, obtained on connecting an external resistance R into the circuit; these characteristics are represented in Fig. 3. As would be expected [1], for a value of R equal to the internal resistance R_i, the value $W_R = \omega S_c$ passes through a maximum, where we obtain $\omega \simeq 16$ w/cm², $V_R \simeq$ ≃ 1.1 v, $R_i \simeq 0.1$ ohm/cm²; furthermore, in this system $\mathcal{E}$ = 1.7 v and $I_0 \simeq 19$ amp/cm². The determination of the conversion efficiency presents considerable difficulties. In the present method of operation the cathode temperature was established pyrometrically with the circuit switched off, and the obtained filament power W_H was kept constant. However, during operation of the lamp the energy balance of the cathode is considerably disturbed. Since the cathode temperature cannot be determined pyrometrically during operation owing to the luminescence of the cesium vapors, we will only indicate the limits within which the value of η should lie; these are:

$$\frac{\omega}{W_H + I_R \varphi_C} \leqslant \eta \leqslant \frac{\omega}{W_H}.$$

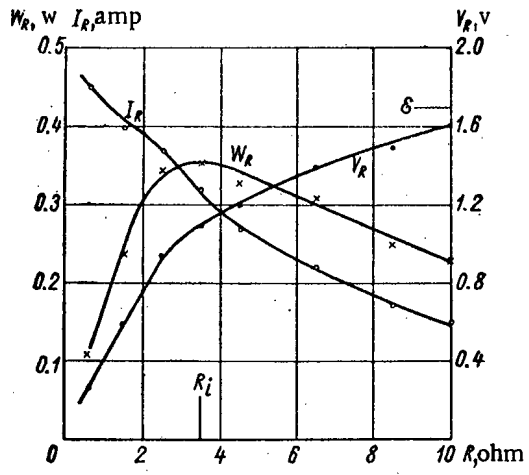

Fig. 3. The load characteristics of the conversion for t = 250°C and T = 2100°K.

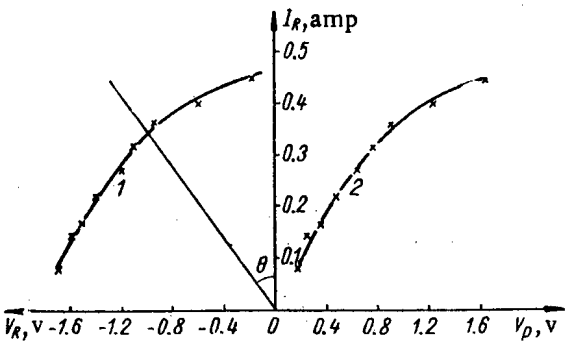

Fig. 4. Volt-ampere curves: 1) external circuit; 2) internal circuit (T = 2100°K; t = 250°C).

In this way for the data of Fig. 3 we obtain a value $\eta \simeq 10$-15%, which together with $\omega \simeq 16$ w/cm^2 is very favorable.

For the more complete characteristics of a similar conversion we give a table for the various systems of T and t. They indicate that at T = 2000-2100°K and t = = 250°C there are stable values of $\mathcal{E} = 1.7$ v, $\omega > 10$ w/cm^2 and $\eta \simeq 10\%$. All these values of ω and η are very satisfactory, judging from the data published in [1], in particular the data for the average T $\simeq$ 2000°K.

Figure 4 shows the two volt-ampere curves obtained on the basis of the data in Fig. 3: of the external circuit, i.e., the electron current I_R in relation to the potential V_R (the dynamic characteristics are given here, i.e., a straight line corresponding to the condition $tg\theta = R$), and the internal circuit of the converter, i.e., of the same current I_R in dependence on the potential $V_p = (\mathcal{E} - V_R)$, falling on its internal section. Curve 1 – essentially a delay curve – characterizes the useful function of the converter, i.e., the values I_R, V_R, and W_R; the saturation region for small values of V_R is expressed very unclearly for reasons which are not yet known. Curve 2 has the interesting feature that it has no sections where the condition $dV/dI \leq 0$, holds, characterizing the usual arc discharge. It can therefore be assumed that in this case, the space between the electrodes of the converter is mainly filled with a thermal ionization plasma, i.e., a medium where the electrons and the ions (having the same concentration) are obtained independent of one another (thermally) on the cathode surface. In this case the medium acts to some extent as an internal resistance [1].

Our preliminary results therefore confirm the possibility of obtaining appreciable values of ω and η in the middle temperature region ~ 2000°K also.

Data on the Various Systems of T and t During Operation of the Lamp in the Energy Conversion System

T, °K	t, °C	$\mathcal{E}$, v	I_0, amp/cm^2	ω, w/cm^2	η, %
1900	200	1.7	5	2	2
1900	250	1.7	12	8	8—10
2000	250	1.7	15	11	8—12
2100	250	1.7	19	16	10—15

The authors are deeply grateful to Professor G. V. Samsonov (Institute of Carbides and Special Alloys of the Academy of Sciences of the UkrSSR) for kindly preparing the thorium carbide.

LITERATURE CITED

1. N. D. Morgulis, Uspekhi Fiz. Nauk 70, 679 (1960).
2. D. Goldwater and R. Haddad, J. Appl. Phys. 22, 70 (1951); D. Wright, Proc. Instn. Electr. Engrs., III, No. 100, 125 (1953).
3. R. Fox and W. Gust, Bull. Amer. Phys. Soc. 4, 322 (1959).

THE EFFECT OF INTERNAL HEAT SOURCES ON CONVECTIVE HEAT EXCHANGE

É. A. Sidorov

Translated from Atomnaya Énergiya, Vol. 9, No. 7,
pp. 51-52, July, 1960
Original article submitted December 28, 1959

It is a well-known fact that in some cases the movement of liquids and gases is accompanied by physical and chemical processes involving the evolution or absorption of thermal energy. In [1, 2] a study was made of the internal thermal evolution during the movement of liquids in a stabilized section of tubes with a constant value of the density of the incoming (or outgoing) thermal stream.

We will consider the effect of internal heat sources on the intensity of convective heat exchange for the general case of flow round curved surfaces for any character of change in density of the thermal stream and any law for change in temperature of the surface round which the flow takes place.

We will write the initial equation for energy in the integral form:

$$\frac{d}{dx}(Ut_0\varphi)=\frac{1}{\varrho c}(q+W\delta). \tag{1}$$

This equation holds both for laminar and turbulent flow. The following symbols are used: x – the coordinate axis coinciding with the direction of movement of the liquid or gas; U – the speed of the medium beyond the limits of the boundary layer; $t_0 = T_0 - T_1$, where $T_0 = \text{const}$ – the temperature of the medium beyond the limits of the boundary layer, $T_1 = T_1(x)$ – the temperature of the surface round which the flow takes place; φ – the extent of the enthalpy loss; ρ and c – the density and specific heat of the medium, respectively; q – the density of the thermal stream at the boundary of the medium and the surface of the body; W – the volumetric power of the internal sources of heat evolution; δ – the thickness of the temperature boundary layer.

As shown by the analysis of [3], the form of the functional dependence $q = q(\varphi)$ is very little affected by the presence of a pressure gradient and the nonisothermal nature of the surface around which flow takes place. It can therefore be assumed that there is an invariant character in the form of the functional dependence $q = q(\varphi)$ in the presence of other factors also, especially internal sources of heat. Substituting the relationships in [4] for the gradient-less flow

$$\delta = m\varphi \tag{2}$$

and

$$q=A\varrho cUt_0Pr^{2/3(s-1)}\left(\frac{U\varphi}{\nu}\right)^s \tag{3}$$

in equation (1) and solving it with respect to φ for the boundary condition $\varphi(0) = 0$, we obtain

$$\varphi=\frac{1}{Ut_0}[A(1-s)]^{\frac{1}{1-s}}Pr^{-2/3}\nu^{\frac{s}{s-1}}\exp\left(\frac{mWx}{\varrho cUt_0}\right)\times\left\{\int_0^x Ut_0^{1-s}\exp\left[-\frac{m(1-s)Wx}{\varrho cUt_0}\right]dx\right\}^{\frac{1}{1-s}}. \tag{4}$$

Here ν is the kinematic viscosity of the medium; Pr is the Prandtl number; A, m, s, are dimensionless constants characterizing the flow (for a liminar system A = 0.222, m = 7.55, s = − 1, for a turbulent system A = 0.00658, m = 10.3, s = − 1/6).

Substituting now the solution of (4), taking into account the effect of internal heat sources in the invariant relationship (3), we find the following expression for the intensity of heat exchange in the presence of internal sources (in a dimensionless form):

$$Nu=(1-s)^{\frac{s}{1-s}}A^{\frac{1}{1-s}}Re^{\frac{1}{1-s}}Pr^{1/3}\exp\left(\frac{msWx}{\varrho cUt_0}\right)\times\left\{\frac{1}{Uxt_0^{1-s}}\int_0^x Ut_0^{1-s}\exp\left[-\frac{m(1-s)Wx}{\varrho cUt_0}\right]dx\right\}^{\frac{s}{1-s}}, \quad (5)$$

where Nu = $qx/\lambda t_0$ is the Nusselt number; Re = Ux/ν is the Reynolds' number. It follows from expression (5) that in the "pure form" the effect of the influence of internal heat sources can only be described analytically for the case of flow round plane isothermal surfaces (U = const; t_0 = const). In this case from formula (5) we have

$$Nu=Nu_0\left[\frac{1}{Z}(\exp Z-1)\right]^{\frac{s}{1-s}}, \quad (6)$$

where $Z = m(1-s)Wx/\rho cUt_0$ is a dimensionless parameter, characterizing the presence of internal heat sources; Nu_0 is the value of the Nusselt number in the absence of sources. Analyzing expression (6) it can readily be seen that the evolution of heat (W > 0) by sources leads to a reduction of the coefficient of heat transfer $\alpha = q/t_0$, and the absorption of heat (W > 0) increases α. It also follows from expression (6) that with laminar flow this influence appears to a greater degree than with turbulent flow. Both these conclusions agree with the results [1, 2].

LITERATURE CITED

1. G. Muller, Am. Soc. Mech. Eng., Paper No. 58-HT-17, 1 (1958).
2. S. S. Kutateladze, N. I. Ivashchenko, and T. V. Zablotskaya, Atomnaya Énergiya, 7, 3, 253 (1959).
3. G. S. Ambrok, Zhur. Tekhn. Fiz. 27, 9, 2134 (1957).
4. L. G. Loitsyanskii, The Mechanics of Gases and Liquids [in Russian] (Moscow, Physics and Mathematics Press, 1958).

AN INTIMATE INTERGROWTH OF URANINITE AND A ZIRCONIUM MINERAL

V. I. Zhukova

Translated from Atomnaya Énergiya, Vol. 9, No. 7, pp. 52-54, July, 1960
Original article submitted November 27, 1959

During a study of complex cobalt-nickel sulfide and uranium ores, localized in dolomites and quartz-albite-chlorite schists, it was discovered that the uraninite in these ores contains a considerable quantity of zirconium and rare earths (especially yttrium and elements of this group).

In the dolomites the uraninite forms thin (fractions of a centimeter) veinlets and nests of colloform material. Minerals associated with the uraninite are chalcopyrite, millerite, polydymite, bravoite, chlorite, talc, and calcite. In the quartz-albite-chlorite schists, uraninite metasomatically replaces rock-forming minerals, fills interstices, and forms small veinlets and lenses. The uraninite is associated with pyrite, chalcopyrite, marcasite, hematite, pyrrhotite, arsenopyrite, cobaltite, gersdorfite, chlorite, tourmaline, quartz, and calcite.

The physical properties of the uraninite containing zirconium are no different from the properties of ordinary uraninite. In particular, the microhardness ranges from 580 to 1070 kg/mm^2.

The chemical composition of the uraninite is shown in Table 1. Because of the difficulty of separating pure uraninite, especially from the schists, somewhat impure samples were analyzed.

TABLE 1

Chemical Composition of Uraninite (in percent)

Oxides	Uraninite from dolomites (analyzed by Z. I. Donskikh)	Uraninite from quartz-albite-chlorite schists (analyzed by L. V. Snegireva)
MgO	0.42	3.32
CaO	0.65	1.10
PbO	0.87	0.56
TR_2O_3	1.85	1.30
Fe_2O_3	0.07	0.64
UO_2	46.14	41.12
UO_3	42.55	31.47
SiO_2	1.52	4.40
CuO	–	0.37
ZrO_2	5.10	2.13
TiO_2	–	0.14
H_2O	0.40	0.7
Loss on heating (300°C)	Not determined	0.2
Totals	99.57	99.60*

*Including 8.40% carbon dioxide gas, 0.15% sulfur, and 3.6% other elements (antimony, tungsten, potassium, and others).

TABLE 2

Determinations of Zirconium and Rare Earths in Uraninite by X-Ray Spectral Means (in percent)

Sample number	Zr	Y	Ce	La	Sm	Nd	Dy	Gd
				Uraninite from dolomites				
1	1	0.65	0.05	Not Found	0.05	0.05	Not Found	0.05
2	2.3	0.70	0.05	» »	0.1	0.1	0.1	0.1
3	3.0	1.2	0.07	» »	0.2	0.3	0.3	0.3
4	4.0	0.9	Not Found	» »	0.3	0.3	0.3	0.3
5	1.5	0.3	» »	» »	Not Found	Not Found	Not Found	Not Found
6	9.5	4.5	0.05	» »	0.15	0.4	0.4	0.5
7	5	2.0	0.1	» »	0.3	0.3	0.3	0.5
8	10	2.5	0.15	» »	0.3	0.4	0.3	0.5
9	2.2	1.4	0.1	» »	0.1	0.1	0.05	0.1
10	2.5	1.2	0.05	» »	0.05	0.2	0.05	0.05
11	3.2	1.5	0.05	» »	0.05	0.05	0.05	0.05
				Uraninite from quartz-albite-chlorite schists				
12	0.4	0.8	0.1	Not Found	Not Found	0.15—trace	Not Found	Not Found
13	0.4	0.4	0.05	0.05	» »	0.15	» »	» »
14	0.4	0.3	0.05	0.05	0.05	0.1	0.05	0.05
15	1.5	0.6	0.1	0.05	0.1	0.1	0.05	0.15
16	1.5	0.3	0.07	0.07	0.1	0.1	0.15	0.1
17	0.9	0.3	0.1	0.1	0.3	0.3	0.05	0.1
18	1.0	0.7	0.07	0.05	0.15	0.15	0.05	0.1
19	1.0	0.3	0.1	Not Found	0.15	0.15	0.07	Not Found
20	1 0	0.1	0.1	» »	Not Found	0.15	0.1	» »
21	0.7	0.4	0.2	0.2	0.15	0.15	0.15	0.1
22	1.0	0.3	0.1	Not Found	0.1	0.1	0.07	0.1

Note: Admixtures of thorium were detected in none of the samples.

TABLE 3

Line Intensities and Interplanar Distances of Zircon (Standard) and of the Insoluble Residue Before Heating

Zircon (standard)									Insoluble residue		
Line No.	*I*	*d/n*	Line No.	*I*	*d/n*	Line No.	*I*	*d/n*	Line No.	*I*	*d/n*
1	2	5.20	11	8	2.06	21	2	1.288	1	Weak, broad	3.31
2	4	4.44	12	3	1.900	22	2	1.256	2	Weak	2.71
3	3	3.65	13	3	1.881	23	1	1.248	3	Medium, broad	2.51
4	10	3.30	14	2	1.819	24	7	1.187	4	The same	1.913
5	1	3.17	15	4	1.750	25	2	1.164	5	Strong	1.682
6	1	2.76	16	10	1.706	26	8	1.107	6	Weak, broad	1.635
7	1	2.70	17	8	1.641	27	8	1.099	7	Very weak	1.563
8	1	2.56	18	7	1.476	28	8	1.057	8	Medium	1.536
9	8	2.50	19	8	1.380	29	8	1.050	9	Weak	1.448
10	2	2.32	20	2	1.360	30	8	1.035	10	Weak, very broad	1.353

Table 2 supplies data of x-ray spectral analyses, which show that the zirconium content in the uraninite ranges from hundredths of a percent to 10%, and the total content of rare earths from 0.5 to 6%. In this regard, the uraninite from the dolomites contains much more zirconium and rare earths than the uraninite from the schists.

Microscope studies, including high-magnification opaque investigation, revealed no rare-earth or zirconium minerals in ore samples. Zirconium and rare earths are absent from all ore and vein minerals that accompany

the uraninite; neither do they occur in the dolomitic host rocks. In the quartz-albite-chlorite schists and in individual rock-forming minerals in the schists, zirconium has been detected in amounts of hundredths of a percent.

X-ray studies of carefully sorted uraninite have shown no supplementary lines pointing to the presence of foreign mineral impurities. The lattice constant is 5.44-5.45 A. The effect of admixtures of zirconium on the lattice parameter was not established. X-ray photographs of the products of roasting (up to 1000°C) zirconium-bearing uraninite and zirconium-free uraninite are completely identical. Heating up to 500°C produces a decrease in the parameter of the cubic lattice, down to 5.39 A, after which the hexagonal phase of U_3O_8 appears. In this process, no supplementary lines belonging to products of zirconium have been detected on the photographs.

When the uraninite is dissolved in 5%-HNO_3 during heating, yttrium (and other rare earths) pass completely into solution along with the uranium, and zirconium is partly dissolved. Most of the zirconium is concentrated in the insoluble residue. The quantity of highly mobile zirconium, determined by dissolving uraninite in concentrated HNO_3, constitutes about 40% of the total zirconium. The color of the insoluble residue is white. Under the microscope (in immersion oils), this residue forms an isotopic mass (with a refractive index no greater than 1.57) in which small highly birefringent crystals may be observed. These crystals suggest zircon in form, but are distinguished by a lower index of refraction (1.60). After roasting the powder at 1100°C, the index of refraction is 1.57-1.60. The differential thermal curve shows a single endothermic effect at 100°C.

X-ray powder photographs of the insoluble residue show weak diffuse lines corresponding to the lines of zircon (Table 3); these become more distinct after heating at 900°C.

Thus, the investigations made on these ores lead us to believe that the ores contain a rare example of intimate intergrowth of uraninite and a zirconium mineral, in all probability zircon. A recalculation of the necessary quantity of SiO_2 to form zircon shows that in the uraninite from the dolomites (considering the undissolved part of zirconium to be 60% of the total zirconium in the uraninite) almost all the silica (1.46% out of 1.52%) may be bound up in the zircon, but in the uraninite from the schists, there is an excess of silica. This latter relationship is explained by the presence of foreign mineral impurities.

The mineral form of the rare earths and of the highly mobile zirconium has not been determined. From the fact that they pass easily into solution during the decomposition of the uraninite, it may be supposed that the rare earths are present in isomorphous admixtures.

A STUDY OF THE SYSTEMS $BeO-Sm_2O_3$ and $BeO-Gd_2O_3$

S. G. Tresvyatskii, V. I. Kushakovskii, and V. S. Belevantsev

Translated from Atomnaya Énergiya, Vol. 9, No. 7, pp. 54-55, July, 1960
Original article submitted January 7, 1960

To study the systems $BeO-Sm_2O_3$ and $BeO-Gd_2O_3$ oxides were taken containing more than 99.5-99.9% of the basic component. The main impurities in the oxides of samarium and gadolinium were other rare earths and in the oxides of beryllium they were calcium, aluminum, magnesium, and certain other elements in quantities from 0.001 to 0.1%.

The temperatures of the liquidus and solidus in the studied systems were measured by high temperature thermal analysis in molybdenum crucibles in an atmosphere of argon using tungsten-molybdenum thermocouples [1]. Figure 1 shows the calibration curve for these thermocouples. The temperatures of the solidus for some mixtures of the system $BeO-Sm_2O_3$ were also determined by thermal analysis with a platinum-platinorhodium thermocouple.

The composition of the eutectic was determined by chemical analysis of the slowly crystallized alloys, the structure of which corresponded to that of the pure eutectic. Chemical analysis was also carried out on hypoeutectic and hypereutectic alloys containing 2-3 mole % of excess component in comparison with the eutectic composition, the presence of which was determined microscopically in reflected light.

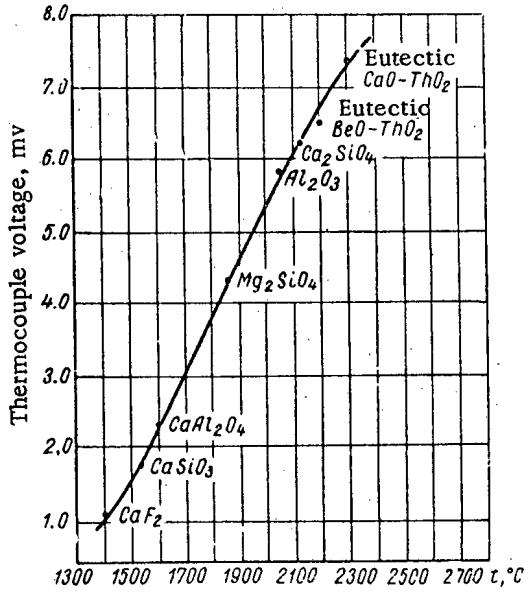

Fig. 1. Calibration curve for tungsten-molybdenum thermocouples.

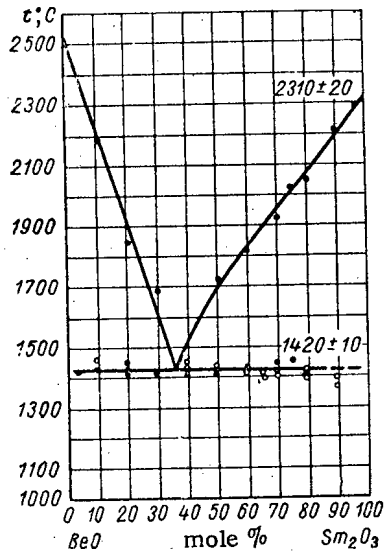

Fig. 2. Phase diagram for the system $BeO-Sm_2O_3$ in a temperature range 1300-2500°C. Temperatures determined by thermal analysis using thermocouples: ●—tungsten-molybdenum; O—platinum-platinorhodium.

The chemical analysis of the above and certain other alloys showed that their compositions hardly differ from the charge composition; this meant that the phase diagrams could be plotted from the charge compositions.

According to the microstructures of fused specimens in the hypoeutectic alloys initially there is crystallization of beryllium oxide and in the hypereutectic alloys there is the crystallization of samarium oxide or gadolinium oxide. The lattice parameters of beryllium oxide (a = 2.698 kX; c = 4.372 kX, c/a = 1.623) in mixtures with rare earth oxides after various heat treatments hardly differed from the tabular values (a = 2.693 kX; c = 4.37 kX; c/a = 1.625) [2], which indicates the absence of solid solutions in the beryllium oxide.

The eutectics in the system contain 35 mole % of samarium oxide or gadolinium oxide and 65 mole % of beryllium oxide.

It was not possible to make x-ray determinations of the phase composition of the specimens rich in the rare earth oxide, due to the lack of clarity in the x-ray photographs and the complexity of the crystalline lattice of the samarium and gadolinium oxides. Studies in reflected light showed that in specimens containing 0.5 mole % and more of beryllium oxide and quench-hardened from temperatures of 1300-1500°C there are two phases. This indicates that in the systems $BeO-Sm_2O_3$ and $BeO-Gd_2O_3$ there is no wide range of solid solutions in the rare earth oxides within the temperature range 1300-1500°C. X-ray methods did not reveal the formation of new chemical compounds in the systems under the described conditions.

On the basis of these investigations phase diagrams were plotted for the systems $BeO-Sm_2O_3$ and $BeO-Gd_2O_3$ in the temperature range 1300-2500°C (Figs. 2, 3). The melting points of the eutectics in these systems are as low as in the system $BeO-La_2O_3$.

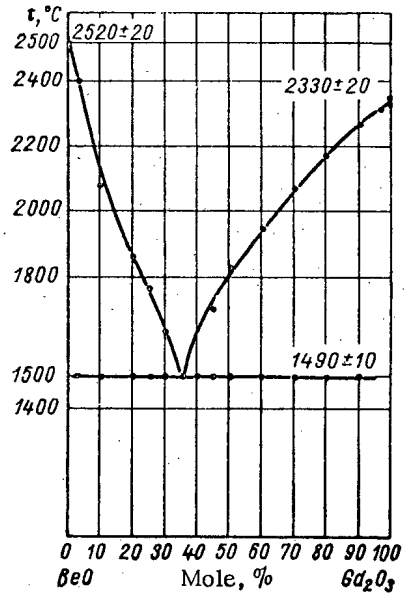

Fig. 3. Phase diagram for the system $BeO-Gd_2O_3$ in the temperature range 1300-2500°C.

LITERATURE CITED

1. P. P. Budnikov and S. G. Tresvyatskii, Ogneupory, 4, 167 (1955).
2. B. F. Ormont, The Structures of Inorganic Materials [in Russian] (Gostekhizdat, 1950).
3. H. von Wartenberg, H. Reusch, and E. Saran, Z. anorgan. und allgem. Chem. 230, 3, 257 (1937).

SYSTEMATIC MEASUREMENTS OF RADIOACTIVE FALLOUT IN THE YEAR FOLLOWING THE CESSATION OF NUCLEAR TESTS

V. Santholzer*

Translated from Atomnaya Énergiya, Vol. 9, No. 7, p. 56, July, 1960
Original article submitted November 23, 1959

In a previous communication** it was shown that in the half year following the cessation of nuclear tests the amount of radioactive fallout had hardly decreased at all. The average amount of daily fallout was 1.8 $\mu C/km^2$. The drop in activity with time is expressed by the formula $A = at^{-n}$, where a is a constant. The time t should be taken from the date of the appropriate nuclear test. Since more than a year has passed since the cessation of the tests, the inaccuracies in determining the dates of the tests are not very important in cases of the approximate determination of the numerical value of the power n. The last specimens of June, 1959 show that the extreme limits for n are 1.4 and 1.8, if the date of the tests is taken as any day of summer or fall, 1958.

The established average value of n, equal to 1.64, remains good at the present time. Approximately the same value n is obtained in the random collection of radioactive deposits for the range of 4-36 months. The oldest of our specimens collected after the cessation of nuclear tests were obtained 17 months ago. The method of collection was described in a previous communication (see footnote**).

In recent months, the radioactive deposits have been collected not only for one to three days but at the same time (in small vessels of about 0.06 m^2 area) for the whole month.

For some months after the cessation of tests the following average amounts were obtained for radioactive deposits per day (in $\mu C/km^2$):

1958		1959	
November	0.3	April	1.5
December	3.4	May	1.3
1959		June	1.4
		July	0.6
January	2.0	August	0.2
February	2.7	September	0.05
March	1.0	October	0.07

The maximum activity of the deposits was observed for only two to four months after the cessation of tests. In October, 1959 even atmospheric deposits did not give high activity, as was the case in spring, 1959. The maximum activity in rain collected on April 6, 1959 was $10.1 \cdot 10^{-9}$ C/liter. In deposits at the end of October, 1959, after a two month period of drought, contrary to expectations, the activity was only $0.03\text{-}0.40 \cdot 10^{-9}$ C/liter.

*Department of Physics of the Medical Faculty of Charles University, Hradec Králové, Czechoslovakia.

**V. Santholzer, Atomnaya Energ. 7, 5, 480 (1959).

A considerable reduction in activity of deposits is also shown by the value of the total activity towards the end of some half years: by April 30, 1959, it was 121 $\mu C/km^2$ and towards October 31, 1959 it was only 54 $\mu C/km^2$. The total activity for the whole year after the cessation of nuclear tests was 104 $\mu C/km^2$.

Systematic measurements of radioactive deposits in the year after the cessation of nuclear tests showed that recently the amount of deposits has been sharply reduced and has settled at values of about 1 μC per month. In the first months after the cessation of nuclear tests the values were about twice as high.

QUANTITATIVE DETERMINATION OF THE CONTENT OF LEAD AND BISMUTH RADIOISOTOPES IN AIR IN UNDERGROUND EXCAVATIONS

V. I. Baranov and L. V. Gorbushina

Translated from Atomnaya Énergiya, Vol. 9, No. 7, pp. 56-57, July, 1960
Original article submitted November 16, 1959

In mining, the greatest radiation hazard consists of the presence in air of radon and its short-lived decay products: RaA(Po^{218}), RaB(Pb^{214}), RaC(Bi^{214}) + RaC'(Po^{214}) (its short-lived product). As a rule, the concentration of radon decay products is below the equilibrium concentration level, and, therefore, special measurements are necessary for a dosimetric determination of their content.

While radon can be simply and very accurately determined by means of the classical emanation method, the methods for the separate determination of short-lived radon decay products which are used in practice [1 and 2] are still not sufficiently reliable.

The radiometric method for determining short-lived emanation decay products was proposed in [3-4] and developed for atmospheric air in 1925 in [5] as well as in [2, 6]. This is an essentially indirect method, and it still cannot be considered as positively proved at the present time. Therefore, we suggest that the method of the radiochemical separate determination of lead isotopes (RaB and RaD) and bismuth isotopes (RaC and RaE), which are collected by means of a BF filter, be used as a control method.

The collection of aerosols with RaA, RaB, and RaC is performed by the usual method [1, 7] at a volumetric rate securing a sufficiently complete deposition of aerosols. After the air is sucked through the filter, the latter is subjected to chemical treatment with the aim of separating the lead and bismuth isotopes deposited on it. For a short period of air filtering, the amount of long-lived decay products (RaE and RaD) can be neglected.

After a sufficient amount of air is filtered, the filter is burned. The sample is subsequently chemically treated according to the method described in [8], where lead and bismuth are separated by adding isotope carriers by means of dithizon. Dithizon with bismuth isotopes and the residual solution with lead isotopes are gradually drained into cups and then evaporated. The complete processing of the filter until a target with bismuth is obtained takes 40 min, and the time required for obtaining a target with lead isotopes is approximately equal to 1 hr.

The targets were measured by means of a B-type device with an end-type β counter. For quantitative calculations, the device was calibrated by means of an RaD-RaE equilibrium standard, which was deposited on a target similar to that used for the samples.

In measurements, due to the short half-life of short-lived radon decay products (T_{RaB} = 26.8 min and T_{RaC} = = 19.7 min), the end portion of the decay curve for these elements is obtained, which is used for calculating the number of RaB and RaC atoms that were deposited on the filter toward the end of air filtering. Experiments in separating such small quantities of lead and bismuth isotopes in an RaD equilibrium solution (RaD in equilibrium with RaE and polonium) were performed first.

The curves representing the variation of the β activity of targets with RaD and RaE in time are shown in Fig. 1. Since the energy of RaD β particles is small (E = 0.0167 Mev), RaD is determined with respect to the rise in RaE β activity in time (curves 1', 2', 3', and 4'). The half-life of the radioisotopes, calculated with respect to the curves 1-4, is close to five days and pertains to RaE.

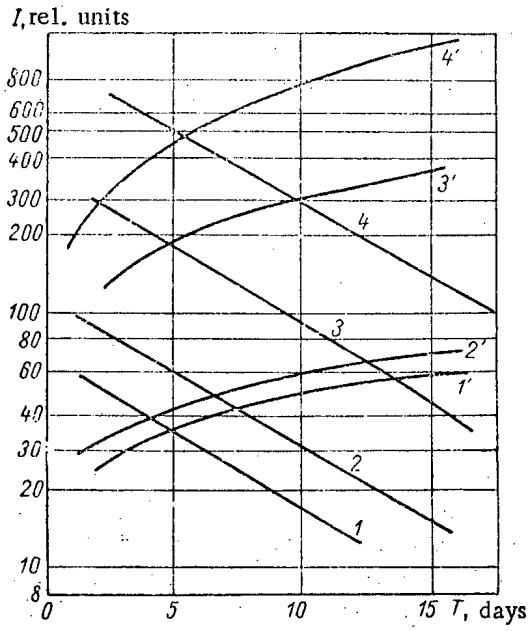

Fig. 1. Variation of the β activity of targets with RaD and RaE in time.

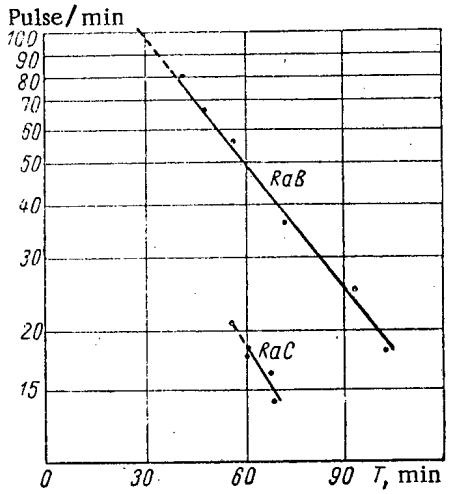

Fig. 2. Variation of the activity of targets with RaB and RaC in time.

Figure 2 shows the time dependence curves of the activities of two targets (with RaB and RaC), which were obtained after processing a filter through which approximately 400 liters of air was filtered. Judging according to the half-life values, the separation of RaB and RaC is satifactory, and, consequently, the number of RaB and RaC atoms which have settled on the filter from air can be calculated with respect to the obtained curves.

LITERATURE CITED

1. E. Tsivoglou, H. Ayer, and D. Holaday, Nucleonics 11, 9, 40 (1953).
2. E. S. Shchepot'eva, Tr. Radievogo Instituta 3, 64 (1937).
3. W. Swann, Terr. Magn. 20, 13 (1915).
4. S. Kinoshita, S. Nishikawa, and S. Ono, Philos. Mag. 22, 821 (1911).
5. V. I. Baranov, Tr. Instituta Fiz. i Krist. 4, 3 (1925).
6. E. G. Gracheva, Tr. Radievogo Instituta 4, 206, 219 (1938).
7. I. I. Gusarov and V. K. Lyapidevskii, Gigiena i Sanitariya, 10, 10 (1958).
8. A. I. Gusev, Bismuth Analytical Chemistry [in Russian] (Izd. AN SSSR, Moscow, 1953) p. 133.

SUMMARY OF THE INTERNATIONAL CONFERENCE AT MONACO ON PROCESSING AND DISPOSAL OF RADIOACTIVE WASTES

V. Spitsyn and B. Kolychev

The use of atomic energy has brought with it the formation of radioactive wastes, the number of which will reach several billion curies annually in the immediate future, solely on account of nuclear power development. If no measures are taken to assure decontamination and reliable, safe disposal of the wastes, a grave danger will ensue. Absence of the necessary agreement, and even of the necessary responsibility in some cases, has had the result that some governments have been disposing of their radioactive wastes without pretreatment and cleanup. This results in completely justified public alarm, and points to the need for an exchange of experience and know-how in this field of activity.

The International Conference on radioactive waste disposal, organized by the International Atomic Energy Agency and UNESCO, convened on November 16-21, 1959 at the Oceanography Institute of Monaco. The deliberations of the conference were participated in by over 300 scientists representing 32 nations and several international bodies, and included representatives of the Soviet Union, whose delegation was led by Academician V. I. Spitsyn. Eighty papers and communications were delivered, of which 70 were heard at the 12 plenary sessions.

The problems discussed at the conference included nature, processing, and shipment of radioactive wastes, modern techniques of waste disposal, and administrative and judicial questions associated with radioactive waste disposal, biological, physical, and chemical aspects of sea disposal of wastes, problems encountered in burial of radioactive wastes at land sites and deep-lying geological formations.

At the inauguration of the conference, Cole, the general director of the IAEA, and Veronese, general director of UNESCO, posed the problem of the need to formulate norms governing waste disposal, and the organization of some international controls over seas and oceans for that purpose, while holding the view that dumping of radioactive wastes in sea and ocean waters was admissible.

Nature of Radioactive Wastes

At the session devoted to this particular question, a report on the topic "The origin and nature of radioactive wastes" was presented by Bruce. The paper gave its attention to the large volume of medium-level and low-level wastes. For instance, during the period 1944-1948, 135 billion liters of discard solutions with activity ranging from 10^{-4} to 10^{-8} C/liter were disposed of at Hanford alone. By 1970, the waste volume is expected to reach 3 billion curies, contained in 27 million liters of solution; and by the year 2000, 60 billion curies contained in 1.1 billion liters of solution is the anticipated figure.

Given the existing techniques in the USA for nuclear fuel processing, the volume of liquid process wastes following evaporation treatment amounts to 1-5 m^3 per ton of irradiated uranium, with over 80% of the volume of wastes being in the form of solutions originating in the dissolution of the fuel-element cladding. In this sense, the mechanical techniques for stripping the fuel elements, since they greatly reduce the volume of wastes attributable to fuel elements, show great promise, although they are not being used currently in the USA.

From the report by Bruce and from other communications, we learn that extraction techniques are being constantly improved upon in the USA, the main line of approach being to seek out new extractants and new ways for engineering the processes. However, no basic change results in the nature of the wastes per se.

Another fact deserving of attention is that new methods of chemical reprocessing of fuel elements are under intensive study in the USA, e.g., chlorination and hydrochlorination at 600°C, fluorination, etc., which may have the effect of greatly reducing waste volumes.

Rodgers (USA) pointed out the possibility of disposing of low-concentration wastes in rivers, in the sewerage system, and in the ground, and of sea disposal of solid wastes in leaktight concrete casks. Kenney (UK) is of the opinion that incineration with ejection of the vented gases to the atmosphere, without any special cleanup treatment, may be recommended for organic and biological wastes (carcasses of animals, rubbish waste, etc.). The USSR delegation pointed out the need to develop methods for decontaminating such off-gases, to avert pollution of the atmosphere.

Dixon (UK), dealing with the problem of radioactive wastes disposal in the context of the British program for nuclear power development, voiced his opinion on the inevitability of getting rid of various forms of wastes at sea, and of discharging low-level wastes into nearby rivers.

From the reports read in this division, the impression is that liquid radioactive wastes are divided into three categories, in both the USA and Britain, viz.: 1) high-level wastes, with concentrations of the order of tens of curies per liter and higher (these solutions are buried in special storage tanks); 2) medium-level wastes, with concentrations of the order of millicuries or fractions of a curie per liter; these wastes are usually subjected to chemical processing, and concentrates of high activity are routed to burial sites, in some cases (notably in the case of Britain) being dumped at sea; 3) low-level wastes, in which the content of radioactive isotopes exceeds the accepted level for drinking water by several orders of magnitude; these wastes are diluted with water down to levels set by medical stipulations, and are then transferred to open reservoirs.

Processing and Shipping of Radioactive Wastes

In a report by Schulte (USA), the point is made that new reactor designs may lead to discarding the bulk of the activity into the atmosphere. Approaching the over-all problem in this light, the reporter reached the conclusion that discharge of wastes to the atmosphere must be properly organized. Small and Storebe (Norway) arrived at the same conclusion. They indicated that the air in the stratosphere varies over a period equal to roughly two years. Release of radioactive wastes at a great height, as has been proposed on occasion, would be ineffective therefore from the standpoint of safety in waste disposal. The reporters described the building of automatic stations for monitoring atmosphere activity in the neighborhood of atomic power installations.

Silverman (USA) discussed the economic aspects of decontamination of air and gases vented as by-products in nuclear processes. Several methods for decontaminating gaseous wastes, including an aerosol approach, have been compared at Harvard University. Fiberglass, which was melted down after use, was the filter material used. Kr^{85} decontamination took place by adsorption on charcoal at a low temperature, or on aliphatic acids. The cost of the gas decontamination differed only slightly from the cost of dilution by air through construction of high stacks.

In the discussion, the British representative stated that all atomic installations in Britain are equipped with filtering devices for gases.

In the section on processing of liquid wastes, a paper was read by Vetsley (Belgium) telling of the use of lignite (brown coal) as ion exchange material to hold back radioactive cations. Studies have been conducted on a laboratory scale. Measurements of the equilibrium constants for systems containing Sr^{90} and Cs^{137} as microcomponents, and calcium, sodium, and hydrogen ions as macrocomponents, have been made. The problem of the mechanism effective in sorption has not yet been studied; it remains obscure which of the components of lignite is the sorbent.

In answer to the query why synthetic ion exchange resins were not being employed, since they give a degree of purification two to three orders of magnitude higher, the reporter laid stress on the importance of the economic factor.

A report by Genguli (India) was addressed to the problem of temperature distribution in waste solids. According to calculations, the maximum temperature at a specific activity of 1 C/g of Sr^{90}, in the center of a sphere of radius 20 cm or cylinder 36 cm in diameter, is 250°C, and 175°C at the surface; at a Sr^{90} concentration of 5 C/g, the corresponding values are 1200°C and 800°C, i.e., $400 \cdot 10^3$ C of Sr^{90} are permissible in 80 kg of material. The author suggests making the same calculations for a mixture of fission products, in the future.

The problem of the processing of waste solids was taken up in a paper presented by Serret (Saclay, France). To achieve more compact disposal, a method of preliminary pulverization and compaction of the wastes prior to burial was employed. Pulverization of the products is followed by placing them in a concrete cask, a cylindrical barrel 1.3 m in diameter and of the same height, with a wall thickness of ~ 16 cm, after which the products are encased in concrete. The concrete mix used (HTS cement 50 kg, sand 76 kg, oxido cement 25 kg, aluminum powder 0.005 kg, water 30 liters) ensures reliable hold-down of the fragments, preventing them from being washed away. The cement block was immersed in water for a year, with no noticeable increase in the activity of the water.

Two papers delivered by Pomarolle (Saclay) discussed various cases of land-burial of wastes, and possible solutions in case shipping of the wastes is required through the home country or a neighbor.

The reporter announced that, besides storage in special buried tanks, burial of low-level wastes by stacking them in trenches with subsequent backfill of the earth is adequately reliable. Cement pipes were built to house casks of high-level wastes below ground.

At the sessions devoted to reprocessing and improved methods of waste disposal, 11 papers were presented.

It was announced in a paper by Beauvoir and Candillion (France) that contamination of the surrounding terrain by radioactive isotopes at the nuclear installations in Saclay, Grenoble, Marcoule, and other localities has reached significant dimensions. In some spots (e.g., at Chinon), soil radioactivity rose to $4 \cdot 10^{-5}$ C/m^3 in 1958, while contamination by $Sr^{90} + Y^{90}$ amounted to $\sim 4 \cdot 10^{-7}$ C/m^3.

A paper by Wormser (France) described a small installation used for decontamination of low-level wastes at Saclay. The activity is concentrated in the precipitates of phosphates, hydroxides, and carbonates, which are then buried in containers and trenches or pits.

A variety of burial techniques resorted to for active wastes were described in reports by Mowson and Russell (Canada). One of the techniques deserving particular mention consists of cementing medium-level wastes in steel casks and then dumping them down deep pits. Despite the fact that wastes containing thousands of curies were buried in those structures, only traces of activity were detected in the surrounding medium.

Burial of various forms of wastes in pits, into which liquid wastes had been placed in polythene containers, and solids were placed unconfined but separated by alternating layers of salt and asphalt, have been tried out. In the case of asphalt, cracks and fissures were discovered in pits where high-level wastes had been buried, which constrains us to approach this burial technique with caution.

Larsen (Denmark) noted that weakly radioactive solutions could not be dumped without pretreatment to keep the activity from exceeding preset levels (activity not to exceed 1/10 of the critically allowable level at a distance of 10 m from the dump point) into the waters of the Rise fjord, despite the unusually slow exchange of the waters.

At Harwell, according to a report by Burns, all of the wastes, even of the low-level variety, are subjected to complex processing. Prior to discard, they are carefully checked, in view of the fact that the Thames, into which they are dumped, is the principal source of drinking water for London.

To handle wastes with a low activity level, caustic soda is added to pH = 9.5, with simultaneous introduction of sodium phosphate. The precipitate of calcium phosphate which forms (on account of the calcium present in large amounts in the original solution) is placed in leakproof cistern tanks, which are then dumped out at sea, while the supernatant liquor is poured off after a careful check.

In processing wastes of medium activity, recourse is had to a facility of 4 m^3/hr capacity, where the Ca-Fe-phosphate precipitate is decontaminated at pH = 11.5. This makes it possible to get rid of 99% of the alpha emitters and 89% of the beta emitters. To remove ruthenium, the solution is acidified to pH = 3 with precipitation of ferric sulfate, making it possible to carry the decontamination on to elimination of 99.8% of the alpha emitters and 91% of the beta emitters. The residue contains ~ 0.3-0.5% of the original β activity. Ultimate decontamination is by ion exchange. Studies are also underway at Harwell to reduce the volume of solid waste through baling and melting.

In the USA, work on decontamination of radioactive wastes proceeds in pretty much the same directions as in Britain and France. Low-level wastes are discharged into rivers, dumped at sea, or buried inland, and problems arising in reprocessing of such wastes were not discussed in the American papers.

An interesting report by Stevens (USA) was devoted to reprocessing of high-level wastes. The inconvenience encountered in methods currently used for burial of liquid high-level wastes in cans was emphasized, since the temperature could not be successfully held below 65° C during the first year, despite the excellent functioning cooling system. It was noted that corrosion proceeds at 0.002-0.005 mm/year.

Studies carried out demonstrated the advantage of burying wastes in solid form, since they take up much less space in that case and the fragments are much more efficiently immobilized, leading in turn to savings and simplification in the storage media, the upshot being that the costs of waste reprocessing are compensated.

Evaporation and calcining of the oxides forming in a fluidized bed at 350-550°C is the method recommended for converting solutions containing aluminum nitrate to solid form. The report describes an existing pilot plant with a throughput of up to 200 ml/min, and another facility being built in Idaho, with a throughput of 5 m^3 per day.

In addition, problems concerning burial of highly active solids have been worked out in detailed fashion. No significant losses of radioisotopes were observed up to 1000°C, but about 100% of the Cs^{137} was removed at 1200°C. The authors came to the view that additional treatment of the calcined materials, with vitrification in particular, will be required for more reliable disposal (to obviate the need for costly cooling systems in the storage dumps).

Reprocessing of wastes was discussed in reports by other scientists, e.g., by Wilson (Australia), Yamamoto (Japan), Rodger (USA), but no new problems were clarified.

The report by Zimakov (USSR) dealing with a study of the composition and behavior of vitrification products of radioactive wastes stimulated a good deal of interest.

Problems involving elimination of radioactive wastes by ground burial and deep-lying geological formations took up two entire sessions.

Considerable interest was evoked by a report of Pierce, Linderot, et al., (USA) on inland burial of liquid radioactive wastes at the Hanford plant. By mid-1959, 139 billion liters of low-level wastes (water, coolant equipment, nontechnological wastes, etc.) with a total activity of 2500 C had been disposed of in natural lowlands ("marshes"); 106 million liters of radioactive wastes, heavily salted down after undergoing various methods of reprocessing and showing a total activity of 647,000 curies, were poured down in special trenches. Finally, 14.9 billion liters of waste containing 1.9 million curies of fission products were pumped into caverns dug out below ground, from which they were expected to gradually seep into the surrounding soil. Test boreholes were drilled down to monitor the progress of the radioactive isotopes in the earth. Considerable migration of the activity has been recorded to date. Despite the low ground water table prevailing in the area (150-200 m), fission-fragment elements have reached it and are being entrained in the water movement. For example, the area of contamination beneath one of the caverns was 370 m^2 at first, and has by now spread out to 7,400 m^2. Ground water samples have shown that contamination has extended to 5 km from the site where the wastes were dumped. The content of β emitters in the water ranges from $1.5 \cdot 10^{-7}$ to $1 \cdot 10^{-4}$ μC per liter, sometimes even higher. The principal offender with respect to migration in the ground water is ruthenium, but sizable amounts of strontium often show up as well. The reporter made clear that trapping of radioisotopes in the soil is primarily attributable to ion exchange reactions. However, if the wastes contain phosphate ions, then these react with the soil calcium carbonate to form an artificial apatite which acts to trap radioactive strontium. When fluorine ions are present in the discard, these react with soil calcium carbonate to form fluorite, which enhances the trapping of the rare earths, strontium, uranium, and plutonium. This report provides strong arguments against directly dumping liquid radioactive wastes into the soil and underlying earth, even under such favorable hydrogeological conditions as prevail at Hanford.

Parker (USA) reported on continuing research geared toward discovery of disposal techniques in handling liquid radioactive wastes, using salt mines as dump sites (a report on this approach was given at the second Geneva conference on the peaceful uses of atomic energy). A pilot project is under study at the present time (in a natural salt bed). However, nonradioactive solutions are being used in simulating experiments.

Hansted (USA), et al., in a report entitled "Migration of radioactive wastes in natural waters at Hanford," discussed questions related to pollution of the Columbia River by radioisotopes. The water used as coolant for the reactors in the Hanford complex was contaminated by over 60 different radioisotopes which came into being chiefly on account of neutron activation of dissolved impurities. These waters are passed through hold-up ponds for 1 to 3 hours, after which they are discharged into the river. The reporter pointed out the fact that the effect of the ionizing radiation on the population near the Hanford plant who consumed the water of the Columbia River averaged 20% of the maximum permissible dose. Taking into account the possibility of accidents and the attendent higher contamination level, one could hardly view the data cited as completely reassuring.

Barbier and Michon (France) reported on calculations of absorption of radioisotopes by tilled soil from low-level wastes entrained in the irrigation water. They arrived at the conclusion that contamination of vegetable crops by radioisotopes will not be proportional to the content of the isotopes in water, but much higher.

V. I. Spitsyn, V. D. Balukov, et al., (USSR) told of the results of laboratory and field tests on sorption of fission-fragment elements when solutions of the latter were allowed to seep into the ground. The paper stressed the fact that radioactive strontium absorbed in soils and earth was readily displaced by the calcium constantly present in natural waters. This undermines any expectation that strontium will be firmly absorbed in soils. On gaining access to the ground water, radioactive strontium begins to migrate with it. Radioactive ruthenium is absorbed weakly by soil minerals. Radioactive cesium is absorbed slightly more readily.

Many of the papers presented by American scientists on burial of wastes at great depths attest to the great interest accorded by scientists to this problem.

Neys gave a detailed review of geological research (carried on in the USA under contract with the atomic industry) centered mainly in the field of radioactive waste disposal. He gave greatest significance to disposal of low-level and medium-level wastes, the dumping of which in areas around atomic enterprises inevitably leads to an appreciable increase in the radioactivity of the earth's surface, a procedure which may entail undesirable genetic after effects, if continued over a protracted period.

The most suitable formations for this type of disposal are synclinal depressions in sedimentary rocks. Compact rocks may become embrittled by hydraulic action or explosives. The USA oil industry has hundreds of thousands of cubic meters of heavily salt-laden waters at its disposal each passing year, in exchange for which radioactive wastes could be pumped into used-up oil wells. The nature of the rocks surrounding the well are of utmost importance. Clayey shales have high sorptive capacity and easily retain radioisotopes. However, they have poor thermal conductivity, and their argillaceous minerals are susceptible to decomposition by acidic solutions. Sandstones are viewed favorably in this context. Limestones fall short by chemical properties; furthermore, they always suffer from cracks and passages permitting the leakage of solutions poured over them. Gypsum rocks are suitable for removal of solid wastes, but their usefulness for removing liquid wastes is held in doubt. Great hopes are placed in a method for burying radioactive wastes in salt mines, particularly rock salt deposits.

Simpson (USA) stated in this report that salt deposits and deep-lying water-permeable formations are being studied at dump sites for high-level wastes. Shallow burial of packaged wastes is considered for medium-level wastes, with pouring into the soil as alternative. In these cases, the ground water movement, the dispersion of impurities introduced into the ground water, ion exchange and adsorption processes are being studied.

Brown (USA) told of the results of geological investigations in the vicinity of the Hanford atomic plant. There were 551 boreholes drilled here; the filtration coefficient, speed of travel and direction of migration of the ground water were studied. At the present stage, information on the geological structure of the region is being supplemented by new data secured with the aid of seismic, magnetometric, gravimetric, and other techniques. The reporter expressed the opinion that until the geological constants of the region are determined more precisely than they have been up to the present, land burial of radioactive wastes should not be stepped up.

A paper submitted by W. de Lagoun (USA), which was not read at the conference, discussed problems of a similar nature. This author feels that the methods in use at present at Hanford and Oak Ridge for waste disposal in the ground are unsatisfactory, since it is impossible to indicate the precise ultimate destination of the wastes.

Kaufman (USA) told of the results of two years of experience in a pilot plant at the University of California, where radioactive solutions have been pumped into a water-bearing layer 1.2 m thick, lying at a depth of 28.5 m. Tritium-tagged water was used to study the hydraulic behavior of the ground water. The results obtained show

that burying wastes deep in the earth makes it possible to attain the same decontamination factors as in the most highly perfected chemical processes.

Wager and Richter (West Germany) reported on the results of geological and hydrogeological research conducted in West Germany with the purpose of finding out the suitable sites for burial of radioactive wastes in depth. A selection of points was found where liquid radioactive wastes could be pumped into structures containing old ground water.

In the summary of the discussion on the papers read, great promise was attributed to further development of methods for burial of radioactive wastes deep in the earth. However, attention was turned to the need for complete localization and keeping the discard under control over protracted storage periods.

The problem of dumping radioactive wastes at sea was the most heatedly discussed item on the agenda, literally from the first day of the gathering. Most of the papers submitted by the American and British scientists dealt directly or indirectly with proof of the admissibility of effecting such disposal at sea without fear of harmful consequences to humanity.

For example, Dunster and Weeks (Great Britain) reported that 10^6 m^3 of low-level wastes containing over 50,000 curies of β activity and 85 curies of γ activity are poured into the Thames River or dumped at sea each year in Britain. They proved the possibility of further disposal in this manner, and stressed that the choice of dump site was governed predominantly by economic considerations.

Burns (Great Britain) stated in his report that radioactive liquid wastes of low activity are being dumped into the Thames.

Rodger (USA) pointed out the fact that burial of high-level wastes in casks at sea depths within the Gulf of Mexico and at a number of shoreline regions of the Pacific and Atlantic Oceans is being carried out in the USA. The reporter laid stress on the need to delineate regions subject to subsequent checking, for burial sites.

Dunster (Great Britain) gave a survey of existing and proposed methods for dumping low-level liquid wastes into the sea; in view of the completely insignificant increase in the average activity of the oceans on a world scale resulting from this procedure, sees the disposal of radioactive wastes in rivers and at sea as harmless.

A detailed study of the justification for the possibility of dumping waste at sea and in oceans was presented by Pritchard (USA). The author strove to demonstrate in this paper that, on the basis of existing knowledge in the field of oceanography, disposal of sizable amounts of liquid waste, including highly active waste, in the sea depths (amounts of the order of several megacuries annually) creates no hazard for humans. Particularly worthy of mention is the position taken by Pritchard to the effect that waste disposal in shore waters may adversely affect the interest of only that nation processing the shoreline in question.

It is clear from the foregoing that the problem of admissible disposal of radioactive wastes in sea basins has acquired particular sharpness, and that would explain why three plenary sessions were devoted to the diverse aspects of this question, with 17 papers, three of them from the USSR, presented at those sessions.

The most interesting papers for mention here include one by Gordon (USA) on a method for studying ebb and flow patterns in the coastal waters by introducing fluorescent dye materials. A mathematical interpretation of the rate of vertical and horizontal mixing of the radioactive material in the ocean was presented by Miyake and Saruhashi (Japan). They pointed out that, while the radioactivity in the Northern Pacific in 1954 was observed only above the thermocline, in 1955, it reached a depth of 600 m, at a time when the thermocline lay at a depth of 75 m.

A paper presented by Morgan (Great Britain) on research devoted to a study of the seasonal migrations of fish in regions neighboring dump sites for radioactive wastes, the radioactivity of those fish, and the percent of the fish population drawn upon annually for food, excited its share of interest for its methodological approach. There were 36,000 head of flounder tagged for the investigation. Within a years' time, ~50% of the tagged flounder had been caught in the fishing grounds. It was found that the number of cases of increased radioactivity in the flounder stock was not high, providing a basis for optimistic inferences. Although, this paper was of unusual interest from the methodological standpoint, objections were still to be raised against the conclusions drawn and the averaging of the probabilistic data regarding the feasibility of using this fish as food.

Schaeffer (USA) devoted his paper to the need for new research work on evaluation of concrete-sea preserves suitable as burial sites for radioactive wastes. He stressed the significance of enormous expanses of open sea where fishing was unfeasible and which constitute a biological wilderness from that point of view. Schaeffer stated that a program has been developed on a broad scale in the USA for similar investigations, to span a five-year period and running into research costs of 30 million dollars.

The gist of the reports reduced to the idea that disposal of radioactive wastes at sea was admissible. However, the ones who delivered papers on this topic [Ketchum, Schaeffer, Chipman, et al. (USA); Morgan, Pritchard, Monas (Great Britain); Valdichuk (Canada)] adduced a wealth of facts which argued strongly against the admissibility of such a conclusion.

For example, it turned out that the concentration of the most dangerous elements, viz., Cs^{137} and Sr^{90}, builds up to 20-30 times higher in the tissues of shellfish and scaled fish than in the surrounding waters, while the phytoplankton evinces a capacity to build up its concentration of some radioisotopes to 1,200 times exceeding the concentration of the water environment.

In the paper mentioned, Morgan referred to the fact that every tenth flounder fished in grounds just adjacent to the disposal sites for the radioactive wastes showed symptoms of radioactive injury, including leukemia symptoms. The data cited by American researchers to the effect that the radioactivity level had increased in zooplankton gathered in regions where wastes were disposed of near San Francisco are familiar.

The Soviet delegation held fast to a negative position on this question from the very first day of the conference. In the papers presented by Zenkevich, Fedorov, Moiseev, as well as in reiterated brief interventions in the discussion by other members of the Soviet delegation, insistence was placed on the position of the inadmissibility of radioactive waste disposal at open sea or in the oceans.

The Soviet delegation motivated its stand by the following fundamental tenets:

1) a series of investigations has established the fact that reasonably intense intermixing takes place in the seas and oceans and even in deep ocean troughs, and that consequently, radioactivity will make its way from any depths to the surface layers;

2) plankton and fish are capable of accumulating radioactivity by two to three orders of magnitude greater than that of the water environment;

3) assuming it is possible to speak of the harmlessness of low concentrations of natural radioactivity to which the human organism is already conditioned, it is certainly not admissible to make statements on the genetic sequelae affecting the organism in the case of even low concentrations of artificial radioactive isotopes;

4) waste disposal operations in coastal waters cannot be dismissed as an "internal" affair, since migration of the activity may well proceed by both hydrophysical and biological pathways, thus, affecting the population of neighboring states;

5) in resolving the problem of the methods to be used in burying radioactive wastes, the economic factor cannot be given priority. Here, as in other respects, the question of the life and health of mankind must be the first question on the agenda. Nor should it be forgotten that at the present time, mankind consumes over 30 million tons of products originating from the sea, annually.

The Soviet delegation advanced, as a fundamental principle, the need to reprocess all forms of liquid radioactive wastes while isolating concentrated products for safe burial in containers or in vitrified form, and the need to use water purified of the bulk of its activity in a closed cycle within the particular nuclear enterprise.

In the ensuing free discussion among oceanographers present, who did not remain uninfluenced by the active interventions of the members of the Soviet delegation, representatives from France, Norway, India, the Netherlands, Italy, Bulgaria, Poland, and Finland expressed, in one form or another, the danger inherent in the drift of radioactivity, especially borne by living marine organisms, over the expanses of the world's ocean bodies. The insistent need to develop research in depth and on a broad front to tackle these questions was stressed.

Rovell (USA), summarizing the discussion, was obliged to acknowledge the extreme inadequacy of the data now available to the scientists, which does not allow them to work with the proper certainty toward a resolution of the problem concerning the possibility of sea burial of radioactive wastes and the appropriate methods.

The trenchant victory won by the Soviet stand was reflected in a statement by the UNESCO representative Vittorio Perez who, in his closing remarks at the termination of the conference, said that the foregoing discussion necessitated a reexamination of previously held concepts on the possibility of disposal of radioactive wastes at sea. He himself remarked that the economic factor should be put into the background in judging this question, and should yield before the problem of the preservation of the health of mankind.

This outcome of the Conference may be viewed as the result of the positive effect of humanistic principles upheld by the Soviet delegation throughout the conference.

Basic Conclusions

1. Despite numerous research efforts conducted in various countries and especially in the USA and Great Britain, disposal of radioactive wastes at sea and in ocean waters cannot be considered as proven safe from the standpoint of the possible spread of radioactivity. Before giving an answer to that question, it is necessary to expand present oceanographic, biological, and genetic research to the fullest.

2. The pathways and trends followed in reprocessing medium-level and low-level wastes in diverse countries differ only slightly from one another on the whole, and boil down in the long run to successive operations involving coprecipitation of hydroxides and phosphates, the use of adsorption for further purification, and oxidation-precipiation operations at the initiation of the process in cases where organic impurities are present.

The one thing we cannot find agreement with here is the practice frequently encountered in foreign countries of dumping solutions of low activity into natural reservoirs and counting on their becoming diluted in time. The principle of closing the cycle and using the water turnover in this case is indisputably more reliable and safe.

3. The burial of concentrated pulps in casks of cement blocks inside of earth caverns, of various types, following processing of the medium- and low-level wastes yields comparatively positive results. It is absolutely inadmissible to approve of burial of such forms of waste without protective encasing, since all studies show the presence of quite extensive migration of the most dangerous active elements.

4. The method of greatest promise for the disposal of wastes of medium and even of high activity must be acknowledged to be burial in vitrified form in earth caverns, pits or trenches, but even here great innovations are to be expected, in all probability, in the technological organization of this procedure, the best studied one to date.

As a provisional measure for disposing of high-activity wastes, we must consider storing them in stainless steel containers, an approach which has been adopted universally.

5. Investigations in the area of burial at depths in wells and closed geological formations must be viewed as promising, but are far from completed at present.

6. The choice of the fundamental technology in the processing of nuclear fuel should be made with observance of such considerations as the volumes of radioactive waste resulting, and the form in which the yield from the processes will appear. In particular, the use of chemical methods for decladding fuel elements results in a sharp increase in the volumes of liquid active waste, which is hardly justifiable in terms of an apparent convenience gained in execution of the process.

Any complex form of fuel elements following machining operations may be brought to a state allowing the nuclear fuel to be dissolved without requiring dissolution of the cladding material. The solid waste from the cladding is small in volume, activity is well localized, and burial is consequently simpler and more reliable.

"THE ATOMS FOR PEACE" PAVILION AT THE USSR INDUSTRIAL EXHIBIT IN IRAQ

In April, 1960, an Industrial Exhibit under the auspices of the Soviet Union ran for three weeks in Baghdad. The exposition was inaugurated by the First Vice-Chairman of the Council of Ministers of the USSR, A. I. Mikoyan. The Iraqi premier, Abdul-Kerim Kassem was present at the inauguration.

The pavilion in which the achievement of the Soviet Union in the field of the peaceful uses of atomic energy were displayed was a center of interest for all those who visited the exposition.

Represented in the pavilion were several fields of the national economy benefited by the use of atomic energy. In the section on power, visitors took an eager interest in the functioning models of the world's first atomic-fuel electric power station, and models of a water-cooled, water-moderated reactor and uranium-graphite reactor. A scale model of the world's first nuclear-propulsion icebreaker, the "Lenin," drew special interest, as did operating models of the 10 Bev proton synchrotron and the 680 Mev synchrocyclotron. The section telling of research conducted in the Soviet Union in the field of thermonuclear reactions was very popular with representatives of scientific circles in Iraq.

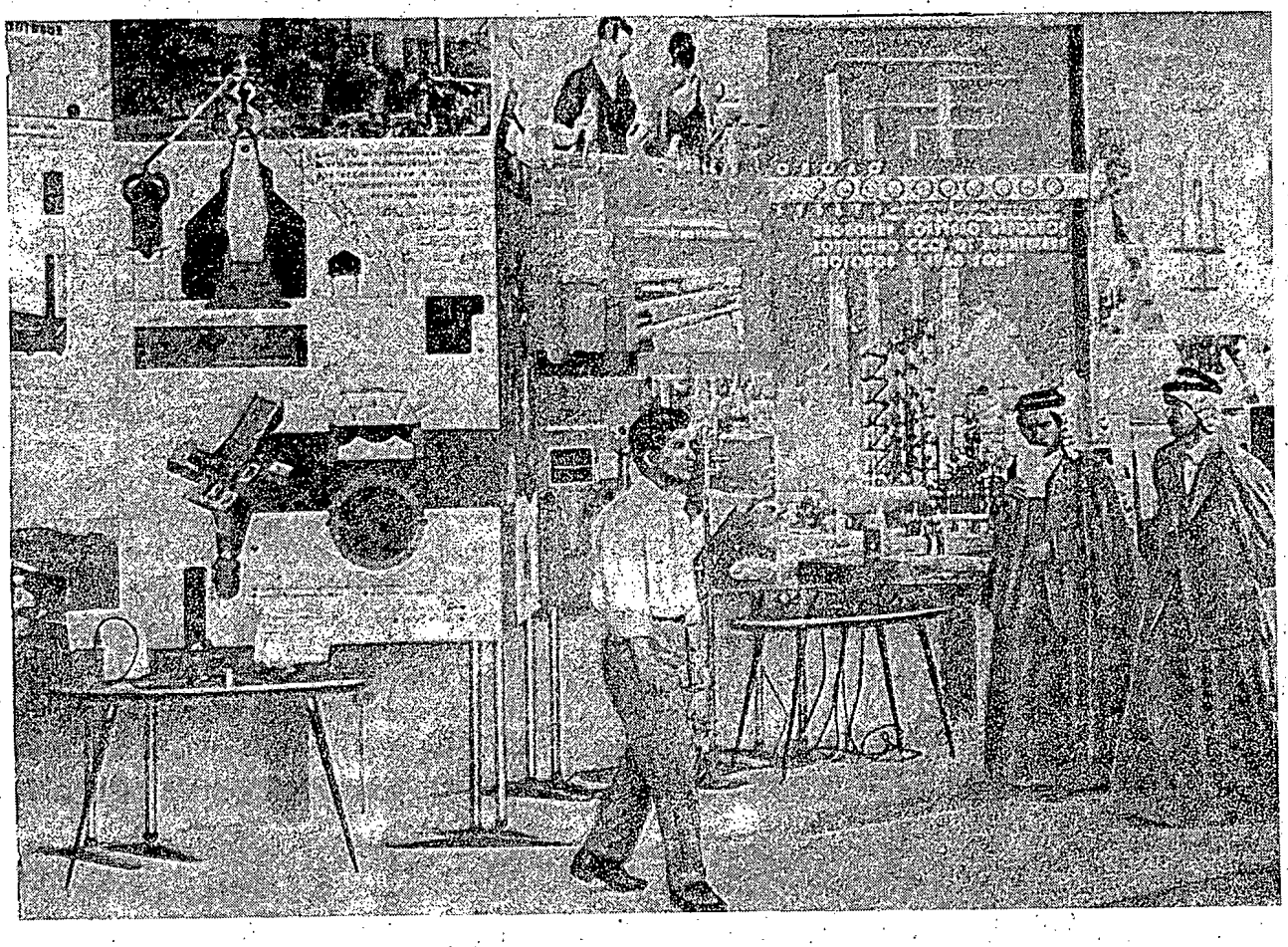

At the Exposition in Iraq.

The equipment used in prospecting for radioactive ores was well represented in the exhibit. These consisted chiefly of portable radiometers with different ranges of measurement.

Those sections of the pavilion telling of isotope applications in geology, medicine, biology, and agriculture were very popular. The reason here is also that these sections were supplied liberally with the appropriate instruments. Specialists visiting the exhibit paid glowing tribute to the quality of the instrumentation.

In the section on shielding and dosimetry, in which a large amount of dosimetry equipment was on display, the manipulator device stole the show.

Fifty-thousand copies of the prospectus drawn up for the exhibit and 50,000 copies of V. S. Emel'yanov's book "The Atom in the Soviet Union Serves the Cause of Peace", both printed in Arabic, were distributed to the visitors during the run of the exposition.

The display attracted the attention of people from outside Baghdad as well; people from the most diverse regions of Iraq traveled to see it. About 40,000 people were on hand on opening day. All in all, the number of visitors totalled half a million.

The activity of the exposition received wide publicity in the Iraqi press. The newspaper "Istiqlal" devoted an entire page to the atomic pavillion in the exhibit. The newspaper "Ittihad Al-Shaab" told of the displays in the "Atoms for Peace" pavillion, concluding: "The Iraqi people left the pavilion with the thought that the Soviet people and Soviet scientists are leaving nothing undone to harness the colossal energy of the atom for the cause of peace and socialism, and not for war and destruction."

Some specialists and other visitors left their impressions about the atomic pavilion in writing. For example, Yussef Abbud, professor at Baghdad University, wrote in the guest book: "Having visited the Soviet Industrial Exhibit, we cannot help expressing our admiration at the tremendous successes achieved by the Soviet Union. What we have seen in the atomic pavilion is worthy of our highest estime. With all our heart, we wish our great friend – the Soviet Union – still greater successes in the field of science, industry, and economics". The worker Tawui Makhdi wrote: "The atomic pavilion has aroused great interest. I wish the Soviet people even greater successes in its noble cause of using atomic energy for peaceful purposes". And here is another salutation: "The Soviet atomic pavilion is a shining piece of evidence of the successes of scientific thinking in the Soviet Union. In getting acquainted with the achievements of that country in the field of the use of atomic energy for the cause of peace, one is astounded by the scope of the work in this field of science so important for mankind."

A. M. Panchenko, G. V. Fedorov

THE DANISH DR-3 HEAVY WATER REACTOR

In January, 1960, the DR-3 heavy-water research reactor, designed chiefly for materials testing, was brought to criticality at Ris (Denmark) (Figs. 1-3).

The reactor was built under a contract dating back to June 20, 1957, between the Denmark Atomic Energy Commission and the Atomic Energy Control Board of Great Britain. Most of the reactor construction work was contracted by Danish firms. The cost of the reactor, including the fuel and heavy water, is 1,564,000 pounds sterling.

The DR-3 reactor is similar to the British DIDO and PLUTO reactors at Harwell [1]. The power rating is 10 Mw in this case too; heavy water functions as both coolant and moderator (10 tons in the system), while the reflector is graphite; fuel assemblies are box types. The fuel elements are manufactured as plate elements of an alloy of enriched uranium with aluminum clad in aluminum [2, 3].

The variation in the design of the DR-3 reactor from its British counterparts is only slight. There are also some differences in the planning of the reactor buildings and in the use of electrical equipment for control of the DR-3 reactor to conform to Danish engineering standards. The pump house was enlarged somewhat to ac-

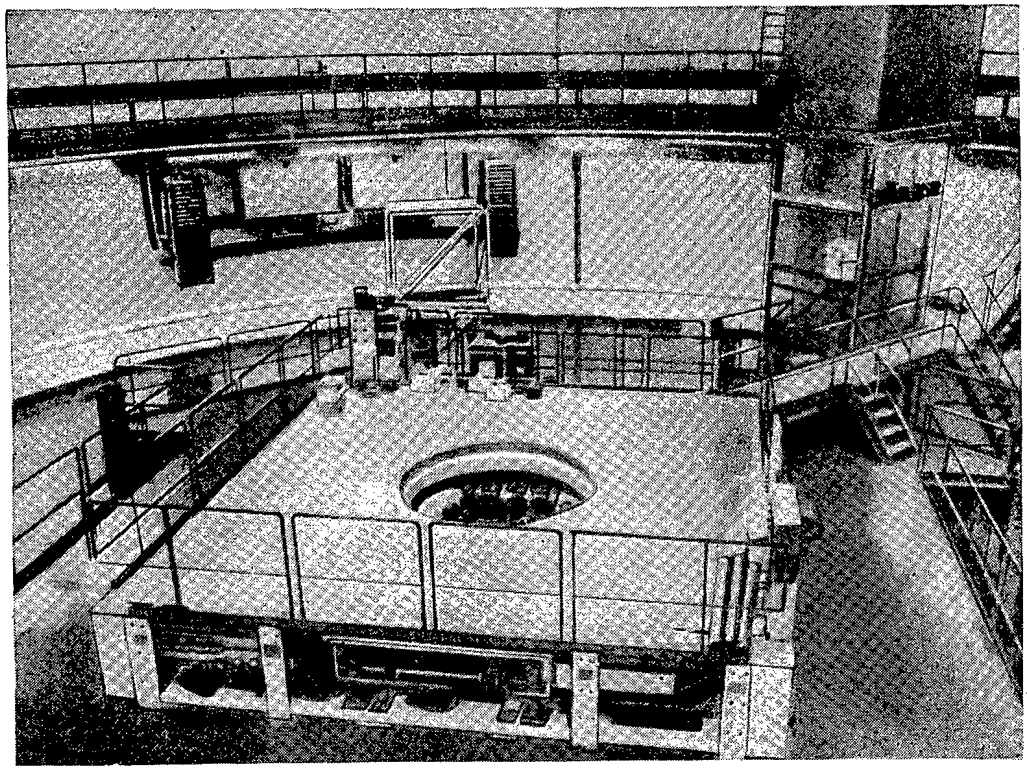

Fig. 1. General view of interior of reactor house.

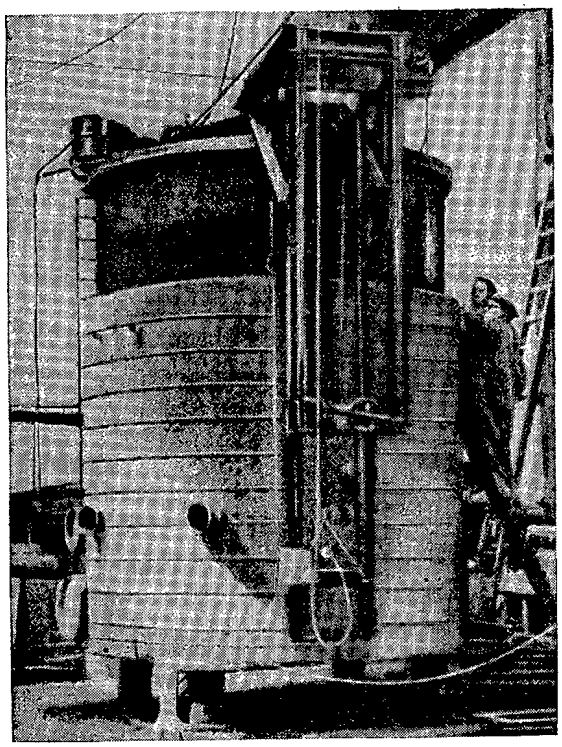

Fig. 2. Assembly of DR-3 pressure vessel.

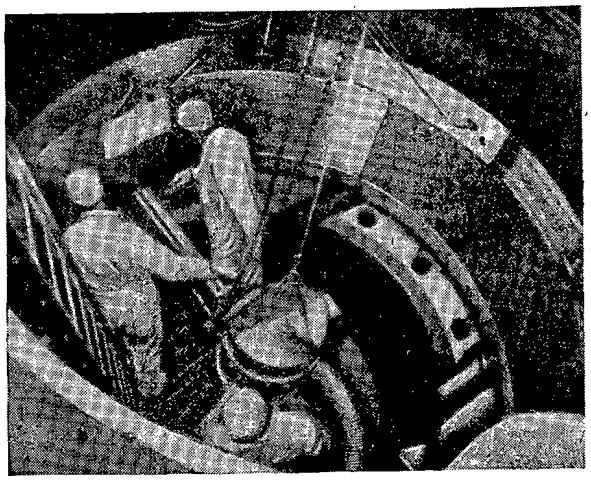

Fig. 3. Assembly of equipment inside reactor pressure vessel.

comodate a ventilation ducting system, a water-treatment facility, and equipment for the air purification system. The ventilation system and the air conditioning system have been altered with respect to the British variants, to satisfy requirements imposed in Denmark. Attention was also given to attainment of high cleanliness and improved deactivation of the rooms and compartments used for operations with radioactive objects. There are differences in the charge-discharge and transportation systems for spent fuel elements. Since the performance of British-make pumps used to pump system heavy water in the DIDO and PLUTO concepts leaves something to be desired, replacement pumps were purchased in France.

A supply of heavy water costing 340,000 pounds sterling was obtained on credit from the US Atomic Energy Commission, under terms of annual payment of 4% of the cost of the heavy water.

After the reactor has been brought up to full power (10 Mw) at the end of the summer of 1960, experiments designed to test the performance characteristics of the British DRAGON concept built at Winfrith Heath will undoubtedly be repeated on the DR-3 [1].

LITERATURE CITED

1. Nucl. Power, 5, 47, 131 (1960).
2. Nuclear Reactor Album [in Russian].(Moscow, Atomizdat, 1959) p. 215.
3. Nuclear Reactor Album [in Russian].(Moscow, Atomizdat, 1959) p. 217.

BERYLLIUM PRODUCTION IN THE CAPITALIST COUNTRIES

Beryllium has come more and more into the forefront in recent times. Until 1957, processing of beryllium concentrates was carried on mainly in order to fabricate copper-beryllium alloys. Beryllium metal has become the important end product in steadily increasing quantities since 1957. The fundamental application for this metal has been found in atomic industry, aviation, rocket construction, and shipbuilding [1]. At the present conjuncture, there are about 50 firms engaged in research on widening the scope of beryllium applications in the various branches of industry [1].

Basic production volume of beryllium concentrates in foreign countries averaged about 10 thousands of tons annually (figures based on concentrate with 10% content of beryllia) during 1957-1959. The main producers of beryllium concentrates are Argentina, Brazil, Belgian Congo, and Mozambique [3].

Production of beryllium concentrates in the USA amounts to a total of about 500 tons annually. The mining of the mineral beryl, in which about 200 firms are engaged, is prosecuted principally in conjunction with mining of other commercial minerals, such as fluorite, feldspar, spodumene, etc. [1-3].

Because of the dearth of rich beryl deposits in the USA, intense work is pursued on enriching the low-grade beryllium raw material, resorting to flotation techniques predominantly. Several flotation plants have been erected in the state of Colorado for the beneficiation of low-grade beryllium ores [3, 4]. Domestically produced beryllium concentrates are listed at higher prices ($529 per short ton) than imported concentrates ($357 per short ton) [5].

Processing of beryl concentrates is carried on in the USA and on a small scale in Britain and France. In recent years, the volume of concentrates processed in the USA rose steeply: 4,400 tons of concentrates were processed during 1956, and 5,000 tons in 1957 [6]; 6,200 tons in 1958, and in 1959, according to a provisional estimate, about 7,250 tons [3].

Increased beryllium consumption in the USA has been accompanied by a reorganization of existing plants for processing and manufacturing this metal, and the building of new ones. For example, The Beryllium Corporation outfitted its plant at Hazleton with new high-productivity equipment (hot-extrusion vacuum presses) [7]. Mineral Concentrates Inc. of the state of Colorado is engaged in building a processing plant for beryllium concentrates yielding beryllium hydroxide as product [8]. Brush Beryllium is building a new plant at Hayward near San Francisco. The construction of the plant is estimated to run into $500,000 [2]. In 1957, these firms completed the building of two new plants for production of nuclear-grade beryllium. Each of the plants boasts 45 tons annual capacity. The plants were completed under contract with the USAEC with delivery terms covering five years for 90 tons of beryllium annually priced at about $100/kg. However, in 1958, the USAEC altered the terms of the contract: the amount of delivery scheduled was cut down to 34 tons annually, and the delivery term was stretched to four years. Production of nuclear-grade beryllium in the USA actually amounted to 21 tons in 1958. The cutback in beryllium deliveries to meet USAEC needs left a surplus over to satisfy the requirements of the

aviation industry and the navy in beryllium metal [1]. Moreover, beryllium is being used in the building of new nuclear reactors in other countries. In particular, Brush Beryllium Company has signed contracts stipulating delivery of beryllium goods totaling 1.2 million dollars for the new Belgian BR-2 nuclear reactor [9].

The yearly consumption of beryllium concentrates by the British economy amounts to approximately 100 tons [1]. Small-scale beryllium production is carried on at the Milford Haven plant and in a pilot plant belonging to Imperial Smelting Company. In line with the use of beryllium for fabricating some reactor parts, and also as cladding for fuel elements in gas-cooled and other reactor types, a plant for producing beryllium metal goods, with 7-10 tons annual capacity, was built and put into operation in 1959. Construction of the plant ran into estimated costs of 1 million pound sterling [10].

At Evenmouth, England, the British-American company Consolidated Beryllium Ltd., is building a plant for fabrication of nuclear-grade beryllium and copper-beryllium alloys. It is expected that this plant will have one of the largest outputs of its kind in the world [11].

Production of beryllium and beryllium compounds is carried on on a small-scale in France [6].

A 15-ton capacity (annual) plant is being set up in India for production of beryllia, and of items made of beryllia and beryllium metal [12, 13].

The last few years have thus witnessed an increase in amount of beryllium concentrates processed to yield beryllium metal, and an expansion of the beryllium-producing areas of the world.

A. Lanin and G. Aref'ev

LITERATURE CITED

1. Metall. No. 12, 1167 (1959).
2. Mining J., 253, No. 6485, 578 (1959).
3. Mining World, 21, No. 5, 67 (1959).
4. Mining J., 253, No. 6473, 237 (1959).
5. Mining J., 251, No. 6411, 18 (1958).
6. Mining World, 20, No. 5, 72 (1958).
7. Mining J., 253, No. 6470, 169 (1959).
8. Mining J., 250, 6408, 695 (1958).
9. Chem. Age, 80, No. 2038, 195 (1958).
10. Mining J., 253, No. 6487, 638 (1959).
11. Mining J., 253, No. 6464, 35 (1959).
12. Mining J., Annual Rev., May, 51 (1959).
13. Mining J., 250, No. 6393, 237 (1958).

CONFERENCE ON THE THEORY OF DISPERSION RELATIONS

In May, 1960, the Joint Institute for Nuclear Research (Dubna) held a workshop conference on the theory of dispersion relations. About 70 theoretical physicists participated in the deliberations, their number including Bulgarian, Hungarian, Vietnamese, Chinese, German, Polish, Rumanian, and Czechoslovak scientists. The conference was opened by N. N. Bogolyubov.

About 20 papers were read at the conference, and might be broken down into two basic groups: 1) proof of dispersion relations and the study of the general analytic properties of scattering amplitude; 2) applications of dispersion relations to obtain approximate equations describing processes of strong interaction and decay processes.

The participants listened with great interest to the report by A. A. Logunov, A. N. Tavkhelidze, I. V. Todorov, and N. A. Chernikov, which develops a method for finding the Majovana operator to Feynman diagrams, and thus makes it possible to investigate in detail the analytic properties of amplitude with the aid of perturbation theory,

and also the paper by V. A. Meshcheryakov, A. V. Efremov, D. V. Shirokov, and Chu Hung-Yuan, on investigations of the possibility of deriving approximate equations for partial waves in meson-nucleon scattering, with the aid of binary dispersion relations.

K. A. Ter-Martinosyan presented a paper in which equations derived with the aid of binary dispersion relations are studied on the basis of examples of concrete models.

Interesting results were reported by V. B. Berestetskii, I. Ya. Pomeranchuk, and V. N. Gribov, in papers linked to a study of the degree of increase in the amplitude of a process with increase in energy.

V. S. Vladimirov, in the course of investigating the general properties of causal commutators, developed a technique which yields the possibility of deriving an integral expression of the Dyson type for the commutator; in addition, this method proved highly effective in the theory of differential equations.

An entire series of papers was devoted to applications of binary dispersion relations to derive approximate equations describing processes involving the participation of unstable particles.

Summarizing the proceedings of the conference, D. I. Blokhintsev noted that the very composition of those in attendance indicated per se the great interest stirred by the theory of dispersion relations, and noted the fact that many interesting pieces of research reporting the solution of concrete problems in scattering theory had been presented. However, D. I. Blokhintsev did not fail to note that insufficient progress had been registered in applications of dispersion relations as the basis of the theory, and that the future would disclose the principal difficulties that still remain to be overcome.

V. Biryukov

NEW LITERATURE

Books and Symposia

REVIEW OF BOOKS ON ION EXCHANGE SORPTION

A wide selection of books on ion exchange have appeared in recent months, containing as a rule very valuable information on the theory and application of exchange resins in uranium technology, radiochemistry, and in the production of nuclear energy. A prominent place must be given, in our view, to the following books:

1. Ion Exchange and Its Application, A Symposium Edited by K. V. Chmutov, Moscow, Izd. AN SSSR, 1959.

2. Ion Exchange Technology, Symposium Edited by Nachod and Schubert. Academic Press, N.Y. Russian translation by Metallurgizdat, 1959.

3. R. Kunin, Ion Exchange Resins. J. Wiley, New York, 1958.

In addition to those books, we shall also discuss "Ion exchange in laboratory practice" by Salmon and Hale, London, Buttersworth, 1959, and "Ion exchange resins" by Kitchener, Methuen & Co., London, 1957.

The symposium "Ion exchange and its applications" has a chapter entitled "Ion exchange resins", compiled by E. B. Trostyanskaya, which gives a classification of ion exchange resins, lists the general requirements imposed upon them in applications, discusses conditions governing the preparation of ion exchange resin beds for practical use, and cites the basic methods used for testing the resins. The principal properties of Soviet ion exchange resins are cited, along with several specimens of exchange resins common in the USA. Of those exchange resins discussed, we were particularly interested in the copolymers of acrylic and methacrylic acid, dimethacrylic acid-ethylene glycol ester, and carboxylic resins based on polyvinyl alcohol and acrylonitrile. Selenic acid cation exchange resins may be prepared by reacting selenic acid with styrene-divinylbenzene copolymer.

For the sorption of a number of radioactive and fission elements, interest focuses on phosphoric acid cation exchange resins, prepared by phosphorylating polymers of polyvinyl alcohol and phenol derivatives, or styrene-divinylbenzene copolymers. Condensation polymerization of hydroxyphenylarsonic acid with formaldehyde yields a cation exchange resin having an arsenic acid residue as ion exchange functional group.

Copolymers based on maleic anhydride and divinylbenzene as a result of subsequent sulfonation of the copolymer to yield cation exchange resins containing carboxylic sulfonic groups may also be of interest to a degree. Great expectations are held for anion exchange resins based on polyvinyl chloride reacted with pyridine or other aminating agents under pressure. A special group is constituted by chelating ion exchange resins of the type which are derivatives of Trilon A and Trilon B, and which are highly valuable in radiochemistry.

In the chapter by M. M. Senyavin, "Elements of the theory of ion exchange and ion exchange chromatography", there appears a critical analysis of contemporary views on the statics, kinetics, and dynamics of sorption, and experimental data obtained for various species of ion exchange resins are reviewed in the light of these approaches. An analysis is made of the three outstanding viewpoints, interpreting the mechanism of the ion exchange process as a membrane equilibrium, as a double-layer heterogeneous chemical reaction, and as an osmotic transport process. The most important criteria determining the effectiveness of separation processes are discussed. The dependence of separation factor on the nature of the ion exchange resin and chelating substance is shown. To amass data needed for arriving at rational separations techniques, it is proposed to determine the equilibrium

constants and diffision coefficients of the ions. Criteria making it possible to distinguish bands of outward and inward diffusion in chromatographic separation are discussed.

In a chapter by the same author, devoted to ion exchange chromatography in analytical chemistry and in the technology of inorganic substances, a eminently complete review is given of Soviet and foreign papers covering all the groups of the Mendeleevian periodic table of elements. This marks the first time such a systematic review of work on ion exchange chromatography has been accomplished, and is a monumental bit of valuable reference material reflecting the current state of the art. Several variants to be pursued in the separation of alkali, alkali-earth, and rare-earth elements are discussed in detail. Valuable information is made available on sorption of uranium, thorium, and other radioactive elements.

The physical-chemical and physical-mechanical characteristics of the most important ion exchange membranes, methods for fabricating them, and their areas of application are treated in the chapter entitled "Ion Exchange Membranes." A correlation is drawn up of the different methods used in desalting ocean water, and it is shown that the most economically feasible technique, where a cheap supply of electric power is available, is the method of electrodialysis using ion exchange membranes.

The book "Ion exchange technology" provides a picture of the state of development of ion exchange technology in virtually all branches of industry where applications of ion exchange resins are possible in the USA. However, for a number of instances the authors of this book adduce only the most general information without making any deep-going analysis of industrial practice in applications of ion exchange technology in the USA.

Readers will find the data on deionization by a mixture of ion exchangers, which makes for more complete removal of electrolytes than may be had using conventional deionization procedures, quite interesting. The use of this procedure for removing radioactive elements yields excellent results. Much attention is given to electrochemical processes entailing the use of ion exchange membranes. The theoretical bases underlying processes of electrodialysis using ion exchange membranes are outlined, and the electrochemical properties of the membranes (electrical conductivity, membrane potential, permselectivity, etc.) are discussed.

A new and interesting process of electrolytic regeneration of ion exchange resins is described, but it is well to note that the authors failed to offer any convincing interpretation of the mechanism involved. A diagram of a multicompartment electrodialyzer for separation of ion mixtures is presented. According to the view expressed by the authors, this process may find applications in the future in separating mixtures of ions possessing similar physical and chemical properties, as for example isotopes. It was found that partial enrichment of D_2O in water may occur as the result of electroosmosis through membranes of the Nepton SP-51 type. The separation constant does not exceed 1.07 in experiments carried out with aqueous solutions of lithium chloride, ammonia, and sulfuric acid in a cell with a single membrane.

In the chapter by F. Spedding and J. Powell, "Quantitative separation of rare earths of high purity by the ion exchange technique", the perspectives envisaged in the use of rare earths are surveyed, and a theoretical justification is given for the ion exchange separation process applied to the rare earths. Practical experience gained in operation of a pilot plant is described.

Of considerable interest in this book are the chapters dealing with the use of ion exchange technology in hydrometallurgy, in processing radioactive isotopes, and in treating radioactive wastes. The broadest area for industrial applications of ion exchangers, following behind water softening and deionization, is found in the hydrometallurgy of uranium. Plants in the USA, Canada, Union of South Africa, and some other countries have made widespread use of ion exchange technology for recovering uranium from leach liquors and pulps. Quaternary ammonium bases (permutit SK, SKB, amberlite IRA-400, or Dowex-1) are used as sorbents.

The effect brought about by high activity levels on the physical and chemical stability of ion exchange resins was studied in relation to an investigation probing the use of exchange resins in radiochemistry, and purifying of discard waters formed in the production of fissionable materials. Some authors have shown that ion exchangers deteriorate partially when exposed to prolonged high activity levels, an effect which is related to the appreciable losses of sorptive capacity.

Very brief data are presented on continuous ion exchange plants for separating nuclear fission products. It is probably that the use of continuous ion exchange processes on an industrial scale is in its early stages in the USA. An extremely important area of ion exchange technology is found in the disposal of radioactive wastes

(cesium, strontium, ruthenium, zirconium, etc.). It was established that the capacity of the resins is dependent on the salt composition of the solution, in cases where the active elements are absorbed. For example, in the sorption of active cesium from distilled water, the capacity of the cation exchanger nalcite HCR is practically infinite, since 1 ml of HCR is capable of taking up 2.07 curies of cesium.

Various opportunities for applications of anion exchangers in the removal of radioactive iodine, ruthenium, tellurium, molybdenum, and zirconium were discussed.

The book by R. Kunin, bearing the title "Ion exchange resins", appeared in print in 1958, and is the second edition of a book of the same name by R. Kunin, and R. Myers, published in New York, in 1950. The first chapters are devoted to the theory of the mechanism of ion exchange, characteristics of cation exchange resins and anion exchange resins, and some supplementary data on the affinity and selectivity of various exchange resins. The dependence of resin properties on the content of divinylbenzene is discussed. A correlation is offered of current theories on exchange (Gregor, Glückauf, Soldano,and others). The chapter on "Synthesis of ion exchange resins" has been largely expanded. A reasonably complete table of the ion exchange resins prepared in the USA and in other countries throughout the world is presented. The basic principles governing the preparation of ion exchange membranes are outlined in concise fashion. Of a number of new sorptive agents listed, those meriting a greater measure of attention are diallyl allyl phosphonate copolymers and allyl phosphonate polymers, which contain an acid group capable of selectively absorbing uranium from nitrate. Resins containing diketone groups selectively absorb copper.

Chapters VI-IX are devoted to ion exchange applications to water softening and water deionization, and deal at bottom with the same questions as in the book's first edition.

Chapter X treats, for the first time, of the use of ion exchange resins in hydrometallurgy. An account is given of the history of the development of methods of uranium recovery from leach liquors and ore pulps. A detailed description is given of a resin-in-pulp technique for processing gold-containing uranium ores. Cyanidation leaching of the gold is the first step, followed by routing of the residue to be leached with sulfuric acid for uranium recovery. The gold from the pregnant cyanide solutions is extracted by means of an anion exchange resin, in the company of nickel, silver, iron, copper, and zinc sorbates. Nickel, iron, copper, and zinc are successfully eluted by dilute hydrochloric acid with sodium cyanide, following which the gold and silver are eluted by a solution of hydrochloric acid in methanol. The uranium is then taken up from the sulfuric acid leach liquor by an anion exchange resin, and passed through a mixture of ammonium nitrate and sulfuric acid as eluants.

Chapter XI is devoted to permselective membranes and their uses. For membrane types C-I and A-I, electrochemical characteristics are given. The most widespread use found for ion exchange membranes is in electrodialysis of water. Among other areas of application, we might cite the possibility of using them in the recovery and precipitation of uranium, and also in decontaminating radioactive solutions.

Ion exchange resins also have a wide range of application in analytical chemistry. This question is the subject of chapter XIII, which cites data on the use of exchange resins for concentration, ion exchange chromatography, determination of the total concentration of electrolyte, determination of equilibrium constants, of activity coefficients, etc.

Chapter XIV considers the principal areas of application of ion exchangers; among these, the field of application for resin exchangers in the atomic industry is of particular interest for us, to remove β and γ activity from reactor coolant water, and for the study of fission products.

Chapter XV goes into detail on some of the methods used in studying the physical and chemical stability of various resin exchangers.

Chapter XVI discusses the economics concerned with processes involving the use of ion exchange resins.

The book by Salmon and Hale, entitled "Ion exchange in laboratory practice", contains familiar data on exchange resins and may be of interest to engineers and technicians having their first fling at the subject. The book offers a large number of exercises which will help in rapidly assimilating laboratory research practices.

Kitchener's book "Ion exchange resins" presents in concise form the basic questions underlying ion exchange theory and practice. Data on the chromatographic separation of the rare earths and the transuranium elements (actinides) are made available, based on familiar work already published.

The chapter devoted to the further development of ion exchange processes and particularly to the production of high-selectivity resins is of some interest. For selective absorption of copper and ferrous oxide, ion exchange resins based on metaphenylene diglycine and other amino acids forming chelating groups are recommended. Resins containing groups of hydroxamic acids exhibit enhanced propensity toward chelation.

B. Laskorin

G. N. Ushakov, The World's First Nuclear Power Station. Construction and Operating Experience. Moscow-Leningard, Gosénergoizdat, 1959, 223 pages, 8 rubles, 40 kopeks.

This book contains three chapters. The first chapter provides a detailed description of the world's first nuclear electric-power generating station. The design of the uranium-graphite reactor and its accessory systems is discussed. The primary and secondary loops of the station, a series of auxiliary low-pressure circuits, the systems for technological and dosimetric monitoring of the station, the drainage, ventilation, accessory electrical power supply, transporting and technological operations systems incorporated into the plant as a whole are described. The experimental possibilities lodged in the reactor and the means relied upon to provide adequate shielding against radioactive emissions are explained.

The second chapter deals with the problems of construction and assembling of the power generating station. The stringent specifications imposed on the quality and precision of the assembly work are stressed. Particular attention is reserved for welding and quality control of welding operations. The organizational measures invoked to bring about correct systems and instrumentation assembly, intermediate testing and checking out of assemblies mounted in place, and the handling of technical documentation of the progress reached in stages of assembly are described. Comprehensive checking-out operations on the facilities, including the physical start-up of the reactor and running of the station through various sets of performance conditions, a prerequisite to putting the station on the line definitively, are discussed.

In the third chapter, we have outlined before us five years of experience in running the plant. Steady-state and transient operations come under discussion. Detailed description of the reactor power transient from zero power to the predetermined level is described, as well as the checkout and setting into operation of various systems, prior to running the power station through the initial power transient. An analysis is given of the performance of various monitoring systems – the system for monitoring the state of the process channels, radioactivity of the working fluids, performance of the heat power section of the power plant, health-physics monitoring, and so forth. Experimental data on reactor reactivity increments as a function of reactor power and period are given. Other items discussed are emergency reactor scrams and routine maintenance shutdowns, charging and discharging of fuel channels to lengthen the life of the channels and to greatly increase nuclear fuel burnup.

Some other questions of a more trivial nature, but nevertheless quite possibly interesting for the operating personnel in nuclear electric power stations, are dealt with in the book. On the whole, the book is directed at the engineer level; if offers an ample selection of graphs, flowsheets, engineering diagrams, and may prove useful not only to specialists in power engineering, but equally to students in power engineering institutes and engineering students majoring in that field.

N. V. Nelipa, Introduction to the Theory of Multiple Scattering of Particles. Moscow, Atomizdat, 1960, 160 pages, 5 rubles, 10 kopeks.

This book elucidates the traversal of γ photons, electrons, and neutrons through matter, with multiple scattering taken into account. A detailed description of various methods used to solve multiple scattering problems referable to those particles is given, for different particle sources. The general methods of solution are illustrated by concrete numerical calculations. Comparison of the results of theoretical prediction and existing empirical data is offered. The book is furnished with tables of build-up factors, energy spectra of photons, etc.

The book is written for physicists and engineers interested in multiple scattering problems, and may also prove useful as a textbook.

B. M. Gokhberg and G. B. Yan'kov, Electrostatic Charged-Particle Accelerators. Moscow, Atomizdat, 1960, 52 pages, 1 ruble, 50 kopeks.

Charged-particle accelerators in which electrostatic generators are used as high-voltage sources are described in this brochure.

A short survey covers various types of electrostatic generators and goes into their operating principles. Most of the attention is reserved for accelerators of recent design with band generators in pressurized gas. An analysis is given of the performance of components determining the energy and stability of the beam of accelerated ions.

J. Kaspar. Minerals of Radioactive Elements, Their Genesis and Extraction. Prague, Statni Nakladatelstvi Technicke Literatury, 1959, 155 pages.

This book is the first monograph on the mineralogy of radioactive elements to be published in Czechoslovakia. It centers its attention on the geochemical peculiarities of the radioactive elements and on descriptive mineralogy.

The introductory portion is devoted to a brief characterization of the processes of radioactive decay. Decay chains for uranium, actinium, thorium, and neptunium are studied. The geochemistry of uranium and the geochemistry of thorium are taken up separately, later on. Both of these chapters include general information on uranium and thorium content in certain rock species, their behavior in the process of magma differentiation, and their behavior in sedimentation processes. Over half the book is given over to a description of uraniferous and thoriferous minerals. This description is richly illustrated with crystal diagrams and color photographs of pertinent minerals. In the following chapter, rather reduced in volume, a concise description appears on the paragenesis of pitchblende and of the stages of mineralization of the most important hydrothermal deposits of uranium. A chart of uranium provinces and their characteristics is appended. The end of the book contains typical flow process diagrams of uranium ore processing operations.

The book is written for specialists working with radioactive ores, and also for students, geologists, mineralogists, geochemists, and chemists.

ARTICLES FROM THE PERIODICAL LITERATURE

I. Nuclear Power Physics

Neutron and reactor physics. Physics of hot plasma and controlled fusion. Physics of charged-particle acceleration.

Doklady Akad. Nauk SSSR, 130, No. 6 (1960).

G. A. Skuridin and K. P. Stanyukovich, pp. 1248-1251. Approximate solution of the problem of the motion of a conducting plasma.

Doklady Akad. Nauk SSSR 131, No. 1 (1960).

G. A. Skuridin and K. P. Stanyukovich, pp. 72-74. Motion of a conducting plasma in response to a plasma piston.

Zhur. Tekn. Fiz. 30, No. 2 (1960).

V. M. Kel'man, et al., pp. 129-137. Achromatic magnetic mirrors.

P. I. Strel'nikov and A. I. Fedorenko, pp. 138-141. Study of focusing properties of a paraboloid magnetic lens.

S. A. Kuchai, pp. 142-152. Optical properties of axisymmetric magnetic fields with a central source of charged-particles.

Zhur. Tekn. Fiz. 30, No. 3 (1960).

K. D. Sinel'nikov, et al., pp. 249-255. Motion of charged-particles in a spatially periodic magnetic field.

K. D. Sinel'nikov, et al., pp. 256-260. Study of a magnetic trap.

A. I. Morozov and L. S. Solov'ev, pp. 261-270. Motion of particles in a toroidal corrugated magnetic field.

A. I. Morozov and L. S. Solov'ev, pp. 271-282. Motion of particles in a helical toroidal magnetic field.

K. D. Sinel'nikov, et al., pp. 282-288. Investigation of ion cyclotron resonance in a dense plasma.

I. F. Kvartskhava, et al., pp. 289-296. Experiments on electrodynamical acceleration of a plasma.

I. F. Kvartskhava, et al., pp. 297-305. Some magnetohydrodynamic effects observed in a pulsed plasma pinch.

R. A. Demirkhanov, et al., pp. 306-314. High-frequency oscillations in a confined plasma.

R. A. Demirkhanov, et al., pp. 315-319. Interaction between a beam of charged-particles and a plasma.

V. D. Kirillov, pp. 320-329. Energy losses from radiation in a gas-discharge plasma.

Yu. V. Vandakurov, pp. 330-337. On the stability of a thin annular plasma conductor in a magnetic field.

Zhur. Éksp. i Teoret. Fiz. 38, No. 2 (1960).

V. I. Veksler, pp. 324-334. Energy distribution of sputtered and scattered ions in bombardment of a tantalum and molybdenum surface by positive cesium ions.

A. N. Protopopov, et al., pp. 384-386. Fission of Th^{232} by neutrons of 14.9 Mev energy.

G. G. Dolgov-Savel'ev, et al., pp. 394-403. Investigation of a toroidal discharge in a strong magnetic field.

G. E. Belovitskii, et al., pp. 404-408. On the mechanism involved in the fission of uranium nuclei by $\bar{\mu}$ mesons.

L. V. Groshev, et al., pp. 588-597. Gamma spectra from capture of thermal neutrons by heavy nuclei. I.

V. M. Strutinskii, et al., pp. 598-611. Gamma spectra from capture of thermal neutrons by heavy nuclei. II.

V. S. Sorokin and I. V. Sushkin, pp. 612-620. Stability of equilibrium of a conducting fluid heated from below in a magnetic field.

D. P. Grechukhin, pp. 621-630. Circular polarization of gamma photons accompanying capture of a slow neutron in the nucleus.

Zhur. Éksp. i Teoret. Fiz. 38, No. 3 (1960).

Yu. A. Vasil'ev, et al., pp. 670-684. Measurement of spectra and average number of neutrons in fission of U^{235} and U^{238} by neutrons of 14.3 Mev energy.

I. F. Kharchenko, et al., pp. 685-692. Interaction of an electron beam with a plasma.

L. M. Kovrizhnykh and A. A. Rukhadze, pp. 850-853. On the instability of longitudinal oscillations of an electron-ion plasma.

Izvest. Vyssh. Ucheb. Zaved. Radiofizika 2, No. 6 (1959).

V. V. Zheleznyakov, pp. 858-868. On the interaction of electromagnetic waves in a plasma. II.

Nauka i Zhizn' 27, No. 3 (1960).

A. N. Lebedev, pp. 38-39. A new accelerator.

Pribor i Tekn. Éksp. No. 1 (1960).

A. V. Kutsenko, pp. 3-16. Coincidence circuits in nuclear physics.

A. P. Babichev and N. D. Fedorov, pp. 16-19. On acceleration of ions in a cyclotron riding a "subharmonic".

A. G. Khabakhpashev, pp. 25-29. A fast neutron scintillation spectrometer.

B. S. Kozachina, et al., pp. 110. Voltage stabilization of the deflection system of a cyclotron.

V. M. Kirsanov, et al., pp. 111-112. Measurement of the current density distribution in the external beam of a cyclotron.

Yu. K. Gus'kov, et al., pp. 143-144. Preparation of uranium monolayers by vacuum evaporation.

Uspekhi Fiz. Nauk 70, No. 2 (1960).

V. L. Ginzburg and A. V. Gurevich, pp. 201-246. Nonlinear phenomena in a plasma immersed in a variable electromagnetic field.

Fizika Tverd. Tela 2, No. 3 (1960).

V. L. Bonch-Bruevich and A. G. Mironov, pp. 489-498. Contribution to the theory of an electron plasma in a magnetic field.

Arkiv Fys. 16, No. 3 (1960).

K. Larsson, et al., pp. 119-217. Time of flight spectrometer with a slow-neutron chopper.

B. Bonnevier and B. Lehnert, pp. 231-236. Motion of charged particles in a rotating plasma.

Canad. J. Physics 38, No. 2 (1960).

J. King, et al., pp. 231-239. Cross section of the (γ, n) reaction for N^{14}.

Industries Atomiques IV, Nos. 1-2 (1960).

R. Levy-Mandel, pp. 71-75. The SATURNE proton synchrotron at Saclay.

I. Linhart, pp. 81-82. New investigations in the area of thermonuclear fusion.

Jaderná Energie 6, No. 3 (1960).

I. Chochlovsky, et al., pp. 80-82. Laboratories for the Van de Graaff accelerator at the Institute of Nuclear Research of the Czechoslovak Academy of Sciences.

Jaderná Energie 6, No. 4 (1960).

J. Habanec. pp. 109. The first Czechoslovak cyclotron.

L. Drška and R. Hejlek, pp. 116-119. A plan drawn up by the department of technical and nuclear physics at Praha-Liben.

Nuclear Energy 14, No. 142 (1960).

------ pp. 112-113. The mass spectrometer at Argonne National Laboratory.

Nuclear Inst. and Methods 6, No. 2 (1960).

B. Cohen, et al., pp. 105-125. The Oak Ridge Relativistic Isochronous Cyclotron. Part II. Design of the magnetic field for the ORIC.

R. Ritchie, et al., pp. 157-163. A spherical condenser as a high-resolution particle spectrometer.

P. Grivet and A. Septier, pp. 126-156. Magnetic quadrupole lenses [in French].

H. Brückmann, pp. 169-175. A modulator for the Bonn FM cyclotron, with a ferroelectric ceramic [in German].

H. Kumagai, pp. 213-216. Design of cyclotron magnets with a wide range of field intensity variation.

Nuclear Inst. and Methods 6, No. 3 (1960).

M. Gordon and T. Welton, pp. 221-233. The Oak Ridge Relativistic Isochronous Cyclotron. Part III. Investigation of ion motion within the cyclotron.

R. Bassel and R. Bender. pp. 234-237. The Oak Ridge Relativistic Isochronous Cyclotron. Addendum. Some recent results on the study of the ion motion.

C. Wagner, et al., pp. 238-242. The techniques of chemical research performed with the Van de Graaff electron accelerator.

Nuclear Inst. and Methods 6, No. 4 (1960).

R. Ballini and S. Shafroth, pp. 331-336. Low-energy neutron detection by the NaI(Tl) crystal in a time-of-flight spectrometer.

Nuclear Phys. 15, No. 1 (1960).

W. Cross and R. Jarvis, pp. 155-165. Scattering of 14.6 Mev neutrons by Mg, Ca, Cd, Ta, and Bi.

Nuclear Phys. 15, No. 2 (1960).

I. Preiss and R. Fink, pp. 326-336. New nuclides of cobalt; activation cross sections of nickel, cobalt, and zinc by 14.8 Mev neutrons.

F. Everling, et al., pp. 342-355. Atomic masses of nuclei from $A \leq 70$.

Nuclear Sci. and Eng. 7, No. 2 (1960).

A. Campise, pp. 104-110. Accuracy of the S_n code in cell calculations.

E. Blue and H. Flatt, pp. 127-132. Convergence of the S_n method for thermal systems.

D. Schiff and S. Ziering, pp. 172-183. Many-fold moment method.

O. Simpson, et al., pp. 187-192. Total cross sections of U^{233} and U^{235} for neutrons of 0.02-0.08 ev energy.

R. Schmunk, et al., pp. 193-197. Total cross sections of titanium, vanadium, yttrium, and tungsten.

Nuova Tecnica, No. 4 (1960).

------ pp. 179-180. The Czechoslovak cyclotron.

Nuovo Cimento 15, No. 2 (1960).

A. Baños and R. Vernon, pp. 269-288. Waves of large amplitude in a collisionless plasma.

Phil. Mag. 4, No. 48 (1959).

A. Hare. pp. 1305-1310. Effect of drag on the stability of incompressible magnetohydrodynamic systems.

L. Kothari, pp. 1325-1338. Scattering of thermal neutrons in aluminum.

Phys. Rev. 115, No. 1 (1959).

R. Sterheimer, pp. 137-142. Range-energy relations for protons in Be, C, Al, Pb, and air.

Phys. Rev. 115, No. 2 (1959).

N. Dreicer, pp. 227-237. Runaway electrons and ions in a fully ionized gas. Part I.

Phys. Rev. 115, No. 3 (1959).

M. Baranger and B. Mozer, pp. 521-525. Electric field distribution in an ionized gas.

Phys. Rev. Letters 3, No. 7 (1959).

J. Tuck, pp. 313-316. Injection of a plasma stream into magnetic fields and entropy trapping into a conservative system.

Phys. Rev. Letters 4, No. 3 (1960).

C. Haaland, pp. 111-112. Confinement of charged-particles by electromagnetic waves in free space.

Phys. Rev. Letters 4, No. 4 (1960).

R. Post, et al., pp. 166-170. Stable confinement of a high-temperature plasma.

Progr. Theoret. Phys. 22, No. 6 (1959).

T. Morita, pp. 757-774. Equation of state of a high-temperature plasma.

II. Nuclear Power Engineering

Nuclear Reactor Theory and Calculations. Reactor Design. Performance of Nuclear Reactors in Nuclear Electric Power Plants.

Vestnik Akad. Nauk SSSR 30, No. 3 (1960).

E. P. Anan'ev, pp. 3-12. Problems of nuclear power engineering.

Prom. Stroitelstvo, No. 2 (1960 [Industrial Construction]

A. N. Komarovskii, pp. 34-38. On the use of prestressed reinforced concrete in building nuclear reactors.

Teploénergetika 7, No. 3 (1960).

P. M. Kessel'man, pp. 83-86. On thermodynamical similitude of light and heavy water.

Teploénergetika 7, No. 4 (1960).

D. D. Kalafati, pp. 74-81. Optimum temperature for regenerative heating of water at nuclear electric power plants.

Atomkernenergie 5, No. 2 (1960).

J. Clauss, pp. 41-52. Contribution to calculating nuclear reactor hot channel factors.

D. Radaj, pp. 53-57. Problem of boundary conditions in calculating thermal stresses in high-pressure reactor vessels.

W. Mayer-Jungnick, pp. 58-66. Aluminum applications in reactor design.

W. Kliefoth, pp. 66-73. Nuclear reactors for ships.

Atomkernenergie 5, No. 3 (1960).

W. Balz and R. Schwarzwälder, pp. 86-91. Calculations of circulation in a boiling-water reactor.

W. Kliefoth, pp. 92-99. American work on reactor projects with spherical fuel elements.

Atomwirtschaft 5, No. 2 (1960).

K. Schmidt-Amelung, pp. 48-52. On perspectives for the use of nuclear power.

Energia Nucleare 7, No. 2 (1960).

V. Surdo, pp. 88-94. Some theoretical questions in the kinetics of circulating-fuel reactors.

Energia Nucleare 7, No. 3 (1960).

I. Casagrande and S. Villani, pp. 141-158. Development of graphite-moderated gas-cooled reactors in Great Britain.

G. Soldaini, pp. 159-168. Studies conducted in the USA on cooling of nuclear reactors by a steam-water mixture.

I. Casagrande, pp. 175-191. Design of a fuel element of uranium metal cooled by wet steam.

R. Bonalumi, et al., pp. 192-209. Calculation of critical nuclear reactor size for a reactor with heavy water moderator and wet steam coolant.

Industries Atomiques 4, Nos. 1-2 (1960).

M. Trioulaire, pp. 57-63, 65-70. Characteristics of swimming pool reactors.

B. Kumleben, pp. 83-88. Survey of nuclear reactor development.

P. Sevette, pp. 89-112. The role of nuclear power in the energy balance of the future.

Jaderná Energie, 6, No. 3 (1960).

T. Margulova and L. Sterman, pp. 74-79. Pathways to more economic exploitation of nuclear electric power stations with graphite-moderated gas-cooled reactors.

Jaderná Energie 6, No. 4 (1960).

L. Sterman and L. Bohal, pp. 110-115. Choice of the optimized thermal economic conditions for Czechoslovakia's first nuclear power station.

M. Poděšť and I. Zvara, pp. 120-124. Water reactors burning slurried fuel.

Kerntechnik 2, No. 3 (1960).

G. Mardus, pp. 98-100. Practical calculations in nuclear engineering.

Nuclear Energy 14, No. 142 (1960).

------ pp. 109-112. The use of electrical heating at nuclear power plants.

P. Lottes, et al., pp. 116-121. Experimental research on natural circulation flow in boiling-water reactors.

Nuclear Energy 14, No. 143 (1960).

------pp. 152-153. The new British research reactor "Consort."

P. Lottes, et al., pp. 156-159. Experimental research on natural circulation flow in boiling-water reactors.

------ pp. 166-169. Equipment for fuel transfer at the Berkeley nuclear electric power station.

------ pp. 170-171. The JANUS reactor for biological research.

Nuclear Eng. 5, No. 46 (1960).

B. Eltham and E. Hicks, pp. 96-98. Safety criteria for low-power research reactors.

------ pp. 99-104. Research reactors. Survey of recent designs. Part I.

W. Hall, et al., pp. 105-111. Demands set by universities on research reactors.

H. Burgess, pp. 113-115. Nuclear engineering in West Germany.

R. Livesley, pp. 116-119. Lattices for graphite blocks in a nuclear reactor.

P. French, pp. 120-122. Vectorial diagram of temperature distribution in reactor channels.

------ pp. 123-128. Roundup of world reactor data.

Nuclear Eng. 5, No. 47 (1960).

------ pp. 150-153. Designing and construction of the HERO zero-power high-temperature reactor.

------ pp. 154-159. Research reactors. Survey of recent designs. Part II.

V. Eldred, et al., pp. 160-163. Changes brought about by irradiation in Calder Hall type fuel assemblies.

------ pp. 164-168. Fuel transfer and handling equipment in the Berkeley reactor.

J. Neuman, pp. 169,171. Health physics on nuclear-powered merchant ships.

------ p. 170. Health physics problems in the design and building of nuclear-powered ships.

------ pp. 172-173. Design of a high-temperature gas-cooled reactor.

------ p. 173. Design for a shipborne reactor with gas turbine.

------ pp. 176-177. A beryllium processing plant.

Nuclear Sci. and Eng. 7, No. 2 (1960).

B. Finn and J. Wade, pp. 93-96. Effects of contamination by light water on lattices of natural uranium rods in heavy water.

J. Busch, et al., pp. 97-103. Thermal stresses in nuclear reactor vessel nozzles.

J. Lewins, pp. 122-126. Use of generation time in equations describing reactor kinetics.

R. Mack and P. Zweifel, pp. 144-146. Calculation of neutron slowing-down in heavy water, using the Greuling-Goertzel calculations.

P. Rude and A. Nelson, pp. 156-161. A statistical analysis of reactor hot channel factors.

W. Rothenstein,pp. 162-171. Probability of collision and resonance integrals for lattices.

D. Donahue, et al., pp. 184-186. Absorption cross section of copper for thermal neutrons.

Nucleonics 18, No. 3 (1960).

P. Balligand, pp. 82-85. Reactor incidents at Saclay.

------ pp. 108, 110. Nuclear superheat design takes final form.

III. Nuclear Fuel and Materials

Nuclear geology and primary ore technology. Nuclear metallurgy and secondary technology. Chemistry of nuclear materials.

Vestnik Leningrad. Univ., Ser. Fiz. i Khim. 4, No. 1 (1960).

A. I. Zaidel', et al., pp. 48-59. Spectral assay of rare-earths extracted from rocks.

Geokhimiya No. 1 (1960).

K. G. Ordzhonikidze, pp. 37-44. Relative abundance of lithium isotopes in uraniferous minerals and meteorites.

Doklady Akad. Nauk SSSR 131, No. 1 (1960).

I. N. Plaksin and L. P. Starchik, pp. 85-86. Separation of minerals in a stream of ions produced by α radiation.

Zhur. Neorgan. Khim. 5, No. 2 (1960).

G. B. Maslova, et al., pp. 359-365. Separation of certain radioactive rare-earth elements by the chromatographic method.

Su Ch'ang and Shih Yi-Yi, pp. 372-380. Investigation of the composition and properties of carbonate compounds of trivalent cerium.

M. P. Pavlovskaya and I. M. Reibel', pp. 393-395. Complex formation between the uranyl ion and 8-hydroxyquinoline.

V. M. Vdovenko and A. S. Krivokhatskii, pp. 494-497. On the extractive power of mixed solvents.

K. A. Petrov, et al., pp. 498-502. Alkylphosphonates, diphosphonates, and phosphine oxides as extracting agents.

Zhur. Fiz. Khim. 34, No. 1 (1960).

V. M. Vdovenko, and D. N. Suglobov, pp. 51-56. Study of solutions of uranyl salts in organic solvents by means of infrared absorption spectra. The spectra of coordination-bound water in uranyl hydrates in region of bending vibration frequencies.

A. N. Murin, pp. 231-233. Contribution to the problem of the utilization factor of various methods for separating isotopes.

Radiokhimiya 11, No. 1 (1960).

A. V. Nikolaev, et al., pp. 3-5. Liquid-liquid extraction of radioactive isotopes by butyl phosphate esters.

V. B. Shevchenko, and I. A. Fedorov, pp. 6-12. Temperature effects on the tributyl phosphate extraction of uranyl, plutonium, ruthenium, and zirconium nitrates.

N. M. Adamskii, et al., pp. 13-19. Temperature effects on the tributyl phosphate extraction of nitric acid.

V. M. Vdovenko, et al., pp. 24-31. Structure of uranyl nitrate hexahydrate.

A. M. Gurevich, et al., pp. 32-43. Spectrophotometric study of the system $UO_2(NO_3)_2-ROH-H_2O_2-H_2O$.

B. P. Konstantinov, et al., pp. 44-49. Separation of radium and barium in exchange between an amalgam and a solution.

B. P. Konstantinov, et al., pp. 50-56. Separation of radium and barium in electrolysis, at the mercury cathode.

V. P. Shvedov and Fu Yi-pei, pp. 57-64. Separation of radioactive isotopes at the mercury cathode. 1. Study of the electrochemical behavior of europium.

V. P. Shvedov, and A. V. Stepanov, pp. 65-67. Separation of rare-earth elements by continuous electrophoresis. II. Separation using ethylenediaminetetraacetic acid.

A. A. Grinberg, et al., pp. 78-82. Determination of the amount of charge on polynuclear complex ions of ruthenium, by the ion exchange technique.

E. A. Isabaev, et al., pp. 94-97. The isotope composition of uranium found in natural specimens.

E. A. Isabaev, et al., pp. 98-103. The investigation of actinium present in natural specimens.

Uspekhi Khim. 29, No. 2 (1960).

A. P. Zozulya and V. M. Peshkova, pp. 234-268. Investigations on chelating in solutions, by the separations method.

Atompraxis 6, No. 2 (1960).

N. Getoff, pp. 41-43. Improved method for fluorometric assay of uranium.

Canad. J. Chem. 38, No. 3 (1960).

D. Santry and L. Yaffe, pp. 421-438. Absolute yield for fission products of U^{233} fissioned by thermal neutrons.

G. Weidmann, pp. 459-464. Separation of a mixture of several heavy metals by extraction methods and paper chromatography.

D. Santry and L. Yaffe, pp. 464-466. Yield of Ba^{140} in fission of U^{233} by thermal neutrons.

Canad. Mining J. 81, No. 2 (1960).

J. Griffith, pp. 135-137. Uranium production in Canada

Energia Nucleare 7, No. 2 (1960).

------ pp. 77-87. The uranium metal plant at Springfield and the program for development of the nuclear industry in Great Britain.

G. Perona, et al., pp. 111-120. Diffusion welding of uranium and zircaloy-2.

Energia Nucleare 7, No. 3 (1960).

F. Vogliotti, pp. 169-174. A fast method for spectrophotometric assay of uranium.

F. Habashi, pp. 210. Extraction of uranium in the heat treatment of phosphates.

Industries Atomiques 4, Nos. 1-2 (1960).

F. Gérard, pp. 76-80. Survey of developments in the chemical and nuclear sciences.

J. Inorg. and Nucl. Chem. 12, Nos. 1-2 (1960).

G. Harbottle, pp. 6-7. Half-lives of Tl^{204}, RaD, and Bi^{207}.

T. Moeller and E. Horwitz, pp. 49-59. Study of the rare earths. LXX. Some characteristics of complexes of EDTA, hydroxyethylethylenetetraacetic acid, and 1,2-diaminocyclohexanetetraacetic acid.

D. Peppard, et al., pp. 60-70. Isolation, physical properties, and infrared spectra of certain organophosphonates.

D. Bradley, et al., pp. 71-78. Compounds of hexavalent uranium. I. Uranyl alkoxides and uranyl hexaalkoxides.

J. Hefley, et al., pp. 84-89. Isolation, preservation, and separation of UCl_4 and UO_2Cl_2 in water, ethyl alcohol, and water-alcohol mixtures.

J. Smit, et al., pp. 95-103. Cation exchange properties of ammonium heteropolyacid salts.

J. Smit, et al., pp. 104-112. Cation exchange on ammonium molybdophosphate. I. Alkali metals.

H. Borchardt, pp. 113-121. Investigation of the reactions of uranium compounds.

S. Siekierski, pp. 129-135. Liquid-liquid extraction using tri-n-butyl phosphate, from chlorate solutions. I. Partition coefficients for zirconium, thorium, cerium, promethium, and yttrium.

G. Best, et al., pp. 136-140. Tri-n-butyl phosphate as extracting agent for inorganic nitrates. VII. Nitrates of the trivalent actinides.

D. Peppard, et al., pp. 141-148. Application of phosphoric acid esters to the isolation of certain transplutonides by liquid-liquid extraction.

D. Grdenic, pp. 149-153. Complexes of tetravalent uranium with dialkylpyrophosphoric acid.

M. Taube, pp. 174-180. Effect of polarity of solvent on extraction of plutonium-organic complexes.

J. Kennedy and R. Davies, pp. 193-198. Absorption of inorganic salts by anion exchange resins from organic solvents.

J. Mines, Metals, Fuels 7, No. 11 (1959).

P. Chakravarti, pp. 1-8. Investigations on the extraction of zirconium dioxide from Travancore zircon. Part I. Zirconium extraction in the form of calcium fluorozirconate.

Mem. Sci. Rev. Metal. 57, No. 1 (1960).

J. Ball, et al., pp. 49-56. Determination of the physical properties of plutonium metal.

Nuclear Energy 14, No. 143 (1960).

P. Jost and W. Bye, pp. 160-161. Lubricants for nuclear industry.

Nuclear Sci. and Eng. 7, No. 2 (1960).

F. Rough, et al., pp. 111-121. Irradiation of uranium monocarbide.

Nucleonics 18, No. 3 (1960).

F. Rough, and R. Dickerson, pp. 74-77. Uranium carbide – reactor fuel of the future?

L. Sarkes and N. MacKinnon, pp. 107. U-enrichment can be checked by gamma-ray spectrometry.

L. Maley, pp. 126,128. Balanced ionization chambers offer sensitive gas analysis.

IV. Nuclear Radiation Shielding

Radiobiology and radiation hygiene. Theory and Practice. Instrumentation for health physics.

Bezopasnost' Truda v Prom., No. 3 (1960) [Work safety in industry].

D. M. Srebrodol'skii and A. A. Korzhev, pp. 18-19. A device for safe radioactive logging operations.

Gigiena i Sanitariya 25, No. 2 (1960)

T. A. Berezina and V. Ya. Golikov, pp. 12-14. Methods for decontaminating sewage effluents from hospitals and clinics of radioactive iodine.

L. B. Dolivo-Dobrovol'skii, et al., pp. 15-18. Data on the deactivation of city sewage systems at biological purification stations.

V. F. Oreshko and Yu. V. Novikov, pp. 64-70. Contamination of atmospheric air by radioactive substances.

Yu. V. Novikov, pp. 71-78. Health physics problems in Britain.

M. A. Gluzman, pp. 79-83. Contribution to the procedure for determining radioactivity of aerosols in air by the aspiration technique.

T. A. Sviderskaya, et al., pp. 27-34. Use of ultraviolet radiation of different spectral make-up to minimize sequelae of radiation injury.

Z. V. Dubrovina and V. I. Katsapov, pp. 44-48. Determination of concentration of radioactive aerosols by the aspiration method.

M. V. Alferov and A. D. Turkin, pp. 49-50. On the question of thermal neutron dose measurement by the activation method.

Izvest. Akad. Nauk SSSR, Ser. Geofiz. No. 2 (1960).

G. M. Voskoboinikov, pp. 263-270. Contribution to the theory on interpreting gamma-logging data in layered media.

Med. Radiologiya 5, No. 2 (1960).

V. I. Prostyakova, et al., pp. 62-66. Working conditions in handling neutron sources for radioactive logging operations.

Radiokhimiya 11, No. 1 (1960).

V. L. Zolotavin and L. K. Ponomareva, pp. 104-106. Determination of radioactive strontium in waters of open reservoirs.

Arkiv. Fys. 16, No. 4 (1960).

R. Björnerstedt and K. Löw, pp. 293-313. Radioactive injuries resulting from exposure to fission products and radioactive precipitates. II. Gamma emission from radioactive precipitates.

R. Björnerstedt and K. Löw, pp. 315-319. Beta activity in fallout.

Atomkernenergie 5, No. 3 (1960).

T. Jäger, pp. 100-107. Power reactor shielding.

Atompraxis 6, No. 2 (1960).

L. Sverak, pp.43-50. Use of radioactive indicators in research on phytopathogenic viruses.

H. Dreiheller and E. Graul, pp. 59-65. Unresolved problems in radiobiology and the comparative method for investigating radiations.

Atompraxis 6, No. 3 (1960).

W. Jahn, pp. 82-87. Absorbing properties of shielding glasses. Part I.

H. Ebert, pp. 88-91. Effectiveness of the use of a lead equivalent to determine the shielding action of materials against gamma radiation.

H. Götte, pp. 99-107. Radiation shielding in handling of uncovered radioactive materials.

Atomwirtschaft 5, No. 2 (1960).

E. Somer, pp. 63-66. Gamma radiometric investigation of reactor shielding.

K. Fink and J. Woitschach, pp. 67-71. Betatron gamma flaw detection for inspection of reaction thermal shielding.

Energia Nucleare 7, No. 2 (1960).

F. Fossati, pp. 95-98. Units used in measuring ionizing radiations.

R. Lonati and F. Tonolini, pp. 107-110. Study of soil α-radioactivity and biological substances, by the α-spectroscopy technique.

Jadernà Energie 6, No. 3 (1960).

Z. Spurný, pp. 83-88. Survey of dosimetric techniques.

J. Rálková, pp. 89-93. Measurement of radioactivity in water.

F. Kepák and Z. Starčuk, pp. 94-95. Filtration of aerosols through fibrous filters.

Kerntechnik 2, No. 3 (1960).

G. Röbert, pp. 81-89. The shielding system of the Westhaut experimental reactor.

H. Helmberger, and W. Dietz, pp. 90-91. Time marker device simplifies determination of half-life using counters.

M. Oberhofer and P. Kienle, pp. 95-97. Radiation shielding in reactors and atomic plants.

------ pp. 100-101. The first scientific conference on processing of radioactive wastes, at Monaco, November, 1959.

Nucl. Sci. and Eng. 7, No. 2 (1960).

J. Watkins, et al., pp. 133-143. The outlook for disposal of radioactive wastes in shallow sedimentary formations.

K. Porges and T. Klippert, pp. 147-155. A broad-range neutron detector and monitoring device.

Nucleonics 18, No. 3 (1960).

R. Nisle, pp. 86-87. Neutron-absorption alignment chart.

J. Schulman, et al., pp. 92, 95-96, 98, 100-102. Thermoluminescent dosimeter has storage, stability, linearity.

R. French, pp. 114, 116. Calculating gamma spectra from reactors.

R. French, and J. Eggen, pp. 117-118, 120. Fast-neutron and gamma spectra for the bulk shielding reactor.

Nuova Tecnica, No. 2 (1960).

J. Šilar, pp. 64-68. Scintillation detectors and their use.

V. Radioactive and Stable Isotopes

Labeled atoms technique. Uses of radioactive radiations. Direct conversion of nuclear energy to electrical energy.

Avtomat. i Telemekh. 21, No. 2 (1960).

A. G. Vasil'ev, et al., pp. 245-253. Reliability criteria for automatic relay devices using radioactive emitters.

Vestnik Akad. Nauk SSSR, 30, No. 3 (1960).

N. N. Shumilovskii and L. V. Mel'tser, pp. 42-46. Development of automatic monitoring techniques, using nuclear radiations.

Atomwirtschaft 5, No. 2 (1960).

L. Erichsen, pp. 72-74. Structural and design materials for a hot-isotope laboratory.

R. Bonhoff, pp. 75-76. Radioactive isotope applications during 1959.

Chem. and Process Eng. 41, No. 3 (1960).

C. Mellish, pp. 83-86. Radioactive isotope applications in the chemical processing industry.

------ p. 87. Radioactive isotope applications for moisture control.

J. Reynolds, p. 88. Industrial radiography.

Contemp. Phys. 1, No. 1 (1959).

E. Wilson and J. Hughes, pp. 62-69. A light source using radioactive isotopes.

Kernenergie 3, No. 2 (1960).

H. Koch, pp. 109-116. Structural materials for hot-isotope laboratories.

Kerntechnik 2, No. 3 (1960).

J. Meissner, pp. 91-95. Use of radioactive isotopes in biology and medicine, Part I.

Nuclear Energy 14, No. 142 (1960).

------ pp. 125-128. Uses of radioactivity in meteorological research.

Nuclear Energy 14, No. 143 (1960).

F. Paulsen, pp. 163-165. Applications for ionizing radiations in the chemical processing industry.

Nucleonics 18, No. 3 (1960).

V. Karpov, et al., pp. 88-90. Radiation makes better woods and copolymers [guest article by Russian scientists].

------ pp. 124. Beta backscattering measures altitude.

R. Ely and J. Pier, pp. 130, 132-133. Tracers test efficiency of air-compressor filters.

Research 13, No. 4 (1960).

D. Powell and B. Bridges, pp. 151-157. The use of ionizing radiations to sterilize pharmaceuticals and drugs.

3 titles of immediate interest!

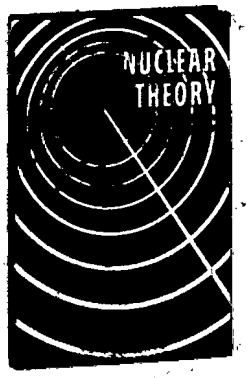

LECTURES ON NUCLEAR THEORY

by L. Landau and Ya. Smorodinsky
Translated from Russian

A concise presentation by these world-famous Soviet physicists of some of the basic concepts of nuclear theory. Originally published at $15.00 per copy.

". . . a real jewel of an elementary introduction into the main concepts of nuclear theory . . ."—NUCLEAR PHYSICS
". . . a decidedly worth-while addition to any experimental nuclear physicist's library."—E. M. Henley, PHYSICS TODAY

cloth 108 pages $5.25

Order from: **PLENUM PRESS 227 W. 17th Street, New York 11, N.Y.**

— of major interest to all researchers in low-temperature physics.

A SUPPLEMENT TO "HELIUM"

By E. M. Lifshits and E. L. Andronikashvili
Translated from Russian

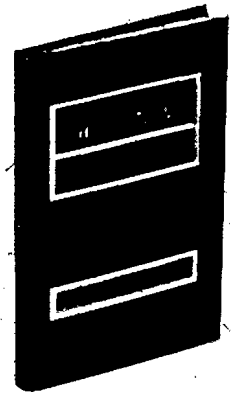

This notable volume consists of two supplementary chapters, by these outstanding Soviet physicists, which were added to the Russian translation of W. H. Keesom's classic book "Helium."
The first chapter, by Lifshits, presents a concise resume of the Landau theory of superfluidity. The second chapter reports in considerable detail the experimental work conducted by Peter Kapitza and E. L. Andronikashvili.

cloth 167 pages illustrated $7.50

Order from: **CONSULTANTS BUREAU 227 W. 17th St. • New York 11, N. Y.**

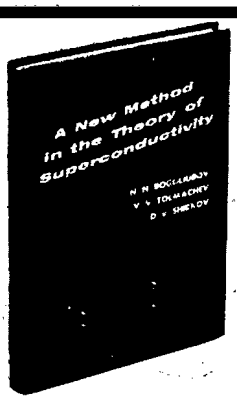

A NEW METHOD IN THE THEORY OF SUPERCONDUCTIVITY

By N. N. Bogoliubov, V. V. Tolmachev and D. V. Shirkov
Translated from Russian

The Soviet authors put forth a systematic presentation of a new method in the theory of superconductivity, developed as a result of the research of N. N. Bogoliubov and V. V. Tolmachev—based on a physical and mathematical analogy with superfluidity. This new method is an immediate generalization of the method developed by Bogoliubov in formulating a microscopic theory of superfluidity. The authors give calculations for the energy of the superconducting ground state using Frohlich's Hamiltonian, as well as of the one-fermion and collective elementary excited states. A detailed analysis of the role of the Coulomb interaction between the electrons in the theory of superconductivity is included. The authors also demonstrate how a system of fermions is treated with a fourth-order interaction Hamiltonian and establish the criterion for its superconductivity.

cloth 121 pages illustrated $5.75

Order from: **CONSULTANTS BUREAU 227 W. 17th St. • New York 11, N. Y.**

Descriptive folders upon request.